PPM
Annual Report
2016

The Annual Report for the PPM Research Centre

DEPARTMENT OF GEOLOGY
UNIVERSITY OF JOHANNESBURG

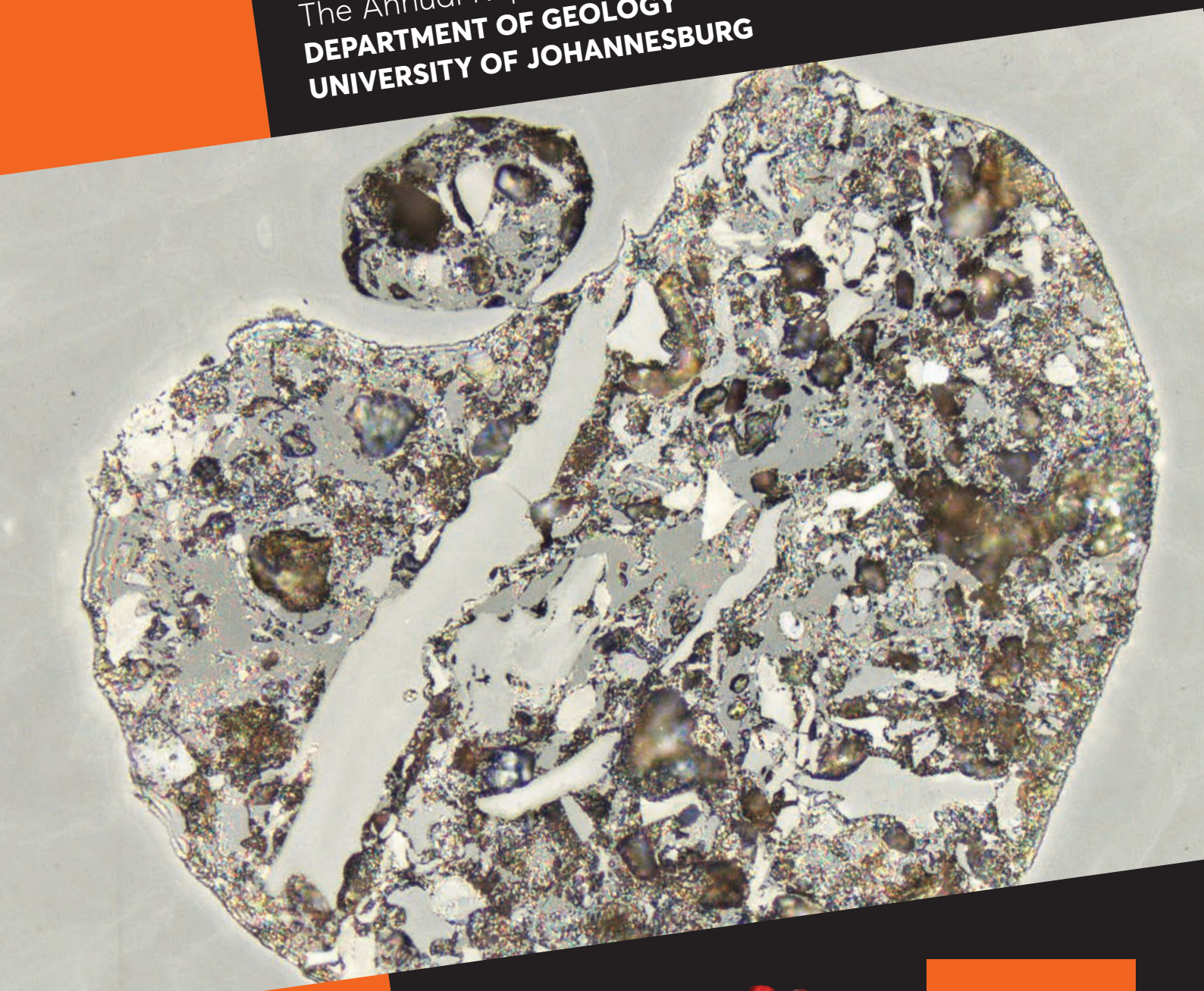

PPM

UNIVERSITY OF JOHANNESBURG

The Annual Report of the PPM Research Centre compiled by Jan Kramers.
Layout and design by UJ Graphic Studio

Special thanks/Acknowledgements
We wish to extend a special word of thanks to all our corporate and governmental financial and logistical supporters (in alphabetical order):
African Rainbow Minerals
Anglo American
Anglo Coal
Anglo Gold Ashanti
Anglo Platinum
Anglo Research
Assmang
Assore
Coaltech
Cradle of Humankind Trust
Department of Science and Technology (DST)
Deutsche Akademische Austauschdienst (DAAD)
Lonmin
National Research Foundation (NRF)
Nkomati Joint Venture
Rand Uranium (Gold One)
Two Rivers Platinum Mine
Vale

Please direct all enquiries and proposals for research to:
Prof. Jan Kramers or Prof. Fanus Viljoen
PPM, Department of Geology
University of Johannesburg
Auckland Park Kingsway Campus
PO Box 524, Auckland Park 2006
Johannesburg, South Africa
E-mail: jkramers@uj.ac.za or fanusv@uj.ac.za
Tel: +27(0)11 559 4701
Fax: +27(0)11 559 4702

Cover photo: Unusual depositional feature in a Limpopo Medium Rank B vitrinite-rich coal. The coal was devolatilised by igneous intrusions, resulting in pore development in vitrinite. In the image, the pore has subsequently been infilled by coal fragments, probably brought in by water at the early stages of coalification. Photograph taken using a Zeiss AxioImager M2M petrographic microscope at a total magnification of x500 under immersion oil. Width of field: 0.5mm. Photo N. Wagner

Header photo: View from the north of the hill above Rising Star Cave, discovery site of Homo naledi. Photo J. Kramers

Footer photo: Joburg Skyline from the Geology Department, 6 AM on 13th April 2017 after dramatic weather. Photo G. Henry

INTRODUCTION

In the course of 2016, Research Centres of the University of Johannesburg were reviewed by a Panel reporting to the University's Executive Director of Research and Innovation. In this process the continuation of the PPM Centre for the following three years (2017-2019) was 'highly recommended'. The Panel specifically endorsed PPM's multidisciplinary diversification of research, which had been a step taken in 2014 and 2015 to coexist optimally with the Inter-University Centre for Integrated Mineral and Energy Resource Analysis (CIMERA). A University Research Centre has more freedom of movement in its scientific endeavours than an NRF-funded Centre of Excellence. One aspect of this is in facilitating internationalization within Africa. In 2016 PPM explicitly supported the applications of three junior Staff members of the University of Ghana for TWAS-NRF PhD bursaries with placement at UJ, and allocated budget for their research. All three applications were successful.

2016 has also been the year in which the new Laser Ablation Multicollector Inductively Coupled Plasma Mass Spectrometry (LA-MC-ICP-MS) became fully operational with the installation of the excimer laser, about which more is written below in the 'Research Highlights and News' section. This is complemented by brief write-ups on the palaeomagnetics and noble gas (aka argon-dating) laboratories, to illustrate this unique combination of analytical equipment available to PPM. Reports on Coal Research and Medical Geology, both having become well established, and a new book announcement complete the news. The section 'Research Projects and Progress' further underlines the new diversity. The new call of UJ is: *the future, reimagined*, and PPM subscribes to this wholeheartedly.

ORGANIGRAM OF THE PPM RESEARCH CENTRE 2016

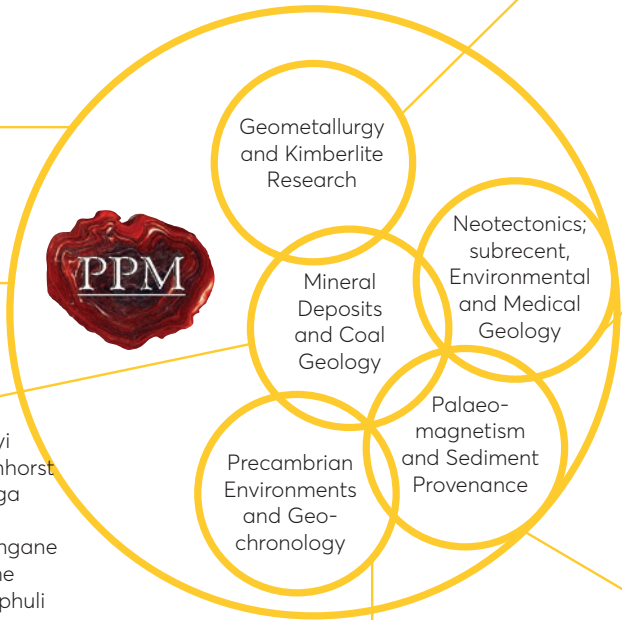

Technical support Staff in PPM
Mr T. Ramaliba
Mr B.T. Tshivhiahuvhi
Mr H. Gugwane

Academic Staff in PPM
Dr. G. Belyanin
Prof. Nic Beukes*
Mr. s Lauren Blignaut
Prof. Bruce Cairncross
Dr. Michiel de Kock
Prof. Marlina Elburg
Prof. Axel Hofmann
Mr. Mike Knoper
Prof. Jan Kramers*
Dr Jeremie Lehmann
Prof. Hassina Mouri
Mr. Freeman Senzani
Dr. Bertus Smith
Prof. Sebastian Tappe
Dr. Herman van Niekerk
Prof. Fanus Viljoen*
Dr. Clarisa Vorster
Prof. N. Wagner

* leading PPM

Mr. T. Dzvinamurungu
Ms. G. Mishra
Ms. B. Mkhize
Ms. S. Mkhatshwa
Mr. E. Moitsi
Ms. Z. Mpanza
Ms. T. Mxinwa
Mr. B.Z. Ndlovu
Ms. T. Nkomo
Mr. C. Radzivhoni
Mr. D. Rose
Ms. M. Vines

Mr. P. Boshoff
Mr P. Gevera
Ms C. Koki
Mr. T.V. Makhubela
Mr. L. Mashamba
Ms. B. McGeer
Mr A. Mgoqi
Ms. R. Shelembe
Mr. N.K. Singo
Mr S. Terblanche

Dr. H. Wabo
Dr. F. Humbert
Ms L. Bowden
Mr. S. Fitzpatrick
Mr. T. Lechekoane
Ms F. Monareng
Nr.R. Ngobeli
Ms S. Zardad

Dr. F. Ossa Ossa
Dr. B. Eickmann
Mr. J. Fitschen
Mrs G. da Costa
Mr. P. Hlungwani
Mr. J. Jodder
Mr. M. Morake

Mr. F. Fabien
Mr. M. Tsunke
Mr. E. Rammilla
Mr. T. Mabundza
Mr. A. Bukanga
Mr. N. Vafeas
Mr. C. Vongani

Mr E. Adeneyi
Ms. C. Badenhorst
Mr A. Bukanga
Ms. J. Lum
Ms. N. Masangane
Mr A. Matiane
Mr. M. Mphaphuli
Ms G. Naude
Mr N. Nendouvhada
Ms. B. Nthloro
Ms. V. Nxumalo
Ms. A. Opperman
Ms. L. Ravhura
Mr. F. Kruger
Mr. C. Schalkwyk
Mr. C. de Kock

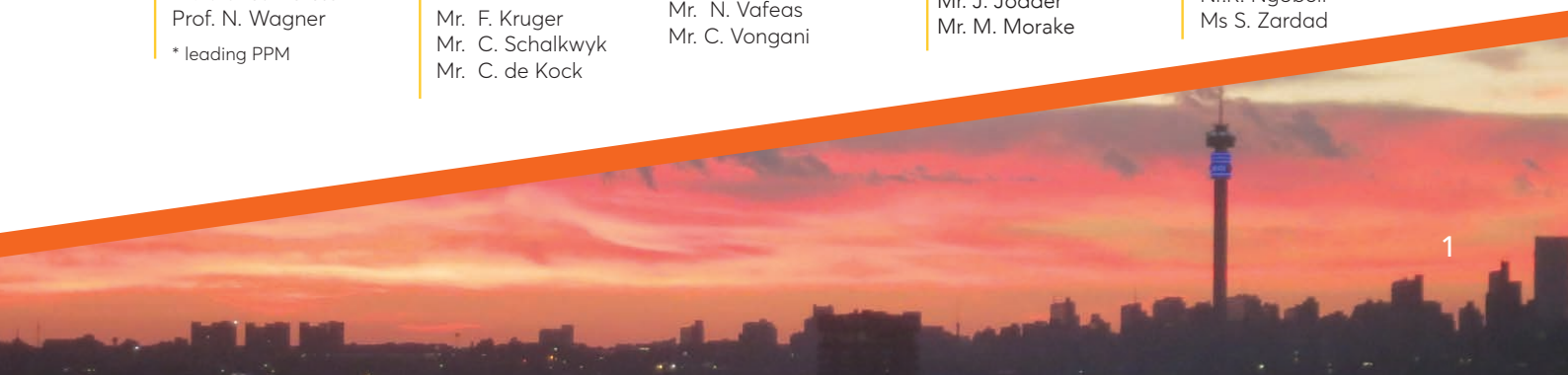

RESEARCH HIGHLIGHTS AND NEWS

The new LA-MC-ICP-MS laboratory now fully established

The UJ isotope facility consists of a Nu Plasma II multi-collector inductively coupled plasma mass spectrometer (MC-ICPMS) that can be connected to an ASI 193-nm excimer laser ablation (LA) system (Fig. 1) or a solution sample introduction system. The laser ablation system can also be connected to the older quadrupole (Q-) ICPMS. Both new instruments were acquired via an NRF-NEP grant to Marlina Elburg and Jan Kramers, and the facility is supported by PPM and CIMERA.

Since the arrival of the MC-ICPMS at the end of 2015, and the laser ablation system in January 2016, as well as the instrument scientist Henriette Ueckermann in February of the same year, several analytical protocols have been developed, and then applied to solve specific geological questions. The main developments have been with the laser as a sample introduction system, as the analysis of solutions is typically preceded by the isolation of the elements of interest from their matrix, which is best done in an ultra-clean environment. For this purpose, the University of the Witwatersrand is building the class-10 "Wits Isotope Geology Laboratory" (WIGL), overseen by Dr Grant Bybee. This will become operational in the second half of 2017.

U-Pb dating of zircon had already been a possibility with the old analytical equipment of 213-nm solid state laser and Q-ICPMS, but the better detection limits of the new set-up makes it easier to detect the presence of common Pb, and thus avoid low-quality sections of the ablation signal. More importantly, the $^{176}Hf/^{177}Hf$ isotopic tracer can now be applied to the same zircons on which the U-Pb ages were obtained, which refines the source information that can be obtained from detrital zircon studies in sedimentary rocks (Fig. 2). A next step will be to obtain Hf isotope and trace element information simultaneously, using the so-called split-stream technique, whereby part of the ablated material goes to the MC-ICPMS for Hf isotopic analysis, and another part to the Q-ICPMS for trace element analysis. However, the by now rather old Q-ICPMS has had a bad run with down time in the past year, and we are only slowly getting back in business with this part of the instrumentation.

In terms of U-Pb dating, we also had success with obtaining ages from titanite, which allowed us to constrain the age of the Pilanesberg Complex as being 1395 ± 10 Ma, and from monazite, which helped to resolve the age of leucosome patches in metapelites of the Southern Marginal Zone of the Limpopo Belt. The latter work was done on ca. 50 micrometer diameter monazite crystals in thin sections (Fig. 3), a job that had been considered as too difficult by the scientists operating the ion microprobe in St Petersburg! We are now looking at the possibility of dating apatite by LA-MC-ICPMS, but this job is somewhat trickier because of the poor quality of available reference materials.

Another tool that has already found several users is the characterisation of plagioclase for its initial $^{87}Sr/^{86}Sr$ ratio, which is a good tracer of the amount of 'crustal' input into magmas. This work is also done on thin sections, and has been embraced enthusiastically by the many people working on the various limbs and sections of the Rustenburg Layered Suite of the Bushveld Complex and the Molopo Farms Complex (see contribution by Peace Hlungwani in Research Projects section).

We have run some trials with in-situ Sm-Nd analyses on titanite, which surprisingly gave us an isochron for one of the Johannesburg Dome granitoids, which, albeit with a large uncertainty, yielded an age only slightly younger that of the U-Pb system in zircon (Fig. 4) – and an acceptable initial epsilon Nd value at the same time! Whether this method will be most suitable for age dating or fingerprinting purposes mainly depends on the age of the rock, and the variability of the Sm/Nd ratios in individual crystals.

Of course the past year and a half hasn't been without its challenges. We had some serious problems with the RF generator in the Nu Plasma MC-ICPMS, whereby we had to replace the unit three times until we finally had one that didn't commit suicide. We also found out that we have to replace the 'defining slits' more often than we had anticipated, as the high energy of the ions rapidly deteriorates the slit material, resulting in an imperfectly shaped beam, and thereby the 'wrong' numbers for reference materials.

However, the overall performance of the equipment has been very good, and we are looking forward to starting analysis on the solutions coming out of the Wits clean lab, and developing the laser ablation capabilities even further.

Marlina Elburg, Jan Kramers, Henriette Ueckermann

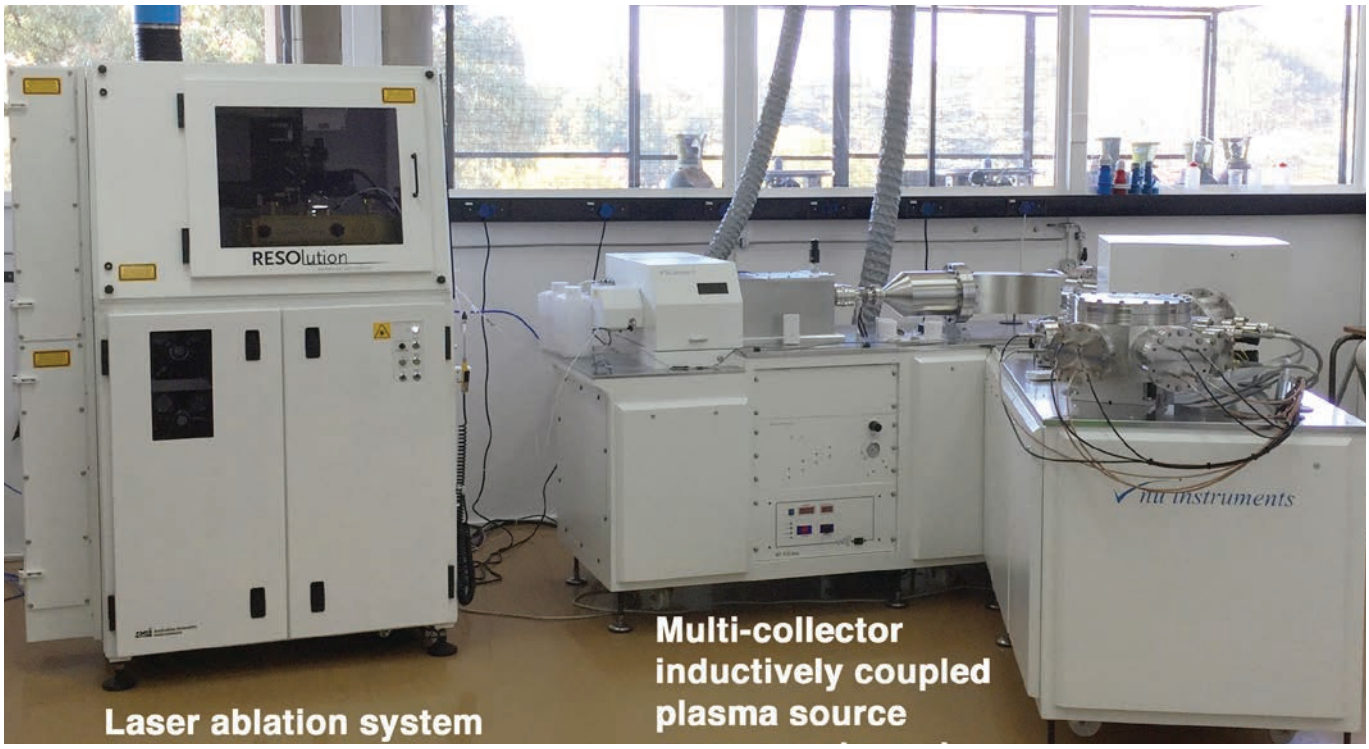

Fig. 1: Laser ablation system (ASI Resolution) and multi-collector ICPMS (Nu Plasma II) at the University of Johannesburg

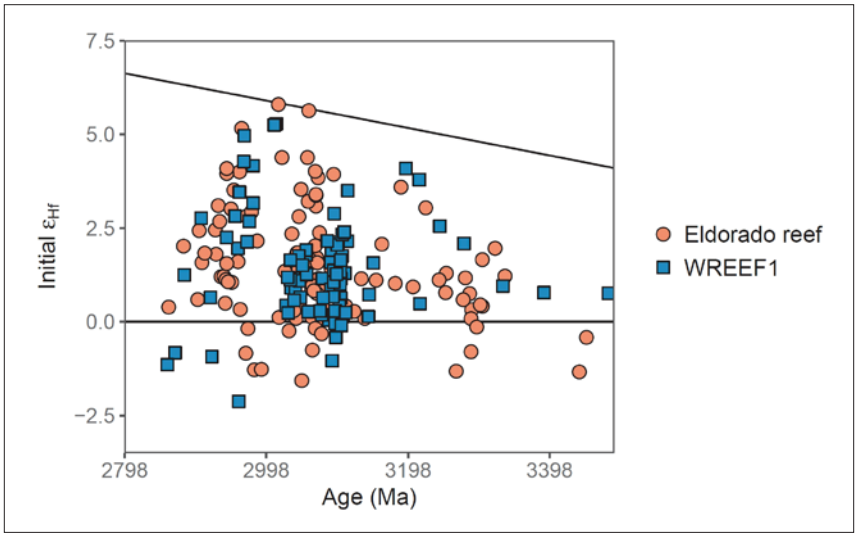

Fig. 2. Age versus initial epsilon Hf value for detrital zircons from the Basal Reef of the Johannesburg Subgroup (Central Rand Group, Witwatersrand Supergroup) compared to published data for the Eldorado Reef in the younger Turffontein Subgroup, showing their close similarity in both parameters.

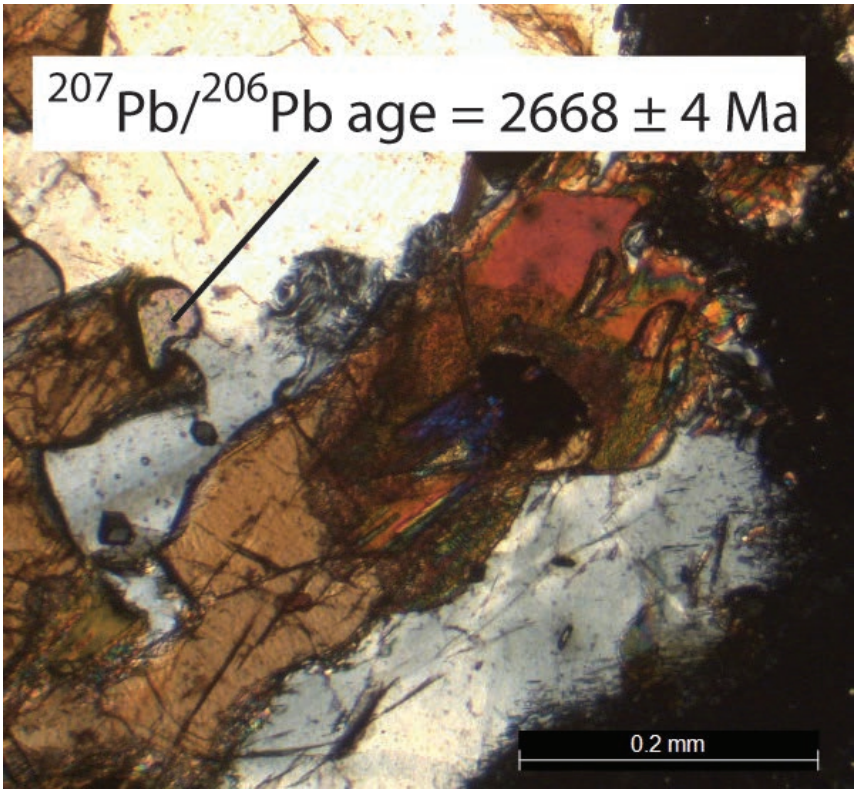

Fig. 3. Dated monazite crystal in thin section of leucosome patch in metapelites of the Limpopo Belt Southern Marginal Zone.

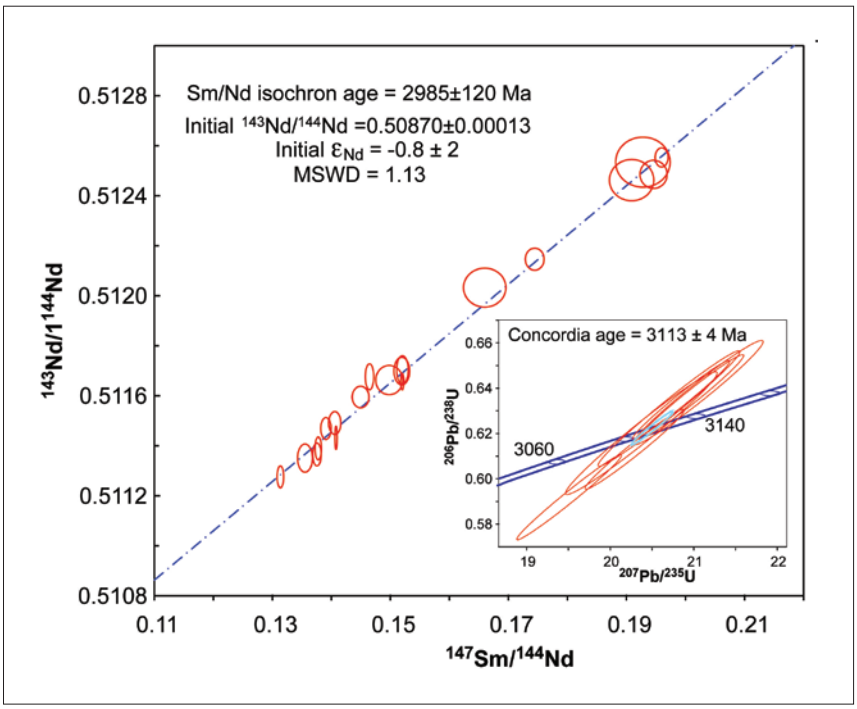

Fig. 4. Sm-Nd isochron of titanite and U-Pb concordia diagram of zircon for one sample of Johannesburg Dome granodiorite.

Research at the UJ palaeomagnetic laboratory

The paleomagnetic method exploits the magnetic information records in rocks to determine their latitudinal position at the time of formation. Ultimately, this allows reconstructions of ancient continents, now fragmented by plate tectonics, with possibility of tracing ore deposits between blocks.

The UJ Paleomagnetic Laboratory is one of the most modern facility of its kind in the world.

The unit is fully equipped in instruments and software necessary for oriented sampling, sample treatments and measurements, and interpretation of data. In 2009, the Paleomagnetic Lab was upgraded with the acquisition of a vertical 2G Enterprises DC-4K (liquid helium free) superconducting rock magnetometer or SQUID. Our SQUID is named for Dr. Alex du Toit, a prominent South African geologist and supporter of Alfred Wegener's hypothesis of continental drift. The UJ Paleomagnetic Laboratory is a member of the Rapid consortium of paleomagnetic laboratories with automated sample-changing systems designed by Prof. Joe Kirschvink at Caltech.

One of the main research goal of the UJ Paleomagnetic Laboratory is to update and expand the paleomagnetic record in order to assist with reconstructing the continental core of Southern Africa- the Kaapvaal craton. Within this frame work, many research projects have been conducted in the Paleomagnetic Lab since 2009 with number of peer-reviewed publications produced (Humbert al., 2017; Gumsley et al., 2017; Wabo et al., 2016a; Wabo et al., 2016b; Kampmann et al., 2015; Gumsley et al. 2013 among others). Many other research projects are currently being conducted in the Lab by UJ Researchers and Postgrads. Examples are (1) Project by Dr H. Wabo on BIFs of the Fig Tree Group in the Barberton Mountainland, (2) Project by Dr H. Wabo and Ms F. Monareng on "bostonite" dykes in the Northern Cape, (3) PhD project of Mr C. Luskin on the ~2.7 Ga Nsuzi Lavas of the Pongola Supergroup (4) PhD project of Mr C. Djeutchou on complexes dyke swarms in Black Hills, Badplaas and Phalaborwa areas, (5) The PhD project of Ms A. Abubakre on Karoo sediments, (6) MSc project of Mr J. OKennedy on Jurassic dykes in Antarctica and South Africa.

The UJ Paleomagnetic Lab also aims to operate as a "National, African and International Facility". With this regard, the unit is involved in various collaborative research projects incorporating paleomagnetism. This is done under the banner of the PPM Group and the CIMERA. Examples of collaborations at a national level include the Univ. of Bloemfontein, the Univ. of Cape town, the Council for Geoscience, etc… International collaborative institutes include the President Univ. and the Indian Statistical Institute in India, the Lund University in Sweden, Yale and Caltech in USA.

If you are interested in incorporating the paleomagnetic technique into your research projects, please contact Dr H. Wabo (hwabo@uj.ac.za)

Herve Wabo

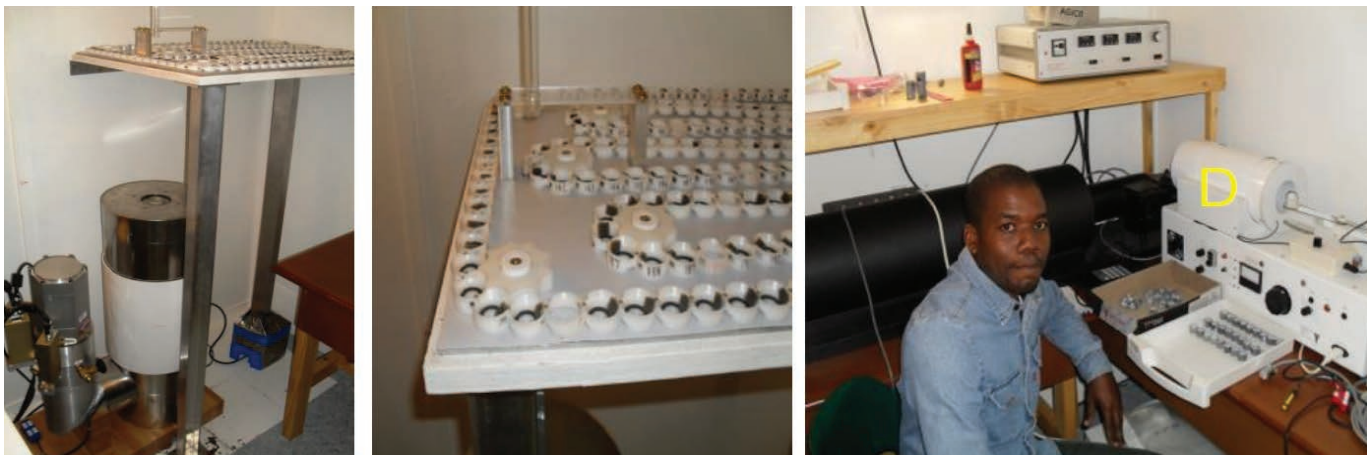

Fig. 1. Left: SQUID magnetometer; centre: SQUID sample magazine; right: Molspin AF demagnetizer (front) and ASC Scientific thermal demagnetization (back).

Noble gas geochronology at UJ

In 2006, the De Beers Geosciences Laboratory donated their noble gas mass spectrometer and coupled gas extraction line to the University of Johannesburg. This was, and still is, the only noble gas laboratory in Africa. The mass spectrometer is a MAP® 215-50 instrument with single on-axis electron multiplier detector and off-axis Faraday collectors, instantaneously switchable, a favoured instrument in the 1990's of which many are still in use today around the world. Heating for gas extraction is done by a SPECTRON® infrared (1064 nm) continuous Nd-YAG laser. Although the companies that manufactured these instruments have long ceased to exist, maintenance and even repairs have up to now been possible with in-house and local expertise.

$^{40}Ar/^{39}Ar$ dating is based on the fact that fast neutrons in a nuclear reactor convert a fraction of ^{39}K in a sample via the reaction $^{39}K(n,p)^{39}Ar$ to ^{39}Ar. This is a radioactive isotope (half life 269 years) and therefore does not occur in nature. Once irradiation parameters are calibrated, the K content of a sample can be derived as a linear function of [^{39}Ar], and age determinations can be made by argon isotope analyses alone, and stepwise heating analysis is a way to check internal consistency of the results. The SAFARI1 research reactor at Pelindaba, currently operated by NTP chiefly for the production of medical radioisotopes, has an irradiation position with fast neutrons. For irradiation, milligram quantities of K-bearing minerals or rocks are wrapped individually in tiny alufoil envelopes and stacked, up to 60 a batch, in a silica glass tube along with standards of known age. After irradiation a 'cooling' period of several weeks is necessary before they can be handled and placed in the extraction line. Up to 50 samples sit in individual pits on a 2 cm diameter aluminium disc placed in an ultrahigh vacuum port with quartz window that sits on a joystick-controlled microscope stage. Selection of samples is manual, but the stepwise heating and analysis cycle, between 10 and 20 steps per sample and lasting from 4 hours to a whole day, is automated.

The lab became operational for general noble gas analyses in 2012, and routine $^{40}Ar/^{39}Ar$ dating started in 2013. Its first claim to fame was the discovery (using Ar isotopes) that the mysterious diamond-bearing stone "Hypatia" from the SW Egyptian desert was extraterrestrial and could be a shocked comet fragment. Since then, the lab has provided significant to dominant input into 12 journal publications, 3 completed and 5 current MSc/PhD projects and 4 Honours projects at UJ. Cooperative projects, all focusing on $^{40}Ar/^{39}Ar$ dating, are running with Staff and PhD projects at UKZN, Wits, Stellenbosch and UWC. A current parallel development concerns (U-Th)-He dating of cave sediments, which is part of the PhD project of Tebogo Makhubela.

Those interested in cooperative work, please contact jkramers@uj.ac.za, gabelyanin@uj.ac.za or tvmakhubela@uj.ac.za.

Jan Kramers

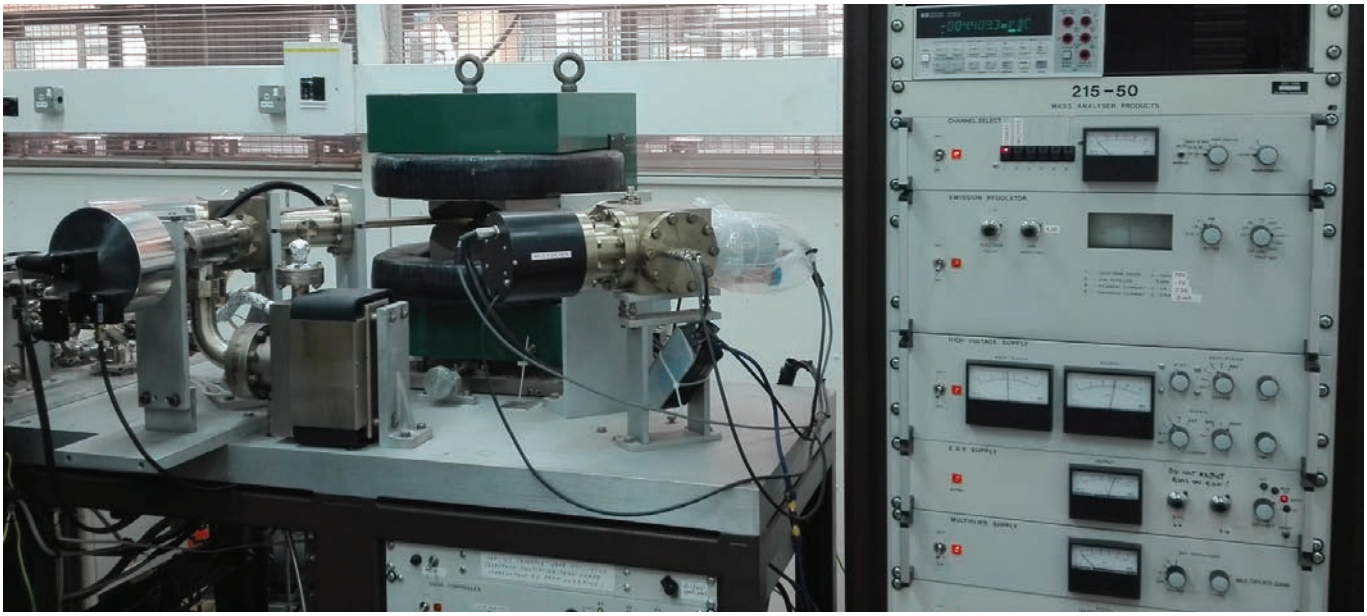

Fig. 1: The MAP 215-50 noble gas mass spectrometer (left) with typical 'old-fashioned' control electronics

Coal Petrography

Coal research continues to grow in the Geology Department at UJ. The petrographic facility was used almost daily by a variety of UJ staff and students, and external postgraduates. Students from Wits, University of Limpopo (MSc), Botswana International University of Science and Technology (MSc), North-west University (MSc & PhD), University of Fort Hare (MSc), and the Council for Geosciences undertook petrographic analyses on coals and organic-rich shale samples. Vitrinite reflectance determination on Karoo shales gas samples received a lot of attention with three students from different institutions submitting samples. Dr Wagner also participated in an international round robin exercise on dispersed organic matter. In addition, several consulting jobs were undertaken for industry. The demand for the coal petrographic facility continues into 2017, with many samples already received from a number of students at Wits (Geology and Mining) and North-West University, amongst others. Two students trained in coal petrography during their MSc studies have been hired on an ad hoc basis to assist with the influx of petrographic samples.

Three students submitted their MSc dissertations in January 2017 for examination. 1) Lateral comparison of coal composition in Botswana coalfields through the use of coal petrography (in collaboration with Analytika Holdings, Botswana, funded via CIMERA); 2) Petrographic consideration of the impact of the Tshipise fault on coal quality in the Soutpansberg coalfield (in collaboration with CoalofAfrica; funded by TESP Eskom grant and the NRF); 3) Consideration of Rare Earth Elements (REE's) associated with coal and coal ash in South Africa (funded by CIMERA). The international ERA-MIN consortium project on "Charphite" progressed well in the latter part of 2016, and the UJ based doctoral candidate appointed to the South African component of the project is progressing extremely well. As of January 2017, seven MSc and four PhD students were registered in the Geology Department to complete or commence research projects on coal and related materials. Eight other postgraduate students based at other southern African institutions are being co-supervised by Dr Wagner.

Four MSc students presented at the International Pittsburgh Coal Conference held in Cape Town (August 2016), and two students presented their research at the Geocongress also held in Cape Town at the end of August. Thus, the coal-based research outputs grew significantly in 2016. Two Msc students (Mr. N. Nendouvhada and Ms. M. Mphaphuli) were awarded the ICCP Student Travel Grant to attend the ICCP Organic Petrology Training Course in Potsdam, Germany (June 2016).

Nikki Wagner

The Medical Geology initiative

Medical Geology is an emerging field of science that is dealing with the impact of natural geological factors, process and material on humans and animals health. This field is based on a multi-, cross- and inter- disciplinary approach bringing together experts from various fields of science including public health experts, animal health professionals, geoscientists, toxicologists, chemists and many more.

The African continent is known for its complex and dynamic geological history and evolution including frequent earthquakes, volcanic activities in tectonically active regions, pervasive dust storms, water toxicity due to interaction with the geological environment..etc. All these naturally occurring processes and material can have serious short and/or long-term health impacts including cancer, asthma, thyroid disorders etc.., which are known to be frequent health issues on the continent. Thus, in order to understand the impact of our environment on our health, it is important to develop this discipline and to train a new generation of researchers who can take the lead in this field in Africa.

Thus, since 2015, 14 PG students were supported to work on various projects related to Medical Geology issues in South Africa and in Africa. 9 of these students are from South Africa and 5 are from other African countries including Kenya, Nigeria, Ghana and Namibia.

The initiative is supported financially by the National Science Foundation (NRF), the University of Johannesburg Global Excellence and Stature (GES) and Research Funds (URC) as well as the UJ- Faculty of Science Research Funds. In addition, several colleagues from SA, Africa and elsewhere are involved in this initiative and support it.

Hassina Mouri

Fig. 1: The Medical Geology Team at the Soweto Campus

New Geology Book!

Microminerals of the Bushveld Complex

By Maria Atanasova, Bruce Cairncross and Wolf Windisch

Published by the Council for Geoscience, Pretoria

Bruce Cairncross has been working for some time with Maria Atanasova at the Council for Geoscience and Wolfgang Windisch on their book "Microminerals of the Bushveld Complex". This went to print in 2016 and was officially launched at the 35th IGC congress held in Cape Town in September 2016. The book for the first time documents over 170 of these minerals and provides a host of other information as well. One major contribution of the research that culminated in this book, is the quantitative identification of 35 mineral species identified for the first time from South Africa. All the minerals are illustrated either in colour or via Scanning Electron Microscope images, or both. The book therefore provides a reference to the complex geochemical and mineralogical evolution that the Bushveld Complex has been subjected to over time and offers a unique contribution to this type of mineralogy.

As several localities are featured, the mineralogical information is complimented by text detailing the history and geological setting of each site, where applicable. Field work by all three authors was undertaken to the various localities. During these field visits, samples, data and photographs were acquired on-site that were then incorporated into the text. The book is therefore a culmination of over 10 year's field work and laboratory analyses. The book disseminates information to the reader via over 1,000 photographs and illustrations, many geological and soil geochemical maps and site photographs, supported by accompanying text. It therefore affords the reader the opportunity to identify these minerals, for the first time, using the book's illustrations and text.

Figure 1. The three authors of the new "Microminerals of the Bushveld Complex" book. From left to right: Bruce Cairncross, Maria Atanasova and Wolf Windisch.

Figure 2. Erythrite ($Co_3(AsO_4)_3 \cdot 8H_3O$) from Kruisrivier cobalt mine, Bushveld Complex. Field of view is 3.1 mm. Wolf Windisch photo.

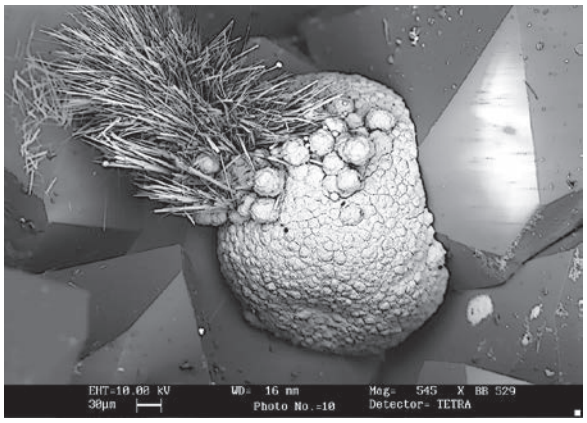

Figure 3. Acicular goethite on botryoidal goethite on quartz. Slipfontein, Bushveld Complex. Maria Atanasova SEM image.

RESEARCH PROJECTS AND PROGRESS

Geometallurgy and Economic Geology

A MINERALOGICAL AND GEOCHEMICAL STUDY OF PLATINUM-GROUP MINERALS AND BASE-METAL SULFIDES IN THE P1 AND P2 UNITS OF THE PLATREEF AT THE LONMIN AKANANI PROJECT AREA, BUSHVELD COMPLEX, SOUTH AFRICA

Brian Z. Ndlovu

The Akanani Project Area is located in the Central Sector of the Northern Limb of the Bushveld Complex. The Platreef has been subdivided into 4 units P1-P4. Mineralization is however only restricted to P1 and P2, even so, P1 has been extensively contaminated by xenoliths of skarn and dolomite with rare appearance of granofelsite xenoliths with the mineralisation being less continuous than that of the P2 unit also considered to be the main ore horizon and is more uniformly mineralised.

The aims and objectives of this study are to determine the nature and abundance of Platinum-Group Minerals (PGM) in the P1 and P2 unit and also gain insight into PGM population variation between the P1 and the P2 units as well as their grain size distribution. It is to further determine the association of these PGM with other minerals, particularly Base-Metal Sulfides (BMS). In addition to this, determine the chemical composition of these BMS and construct a mineralisation model. An earlier study did demonstrate an abundance of Pt-Pd bismuthotellurides at Akanani, and a strong association of these with base-metal sulfides, but the sample spread was limited to only two boreholes, drilled through the P2 unit. A more comprehensive sample set is now available incorporating both P1 and P2, thereby allowing for a more comprehensive study, with a view on mineralogical variability of the PGMs.

PGE-bismuthotellurides have been found to be the most abundant PGM in the P1 and P2 units, however their end member appeared to have varying proportions and this being a result of a possible lack of or abundance of the constituents of these minerals (Figure 1A and B). The nature of these platinum-group minerals can be seen in (Figure 2 A-H). It was further found that the different PGM groups (e.g. PGE-(sulf)-arsenides, PGE-alloys, PGE-Fe-alloys as well as Electrum) of P2 contained twice as much the concentration as P1 (Table 1).

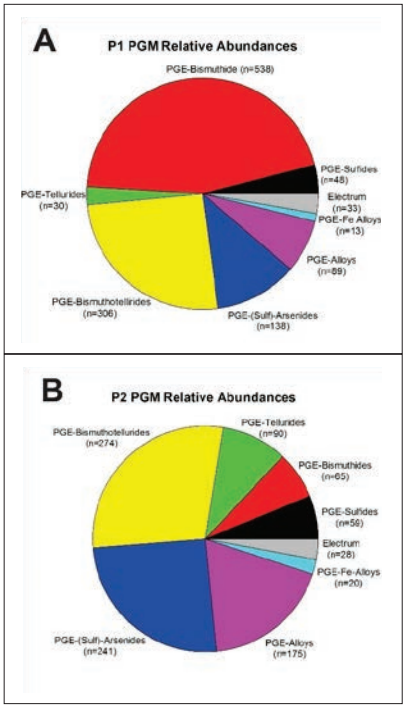

Figure 1: A and B showing the relative abundance of the platinum-group minerals in P1 and P2.

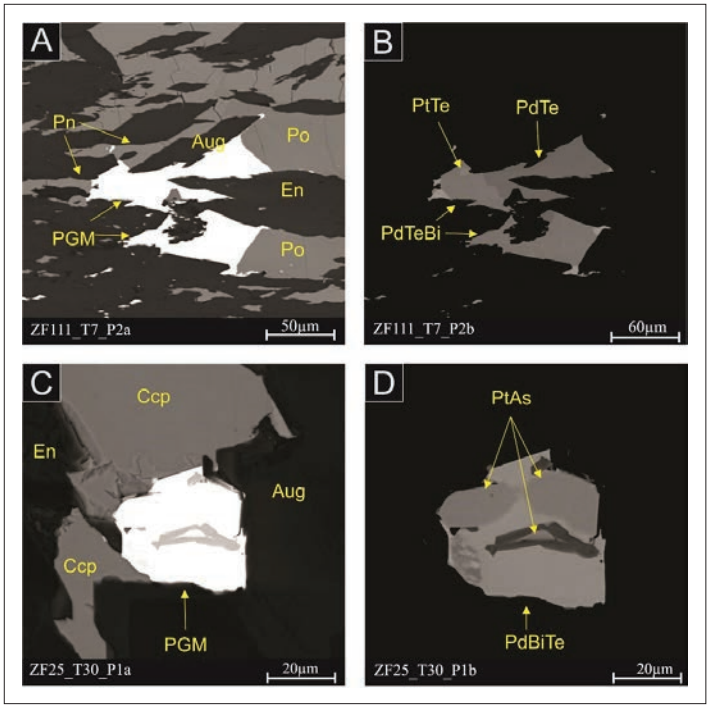

Figure 2 A-D: With the use of different contrasts an exsolution textures can be observed in the platinum-group minerals. These can be further seen to be highly associated with primary silicates and base-metal sulfides.

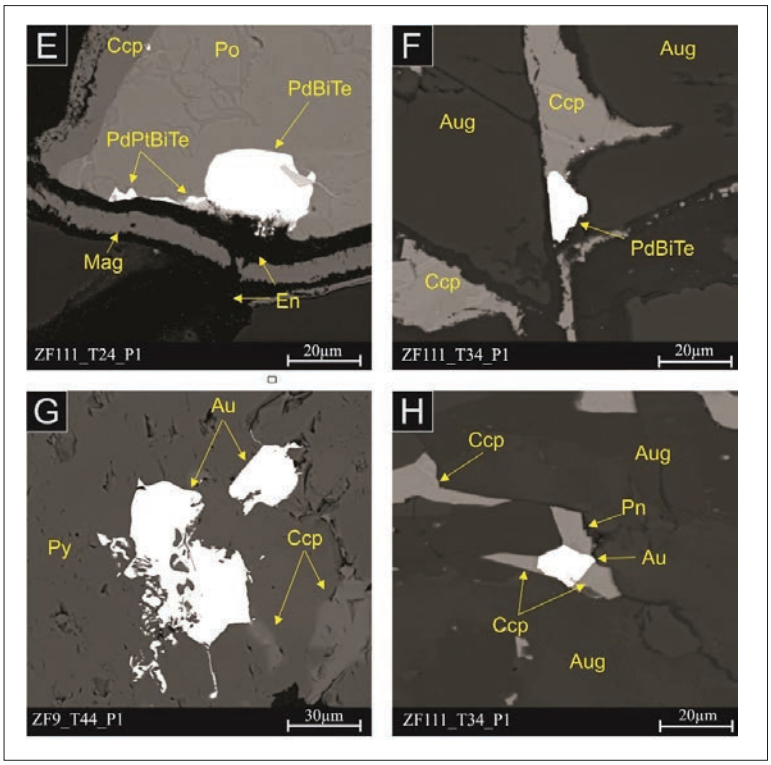

Figure 2 E-H: Platinum-group minerals as well as gold can be seen to be highly associated with base-metal sulfides and primary silicates.

Table 1: The different platinum-group mineral groups and the minerals found in the study for both the P1 and the P2 units. The relative abundance of these minerals is shown by area percent and grain count.

Group	Mineral	Area% P1	Grain Count P1	Area% P2	Grain Count P2
PGE Bismuthide	Insizwaite ($PtBi_2$)	28.06	492	8.84	60
	Sobolevskite (PdBi)	3.80	46	0.15	5
	Total	**31.86**	**538**	**8.99**	**65**
PGE Telluride	Moncheite ($PtTe_2$)	0.12	28	18.94	85
	Kotulskite (PdTe)	4.02	2	0.88	5
	Total	**4.14**	**30**	**19.82**	**90**
PGE Bismuthotelluride	Maslovite ((Pt,Pd)BiTe)	3.28	55	16.87	85
	Michenerite (PdBiTe)	28.35	251	16.90	189
	Total	**31.63**	**306**	**33.76**	**274**
PGE Sulfide	Braggite (Pt,Pd,Ni)S	0.39	25	2.92	29
	Cooperite (PtS)	1.36	13	1.19	23
	PtSnS	3.80	10	0.09	7
	Total	**5.55**	**48**	**4.20**	**59**
PGE (Sulf)-Arsenide	Sperrylite ($PtAs_2$)	15.63	42	16.65	103
	Hollingworthite ((Rh,Pt)AsS)	4.48	79	6.66	89
	PtSbAs	0.05	12	0.28	14
	PdSbAs	0.01	5	1.66	21
	PdAsNi	0.00	0	0.86	14
	Total	**20.17**	**138**	**26.11**	**241**
Gold	Electrum (Au,Ag)	0.85	33	2.04	28
	Total	**0.85**	**33**	**2.04**	**28**
PtFe-Alloy	PtFe-Alloy (Pt_3Fe)	1.71	13	0.62	20
	Total	**1.71**	**13**	**0.62**	**20**
PGE-Alloys	Atokite $(Pd,Pt)_3Sn$	2.66	30	1.78	62
	Plumbopalladinite (Pd_3Pb2)	1.37	57	2.52	106
	Stibiopalladinite (Pd_5Sb_2)	0.06	2	0.14	7
	Total	**4.09**	**89**	**4.44**	**175**
	TOTAL	**100.00**	**1195**	**100.00**	**952**

The PGM of the P1 for an 80% population have been found to be slightly coarser grained than P2 (Figure 3A). These PGM are highly associated with Primary Silicates (albite, anorthite, bytownite, augite, enstatite and olivine) and this being predicted by their high abundance. Their association has also been found to be profoundly with Base-Metal Sulfides (chalcopyrite, pentlandite, pyrrhotite and pyrite), Secondary Silicates (actinolite, tremolite, hornblende, biotite, chlorite, serpentine and talc) and to a lesser extent other minerals (barite, calcite, chromite, dolomite, galena, hematite, ilmenite, millerite and sphalerite). Amongst these Base-Metal Sulfides, pentlandite has been found to have the highest association with PGM and least association with pyrite in both P1 and P2 (Figure 3B-D).

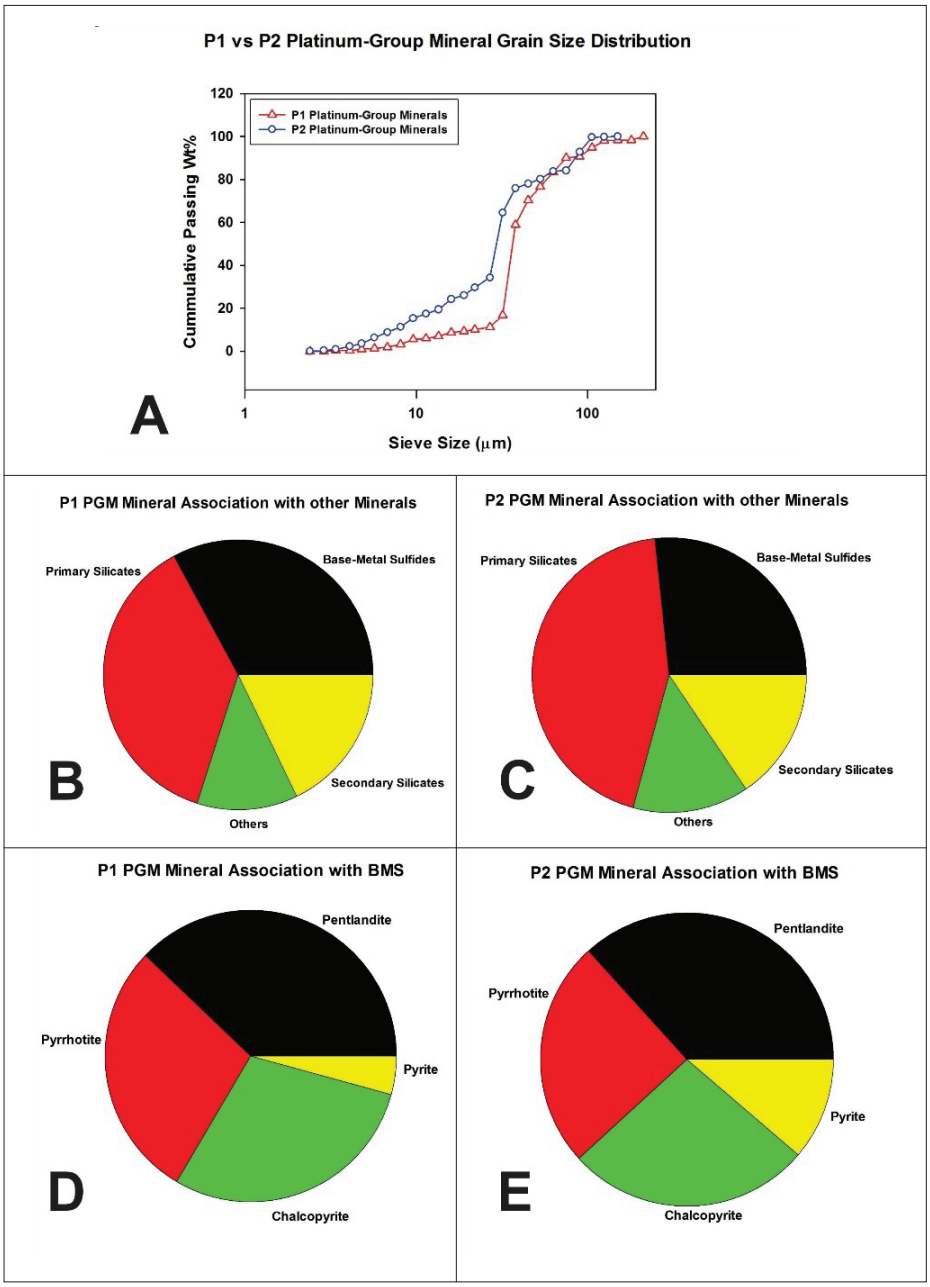

Figure 3: (A) grain size distribution of P1 and P2. (B) and (C) showing the mineral association of platinum-group minerals with different mineral groups in P1 and P1. (D) and (E) further showing the association of platinum-group minerals with the main base-metal sulfides.

The base-metal sulfides found in the P1 and P2 unit were strongly associated with primary silicates such as augite, hypersthene, albite, anorthosite, labradorite and occasionally an oxide which is chromite (Figure 4A-H). Allanite was another mineral that the base-metal sulfides were not strongly associated with but was quite interesting to find given its rare earth element content (Figure 4C). Another mineral that was interesting to find and also associated with pentlandite was apatite (Figure 4C). These base-metal sulfides were also found to be strongly associated with themselves, not only through grain boundary contact, but through grain inclusions as well (Figure 4A-H) this can be seen with pentlandite and pyrrhotite. This association of base-metal sulfides with themselves is a representation of a monosulfide solid-solution, where upon cooling of a monosulfide solid-solution, pentlandite and pyrrhotite get exsolved (Mostert et al., 1982).

The pentlandites appeared to be highly fractured and consisted of some form of a replacement texture of augite (Figure 4B and C) and hypersthene (Figure 4H), where the augite and hypersthene appears to be channelling itself through the pentlandite fractures. The pyrrhotite appeared to have almost spherical voids and spherical inclusions of pentlandite, this has also been seen in pyrite (Figure 4A-C and F). Millerite which does not always form part of the main four BMS and is rather considered to be a replacement mineral alongside pyrite (Zientek, 2012) had been observed (Figure 4A). This mineral has not been observed in the P2 samples but only in the P1 samples and the presence of this mineral in the P1 unit can therefore confirm the observed chemistry.

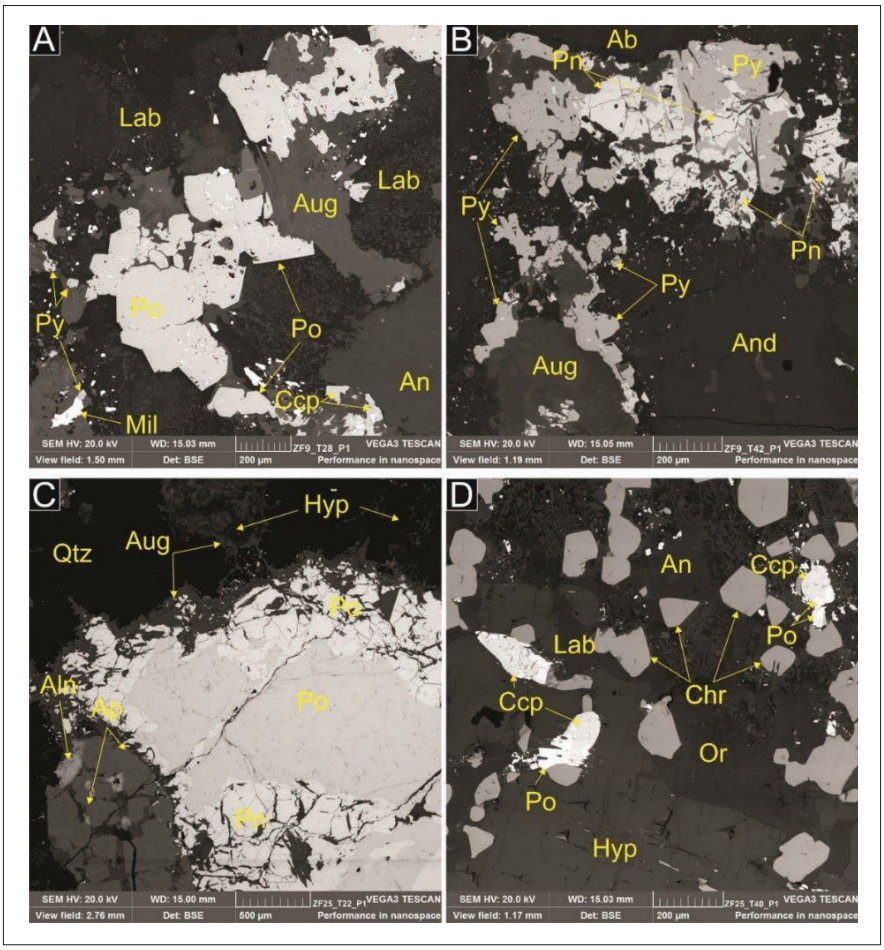

Figure 4: Some backscatter electron (BSE) images of the base-metal sulfides in the P1 and P2 unit. (A) Showing pyrrhotite as well as pyrite and millerite. (B) and (C) consist of highly fractured pentlandite grains as well as their strong association with pyrrhotite. (D) Showing an association of chalcopyrite, pyrrhotite and chromite.

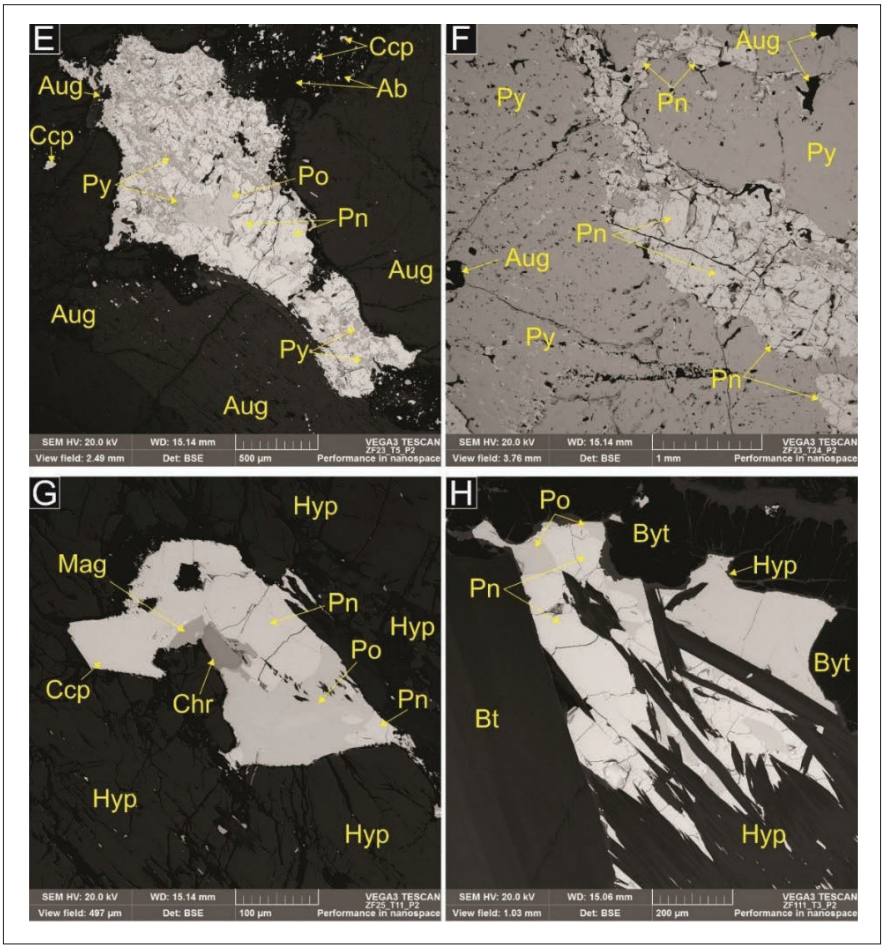

Figure 4: (E) Highly fractured pentlandite with a high association with pyrrhotite and pyrite. (F) Pyrite with augite and pentlandite inclusions. High fracturing in pentlandite grain which appears to be a larger inclusion in the pyrite. (G) Chalcopyrite associated with pentlandite and magnetite; pyrrhotite associated with pentlandite and chromite. (H) Fractured pentlandite being cross-cut hypersthene and also associated with pyrrhotite, bytownite and biotite.

A high chemical variation was observed for the Base-Metal Sulfides of P1 as compared to P2. For example the chalcopyrite for P2 were chemically uniform whereas those of P1 showed a slight depletion in copper and respective enrichment in iron (Figure 5A). The pentlandite for P2 as well were chemically uniform and those of P1 showed high chemical variation where the compositions ranged from a pyrrhotite composition (Ni deficient) to a millerite composition (Fe deficient) (Figure 5B and C). The high chemical variation in P1 as opposed to P2 has been thought to be due to P1 being highly contaminated and altered and therefore the appearance of alteration minerals such as millerite and violarite. There is also the possibility of the monosulfide solid solution in the P1 system having cooled down much slower and therefore resulting in an exsolution of high temperature minerals (pyrrhotite) all through to low temperature minerals (millerite) which represent a complete solid solution series.

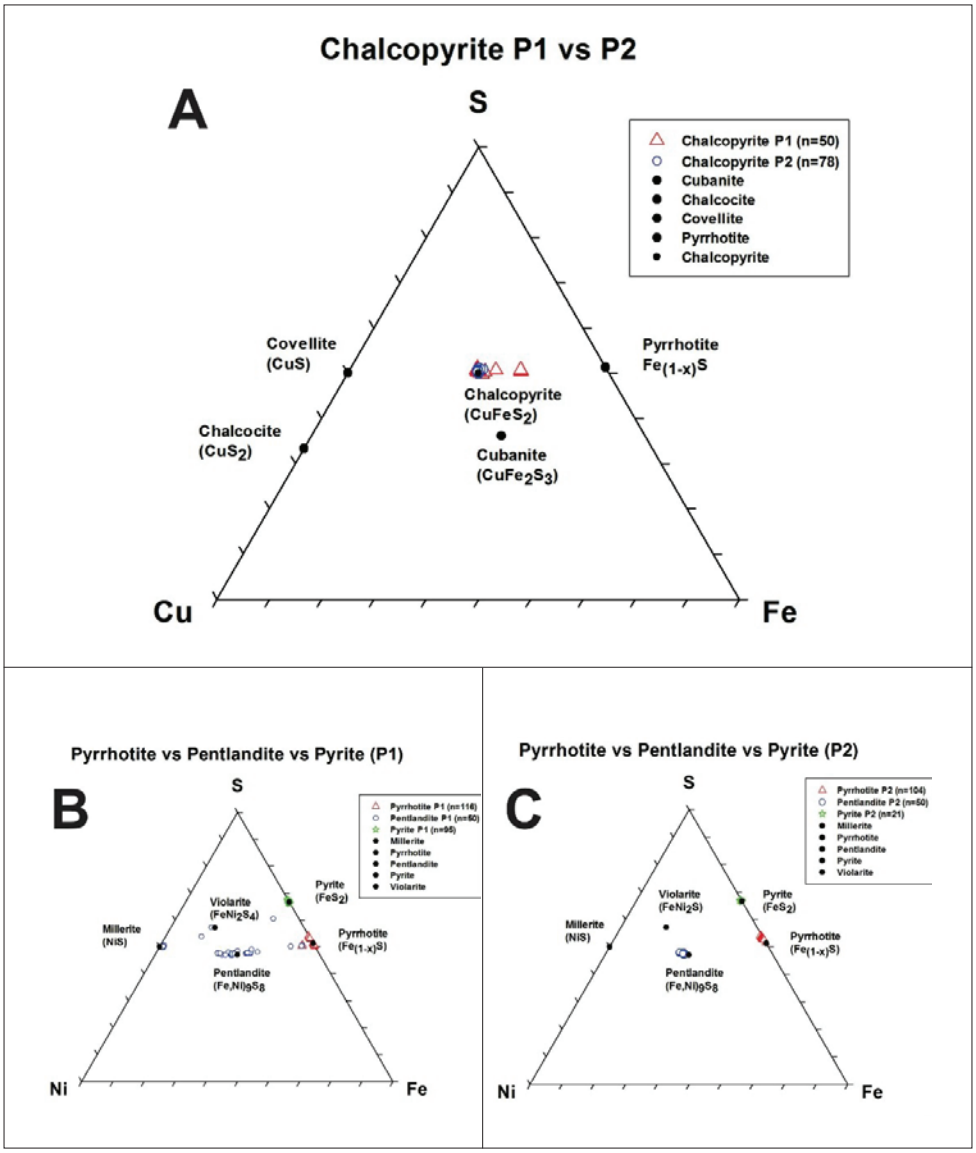

Figure 5: (A) plot of the chemistry of the chalcopyrite grains from P1 and P2 with C and D further showing the chemistry of pyrrhotite, pentlandite and pyrite grains for P1 and P2.

A PETROGRAPHIC AND GEOCHEMICAL ANALYSIS OF THE KALAHARI MANGANESE DEPOSIT, SOUTH AFRICA

Lauren Blignaut, Fanus Viljoen and Harilaos Tsikos[1]

[1] Rhodes University

The manganese (Mn) ores in the Kalahari Manganese Deposit (KMD), were ultimately affected by hydrothermal alteration, which involved the addition and removal of elements and metals, and the subsequent upgrading of the protolith and low-grade ores into the high-grade ores. Normal and thrust faults localised the alteration system, as they acted as conduits for hydrothermal fluids. The flow of isotopically light, low temperature meteoric fluid from the overlying Mapedi/Gamagara unconformity also contributed to the enrichment of the ores. Three distinct ores, based on mineralogical associations, textural features and geochemical characteristics were distinguished: (1) the protolith ore; (2) the low-grade (carbonate-rich) ore, and (3) the high-grade (carbonate-poor) ore. The protolith ore exhibits a decrease in Fe and Si concentrations, and an increase in Mn and Ca abundances with depth. The Ca abundances are generally high throughout, suggesting less alteration and replacement of carbonates. The low-grade ore is far more enriched in Mn within the upper ore as a result of carbonate loss and conservative Fe enrichment. Both ore types display high abundances of braunite and carbonates, with minor secondary oxide minerals of braunite-II and hausmannite. Tephroite, friedelite and the serpentine-group minerals are ubiquitous throughout these ores. The high-grade ores generally exhibit conservative Fe and Mn enrichment, suggesting normal residual enrichment, with abundant carbonates and hematite, as well as bixbyite, braunite-II and hausmannite. Two ores, however, display a highly ferruginised, decarbonated upper ore, and a highly Mn-enriched lower ore, with Fe being removed. As a result of this significant enrichment, these ores have been affected by the movement of the meteoric fluid flow into the Mn ores, 'aided' by an impermeable dyke.

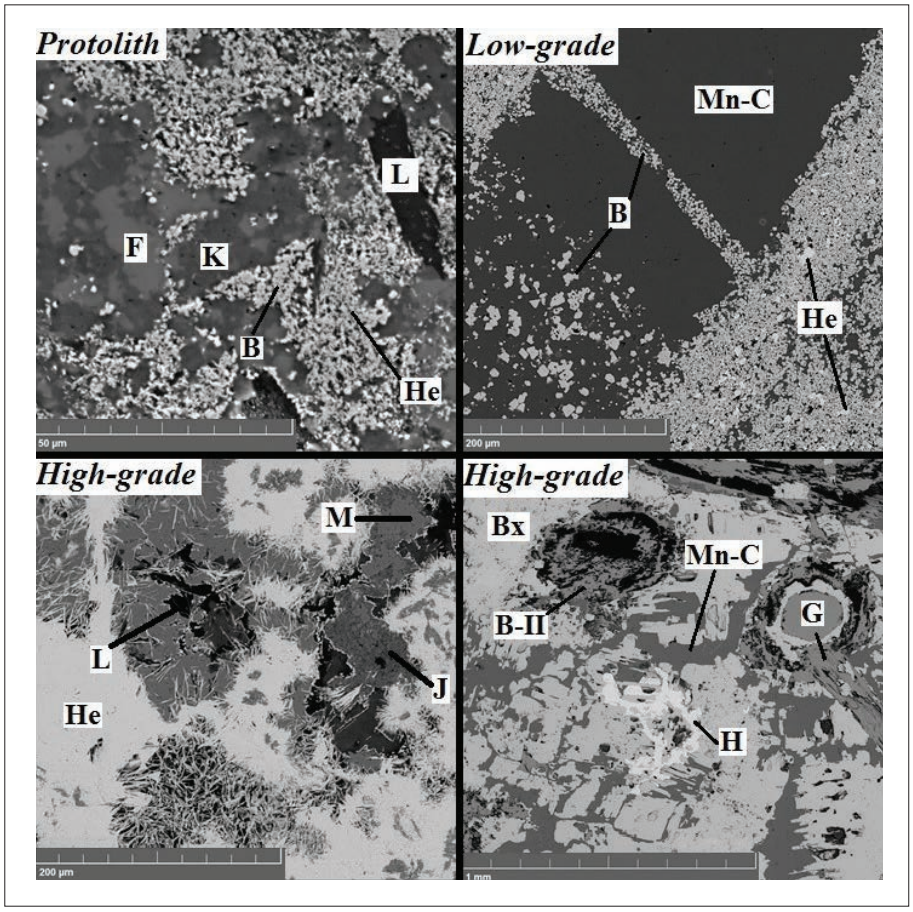

Figure 1. Backscattered electron images of (A) the protolith ore, with a kutnohorite-hematite-jacobsite (K-He-J) matrix with intergrown friedelite (F), braunite and lizardite (L); (B) low-grade ore, with braunite (B) scattered throughout an ovoid with hematite and Mn-calcite (Mn-C) interstitial to braunite; (C) high-grade ore, with hematite intruding into jacobsite (J) and manganite (M) with lizardite (L) inclusions; and (D) high-grade ore, with hausmannite (H) replacement of bixbyite (Bx) and Mn-calcite, with braunite-II (B-II), gaudefroyite (G) and hausmannite replacing carbonate ovoids.

In terms of trace elements, the high-grade ores are enriched in boron (B), which is an important component in the steel-making industry. B, overall displays a higher average abundance in the upper ore, and is mineralogically controlled and hosted by braunite, braunite-II, gaudefroyite, tephroite and the carbonate- and serpentine-group minerals. B isotopes within these ores exhibit a wide range of values, suggesting that B might have originated from multiple sources. The large variations in $\delta^{11}B$ values reflect the mixing of different B sources and B isotopic fractionation during the hydrothermal evolution of the Mn ores.

High δ11B values are predominant, and are generally caused by an interaction with an external B source, such as seawater. The protolith and low-grade ores represent primary sedimentary water-rock interactions and diagenesis, and the B is most likely derived from clays that occurred in equilibrium with seawater, as well as marine carbonates. The $\delta^{11}B$ values of the high-grade ores are as a result of secondary hydrothermal alteration processes, in which the Mn ore is enriched (by low temperature B-rich hydrothermal or meteoric fluid) and reworked. Due to the alteration and recrystallization of the B-hosted minerals, a large amount of B is incorporated into the mineral structure, as a result of quantitative scavenging of B from seawater, which results in the high B concentrations. Overall, HREE enrichment occurs within the Mn ores, with positive La and Eu anomalies and a strong negative Ce anomaly, indicating a seawater signature. The Ce appears characteristic of marine chemical sedimentary precipitates. The REE signature is similar to modern seawater, with a small presence of mid-ocean ridge-related hydrothermal components in the deeper, anoxic ambient seawater.

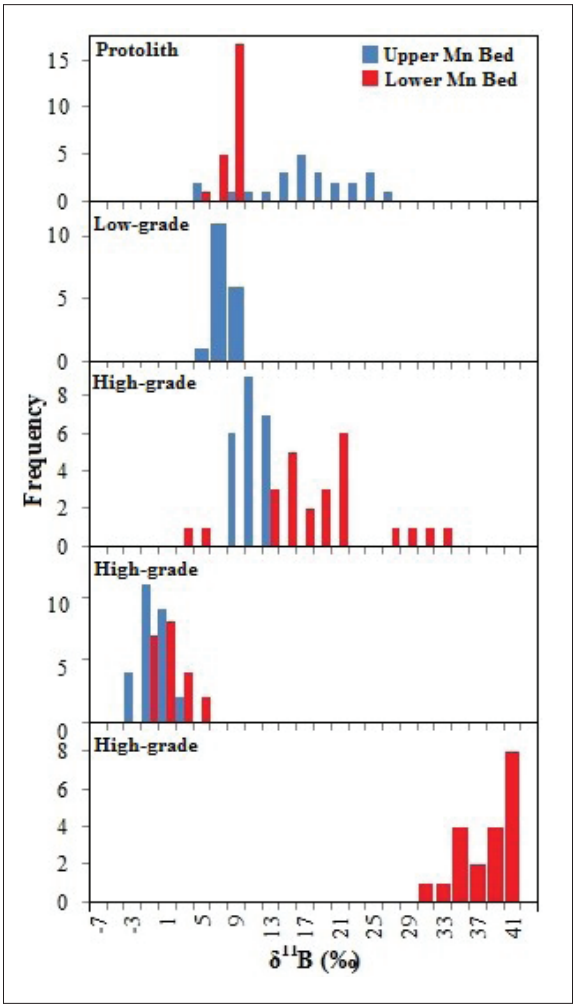

Figure 2. Comparative histograms of $\delta^{11}B$ values for the upper and lower Mn ore bodies from the KMD.

PROGRESSIVE MINERALOGICAL PHASE CHANGE OF THE LOW-GRADE, HIGH CARBONATE MANGANESE ORE OF THE SOUTHERN KALAHARI MANGANESE FIELD DURING HIGH TEMPERATURE X-RAY DIFFRACTION ANALYSIS.

Nick Vafeas and Fanus Viljoen

To date, there have been few studies on the mineralogical phase changes that occur within the manganese ore from the southern Kalahari Manganese Field (KMF) at high-temperatures under oxidative conditions. The low-grade manganese ore is well known for its high, 40-60 percent carbonate content, making it a prime subject for high temperature X-Ray diffraction (XRD) analysis.
20 to 50kg stock-piled ore samples from five separate low-grade mines were collected. The ore was then split to 10g samples and dry milled in preparation for analysis. Using the X-ray diffractometer housed at the University of Johannesburg, an XRD Analysis was conducted using incremental heating steps from 25˚C to 250˚, 500˚, 525˚, 550˚, 600˚, 625˚, 650˚, 700˚, 800˚, 900˚, 1000˚ and back to 25C˚. PANalytical's Highscore Plus software V4.1. was used in the Rietveld analysis.

A Scanning Electron Microscope (SEM) analysis was conducted on the stockpiled ore to establish the dominant mineral phases present prior to heating (Figure 1). Prior to heating the manganese ore comprised abundant kutnohorite and calcite diagenetic concretions and laminae with lesser amounts of hausmannite. The matrix of the ore comprised a fine intergrowth of kutnohorite and braunite I.

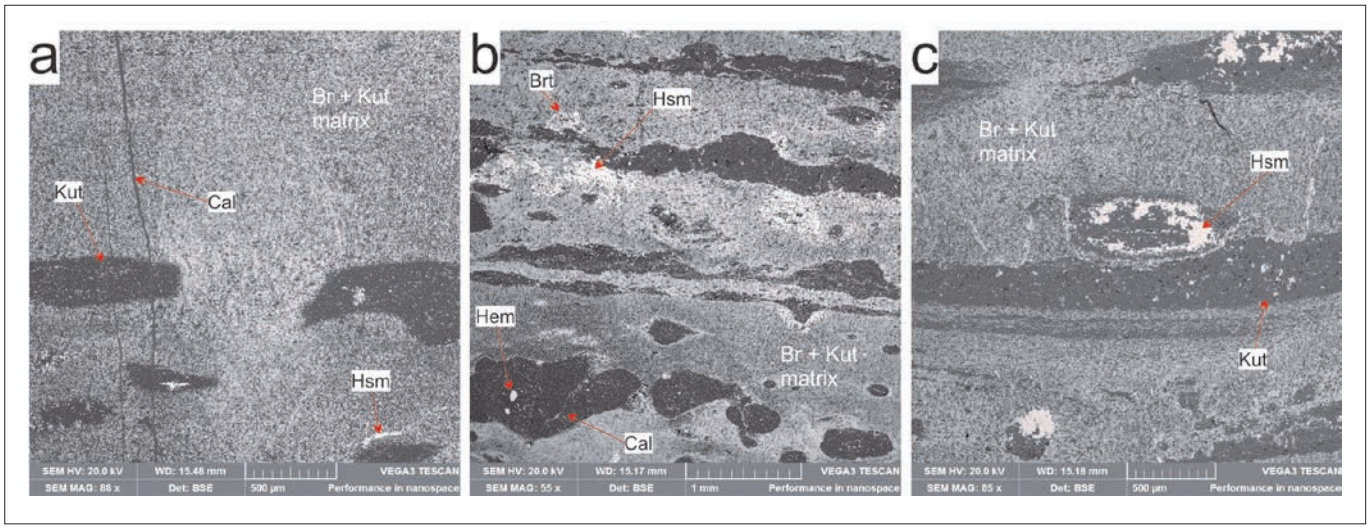

Figure 1. Back-scatter SEM images of the M (a), C(b) and Z (c) sub-zones from core samples. These three sub-zones represent the bulk composition of the stock-piled ore.

During high-temperature XRD analyses, carbonate peaks, including calcite and kutnohorite are shown to diminish due to oxidation and thermal decomposition (Figure 2) as follows:

$$CaMn^{2}(CO_3)_2 + ¼O_2 \rightarrow CaO + ½\ Mn^{3}{}_2O_3 + 2CO_2 \ldots \text{(Oxidation)}$$

And

$$CaCO_3 \rightarrow CaO + CO_2 \ldots \text{(Thermal Decomposition)}$$

By 650°C, all carbonate phases have been removed from the ore. Similarly, by 700°C, all pre-existing oxides i.e. braunite and hausmannite have been oxidised.

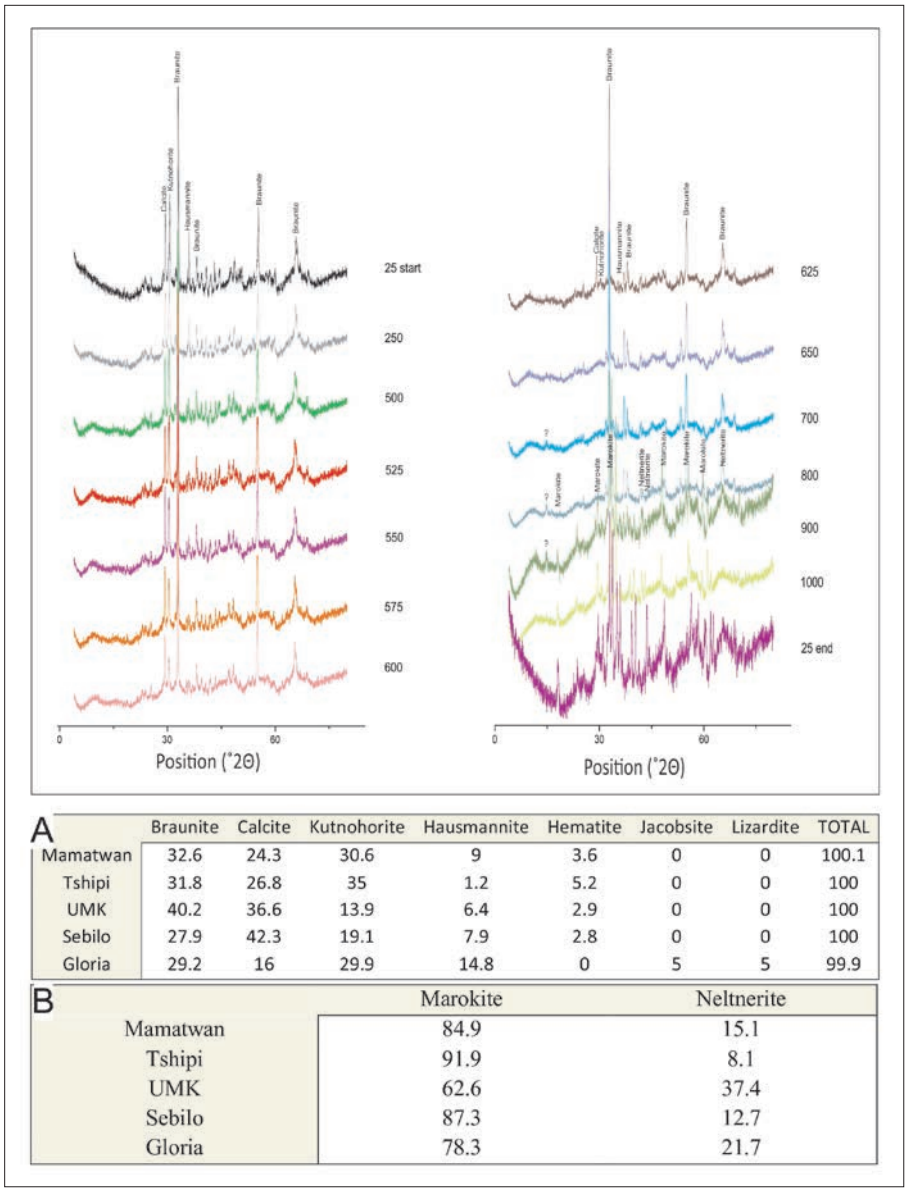

A

	Braunite	Calcite	Kutnohorite	Hausmannite	Hematite	Jacobsite	Lizardite	TOTAL
Mamatwan	32.6	24.3	30.6	9	3.6	0	0	100.1
Tshipi	31.8	26.8	35	1.2	5.2	0	0	100
UMK	40.2	36.6	13.9	6.4	2.9	0	0	100
Sebilo	27.9	42.3	19.1	7.9	2.8	0	0	100
Gloria	29.2	16	29.9	14.8	0	5	5	99.9

B

	Marokite	Neltnerite
Mamatwan	84.9	15.1
Tshipi	91.9	8.1
UMK	62.6	37.4
Sebilo	87.3	12.7
Gloria	78.3	21.7

Figure 2. High-temperature XRD spectra showing the incremental temperature increases and the effect on the peak intensities. The Rietveld Refinement results before (Table A) and after (Table B) heating are also given.

The resultant products of oxidation and thermal decomposition of the ore-bearing phases during the analysis, further react to produce a macroscopically homogenous mix of marokite and neltnerite. These final phases are seen to develop at a temperature of approximately 700°C. Whilst marokite only requires calcium and manganese to form, minor amounts of silica are required for the formation of neltnerite. This silica is derived from the oxidation and subsequent break-down of braunite. The neltnerite therefore correlates to the original braunite content of the primary ore sample.

ALTERATION FEATURES OF THE MN2-MANGANIFEROUS BED FROM THE ROOINEKKE IRON FORMATION, NORTHERN CAPE PROVINCE

Fanie Kruger

Apart from the larger deposits of manganese in the Kalahari Manganese Field, other (smaller) deposits in the Transvaal Supergroup do also exist, including the one at Rooinekke. The following description is quoted (Mineral Resources of SA, 1980):

"In the vicinity of Rooinekke, 70 km southwest of Postmasburg, low-grade supergene manganese deposits occur at various horizons in banded iron formation and flagstones near the top of the Koegas Formation. The ore is of a low grade, the Mn-content being about 35%, with Fe ranging from 25-27%".

A number of years back two deep holes were drilled immediately to the west of the old Rooinekke iron and manganese mine to obtain unweathered supergene enriched manganese ore. The SAR-4 borehole and its intersection with the stratigraphy is indicated in Figure 1:

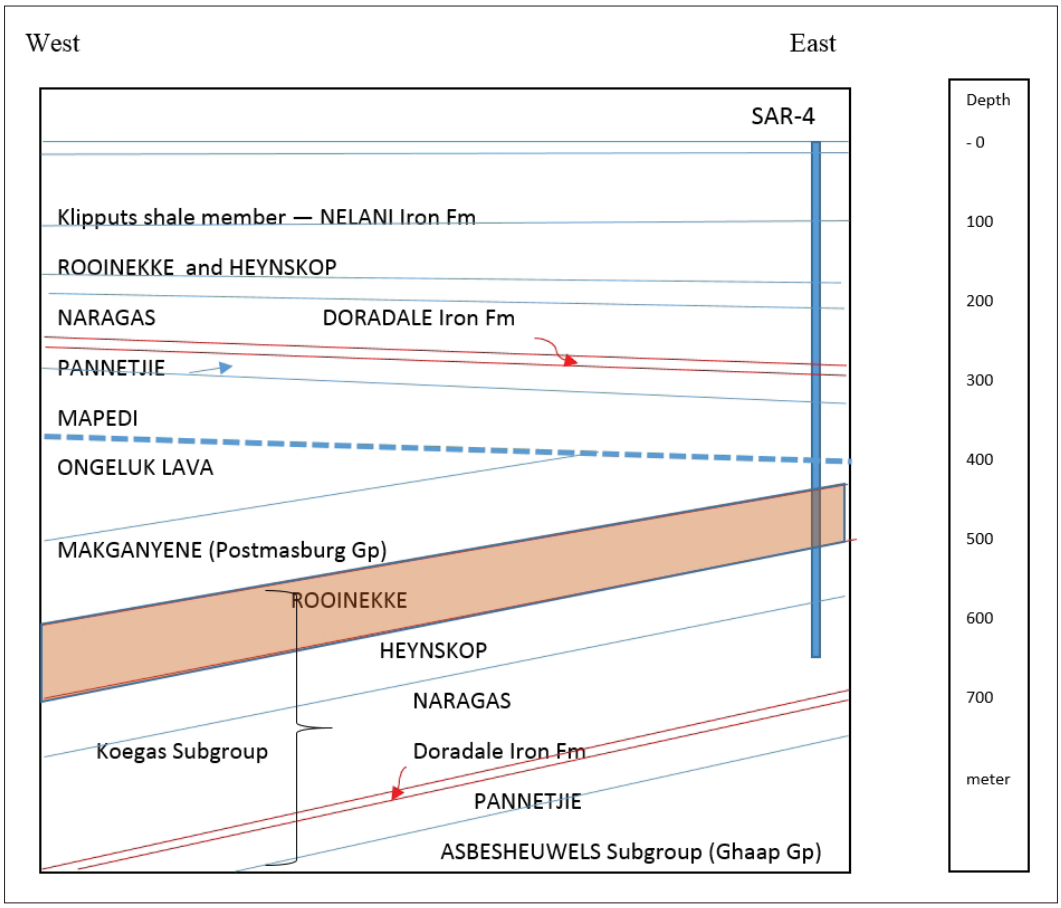

Figure1. Stratigraphic cross section — borehole SAR-4, intersecting members of the Koegas Subgroup and Postmasburg Group of the Transvaal Supergroup (diagram modified after Gutzmer and Beukes, Report January 2002).

Two manganese bearing layers were intersected in the Rooinekke Iron Formation, namely the shallower Mn-1 and deeper Mn-2 layer. Only the Mn-2 layer has been investigated in more detail at this stage to determine the mineral assemblages and other features that characterize the ore. It was soon realized that alteration of different kinds had a prominent effect.

Two major types of mineralization were determined, each with characteristic mineral assemblages. (See photo's with summary of mineral assemblages for each hereafter):

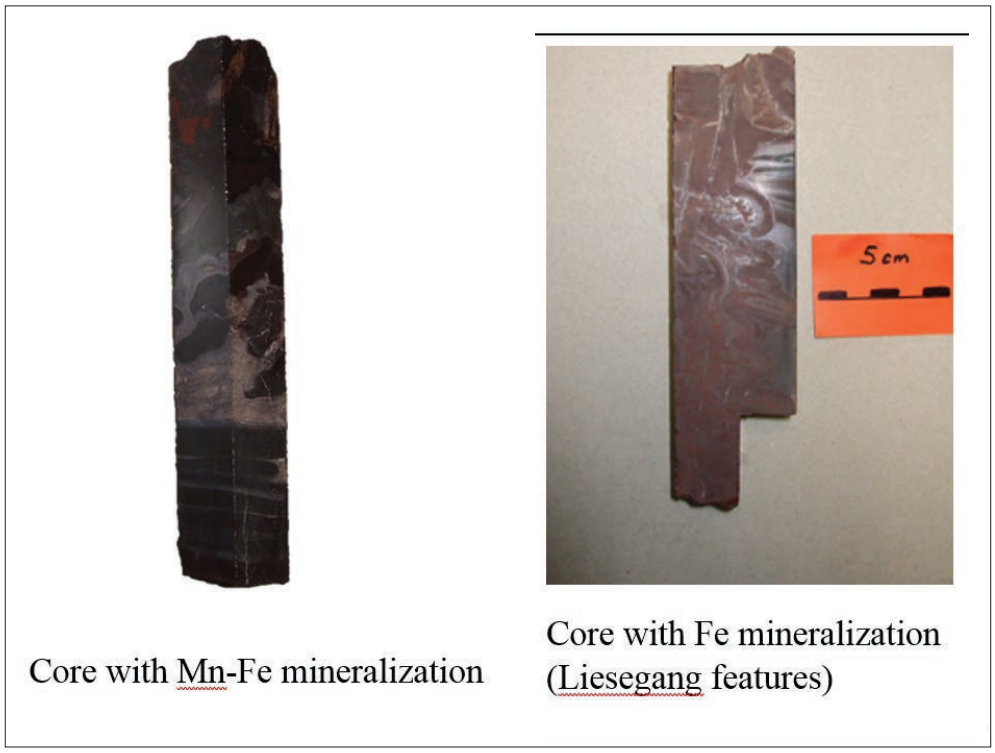

Fig 2. Macroscopic features present in portions of jacobsitic-tephroitic (left) and hematitic enriched cherty shale (right)), both with prominent Liesegang features.

Mn- and Fe-mineralization:

- Jacobsite ($MnFe_2O_4$) occurs as major mineral with subordinate tephroite (Mn_2SiO_4) in the darker Mn-rich zones, sometimes associated with anhydrite ($CaSO_4$), quartz and also bementite ($Mn_5Si_4O_{10}(OH)_6$).
- The lighter coloured zones are more silica rich, while tephroite is also present in lower quantities. Mn-chlorite, pennantite [$(Mn^{5+}+2Al)(Si_3Al)O_{10}(OH)_8$], was also identified and anhydrite is sometimes present in minor quantities, as well as small pockets of barite ($BaSO_4$).

Fe-mineralization:

- This material could have a very high Fe-content (hematite) in a mainly quartz matrix, with less feldspar/ chlorite and kutnohorite. The latter assemblage agrees to some extent with the mineral composition of a shale as protolith before ferruginization.

Alteration and veining

- Parts of the matrix is replaced in certain zones by carbonates, mainly kutnohorite and rhodochrosite
- Veins: Rhodochrosite appears more commonly in veins, while calcite occurs as an associated mineral. A variety of vein types (also bementite) were identified as late stage phenomena, but these can be complex and varied. Barite is quite often observed as an associated mineral.

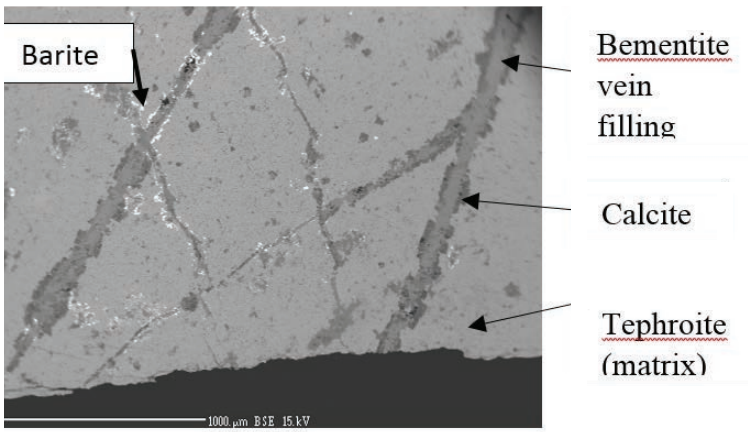

Fig. 3. Example of mineralization associated with veining in tephroite (Mn_2SiO_4) matrix (BSE-image)

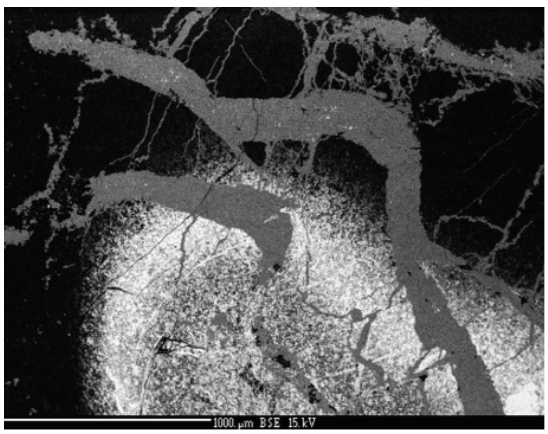

Fig. 4. Rhodochrosite ($MnCO_3$) invasive in a Liesegang dendrite, all in silica matrix (BSE-image)

PETROGRAPHY AND GEOCHEMISTRY OF THE PRE-MAPEDI "BOSTONITE" DYKES AND SILLS IN THE KALAHARI MANGANESE FIELD, NORTHERN CAPE PROVINCE

B. Fisah Monareng

Mafic dykes and sills intruding and affecting ore deposits are a well-known phenomenon around the world. The role played by magmatic hypogene fluids globally in the genesis of high-grade hematite ore is well-recognized. In the Northern Cape Province of South Africa, a series of intrusions have been emplaced in association with various sedimentary-hosted iron and manganese deposits. In the Kalahari Manganese Field (KMF) of the Northern Cape Province, the intrusions are referred to as "bostonites". These dykes and sills are pre-Mapedi in age and contact metamorphosed the ore resulting in a general decrease of ore quality.

The main aim of the study is to characterize the "bostonite" dykes and sills more extensively than previously by determining whether they are related to the same magmatic event and by evaluating the style of alteration that affected the "bostonite" chemistry. Comparison with the previously studied "bostonites" and the well-known large igneous provinces of the Kaapvaal Craton was made to determine the comagmatism. A paleoweathering profile on the mafic intrusive rocks (so-called "Bostonite") was intersected during the exploration drilling of the Avontuur Deposit and provides an opportunity to describe the behavior of major, trace and REE in weathered rock relative to the unweathered parent rock. This weathering profile developed below the basal Gamagara/Mapedi unconformity overlying the iron formation (IF) and manganese formation (MF) of the Hotazel Formation and marks the base of Olifantshoek group. The "bostonites" of the Main Kalahari Deposit are composed predominantly of pyroxenes (diopside and augite), plagioclase (labradorite and andesite), Fe-Ti oxides (ilmenite, titanomagnetite) and minor rutile. The "bostonites" of the Avontuur Deposits, on the other hand, are composed predominantly of pyroxene (augite), plagioclase (albite) and Fe-Ti oxides (ilmenite, titanomagnetite, titanite).

Based on the geochemistry, "bostonites" of both the Main Manganese and Avontuur Deposits are characterized by low Mg# indicating an evolved nature of the magma, as well as low Cr, Co and Sc signifying fractionation of the mafic minerals within the magma chamber. These mafic intrusives are characterized by negative Sr, Nb and Ta anomaly and positive K and Pb anomalies on the trace element spider diagram. The "bostonites" of both the Main Kalahari and Avontuur Deposits represent plate basalts.

Based on the weathering profile with an increase in weathering, a slight loss of silica and an intense decrease in alkali and alkali earth elements (Mg, Ca and Na) is noted. Potassium behaves differently from other alkali and alkali earth metals as it increases dramatically reaching a maximum of 245 %. The chemical indexes of alteration (CIA) values are typical of a warm and humid climate with chemical weathering, and the Ce anomalies suggest oxidative weathering.

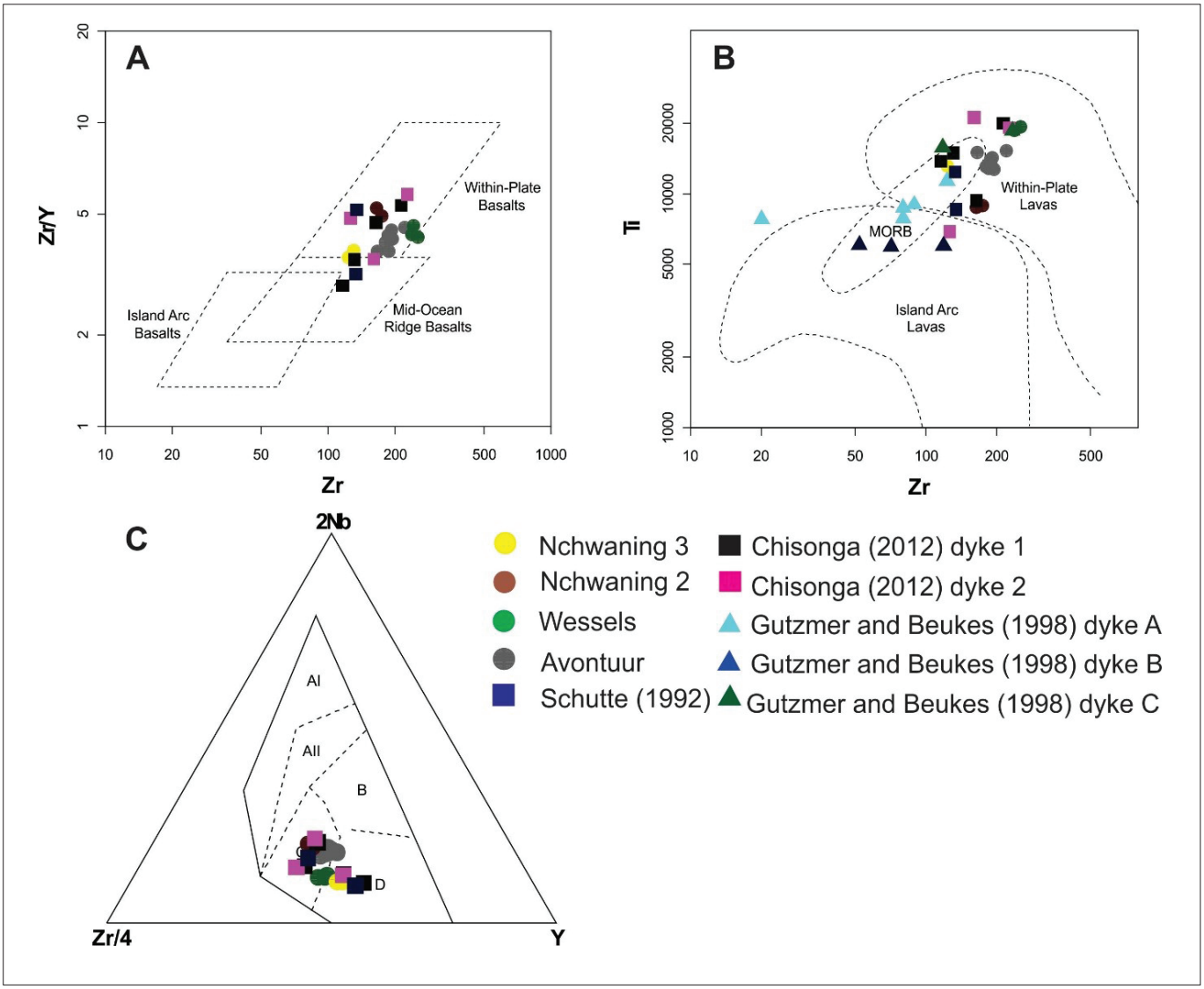

Figure 1. Tectonic discrimination diagrams for the "bostonites" sills and dykes of both the Main Kalahari Manganese Deposit and Avontuur Deposit compared with the previously studied "bostonites": A) Zr-Zr/Y of Pearce and Norry (1979); B) Zr-Ti of Pearce and Cann (1973) and C) Zr/4-2Nb-Y of Meschede (1986).

Meschede, M. (1986). A method of discriminating between different types of mid-ocean ridge basalts and continental tholeiites with the Nb-Zr-Y diagram. Chemical Geology, 56, 207-218.

Pearce, J.A. and Cann, J.R. (1973). Tectonic setting of basic volcanic rocks determined using trace element analyses. Earth and Planetary Science Letters, 19, 290-300.

Pearce, J.A. and Norry, M.J. (1979). Petrogenetic implications of Ti, Zr, Y, and Nb variations in volcanic rocks: Contributions to Mineralogy and Petrology, 69, 33-47.

PETROGENESIS OF NAMAQUALAND RARE ELEMENT PEGMATITES: ANATECTIC OR RESIDUAL?

Christophe Ballouard, Marlina Elburg, Sebastian Tappe, Mike Knoper

Pegmatites are typically coarse grained (> 2 cm) felsic magmatic rocks, occurring as irregular dykes or lenses. Most are barren but others, called rare element pegmatites, contain lithium (Li), cesium (Cs), tantalum (Ta), beryllium (Be), tin (Sn), niobium (Nb), yttrium (Y), fluorine (F), rare earth elements (REE), thorium (Th) and/or uranium (U)-bearing minerals and have economic importance. Two main families of rare element pegmatites exist: NYF pegmatites, of metaluminous to slightly peraluminous composition, are characterized by Nb, Y, F enrichment whereas LCT pegmatites are highly peraluminous and enriched in Li, Cs and Ta (Černý and Ercit, 2005). LCT pegmatites are generally interpreted as the result of partial melting of middle to upper crustal rocks whereas lower crustal, mantle and hybrid origins have been proposed for NYF pegmatites (Černý and Ercit, 2005).

Despite decades of research, the origin of rare element pegmatites is still poorly understood. Although many workers (e.g. Černý and Ercit, 2005, London, 2008) believe that they are the product of extreme granitic differentiation ('residual pegmatites'), the common absence of spatially, temporally or geochemically associated granites casts doubt on this scenario (e.g. Deveaud et al., 2015). However, the extreme enrichment in rare elements is more difficult to explain if the pegmatites form by direct partial melting ('anatectic pegmatites'). We propose to address these questions by studying the 450 km long northern Namaqualand pegmatite belt, which intruded at the end of the Namaqua orogeny (Fig. 1) – (Thomas et al., 1994). The rare element pegmatites of this belt transect different crustal terranes, their intrusion significantly postdates high-grade metamorphism and no contemporaneous granitic intrusions are exposed nearby, thus posing problems for both the residual and anatectic scenarios. Zonality exists in the pegmatite belt, with lithium-cesium-tantalum (LCT) pegmatites occurring in the west and east, and niobium-yttrium-fluorine (NYF) pegmatites in the middle (Hugo, 1970; Schutte, 1972). Preliminary studies of the NMC pegmatites shows that they were emplaced in strike-slip deformation setting between ca. 1040 and 960 Ma, after the peak of metamorphism in the region (Lambert et al., 2013; Doggart et al., 2017).

Structural studies, as well as sampling of pegmatites, host rocks and potentially genetically related rocks, will be performed to characterize the tectono-magmatic context of emplacement of the pegmatites. Intrusive ages will be determined by LA-MC-ICPMS U-Pb analysis on selected minerals (zircon, monazite, apatite columbite-tantalite). Stable (O, Li) and radiogenic (Sm-Nd, Rb-Sr, U-Pb) isotope analyses of whole rocks and minerals, in combination with major and trace element studies, will help to characterize their source, and document differentiation and host rock interaction processes. The data from the different aspects of the project will be integrated to formulate a comprehensive petrogenetic model for the pegmatite belt.

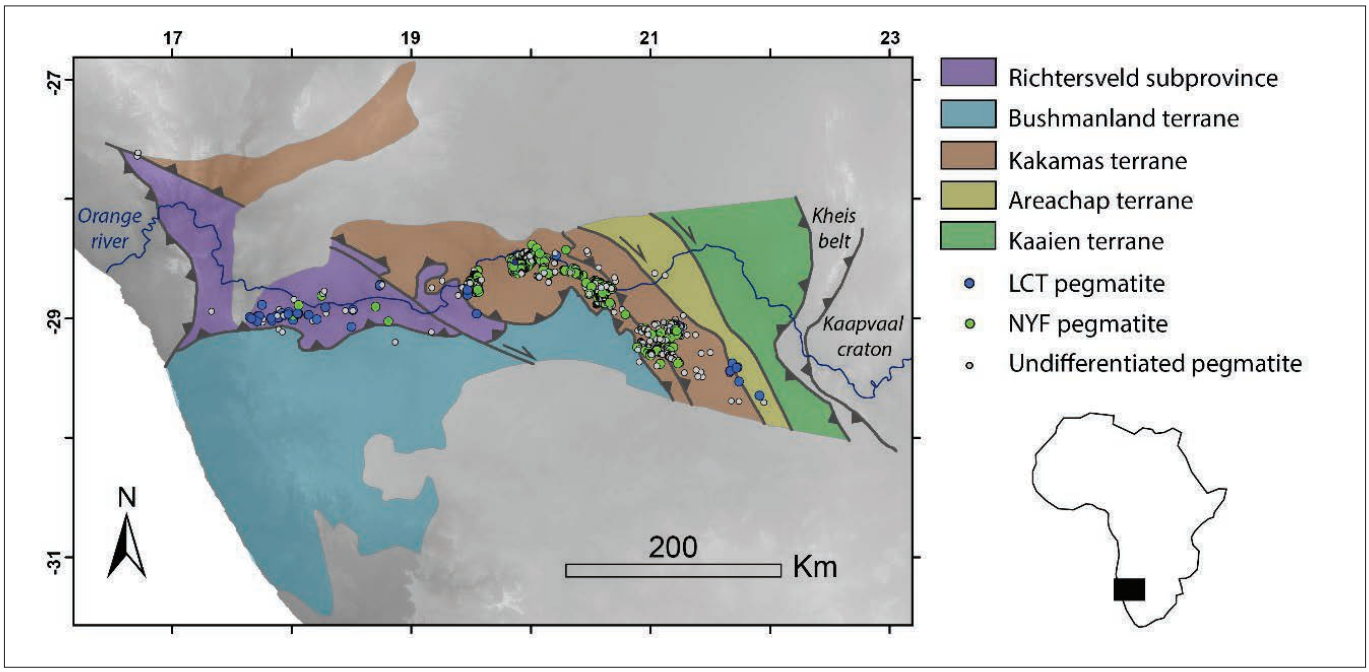

Figure 1: Terrane map of the Namaqualand province showing the location of rare element pegmatites. Pegmatite typology after Hugo (1970) and Schutte (1972).

Černý, P., Ercit, T.S., 2005. The Classification of Granitic Pegmatites Revisited. Can. Mineral. 43, 2005–2026.
Deveaud, S., Millot, R., Villaros, A., 2015. The genesis of LCT-type granitic pegmatites, as illustrated by lithium isotopes in micas. Chem. Geol. 411, 97–111.
Doggart, S.W., Buick, I., Frei, D., Lana, C., Macey, P., Lambert, C.W., 2017. Monazite U/Pb geochronology and geochemistry of the orange river pegmatite belt. The 9th Igneous and metamorphic studies group meeting. Glenburn Lodge, Muldersdrift.
Hugo, P.J., 1970. The pegmatites of the Kenhardt and Gordonia districts, Cape Province. Memoir of Geological Survey of South Africa 58.
Lambert, C.W., 2013. Granitic melt transport and emplacement along transcurrent shear zones: Case study of the Pofadder Shear Zone in South Africa and Namibia. Master thesis, Stellenbosch University.
London, D., 2008. Pegmatites. Can. Mineral. Special, Publication 10 p. 363
Schutte, P.J., 1972. The pegmatites of the Kenhardt and Gordonia districts, Cape Province. Memoir of Geological Survey of South Africa 60.
Thomas, R.J., Agenbacht, A.L.D., Cornell, D.H., Moore, J.M., 1994. Kibaran (Mid-Proterozoic) Metallogeny in Central and Southern AfricaThe Kibaran of southern Africa: Tectonic evolution and metallogeny. Ore Geol. Rev. 9, 131–160.

Magmatism and Igneous Petrology

THE PETROGRAPHY AND GEOCHEMISTRY OF THE LAYERED MOLOPO FARMS COMPLEX, SOUTH AFRICA: A PRELIMINARY REPORT.

Peace Hlungwani and Marlina Elburg

The Paleoproterozoic layered Molopo Farms Complex (MFC) is a mafic-ultramafic layered intrusion. Unlike the nearby mafic-ultramafic Bushveld Complex (BC), the Molopo Farms Complex has no surface exposure. An association of the MFC with the BC has been proposed (Day, 1984; Thomas and Bowen, 1986; Prendergast, 2012), but the data supporting this assumption has up to now been limited. The present petrographical and geochemical study of the MFC is aimed to provide a comparison between the two complexes (MFC and BC) and complements the study by Ravhura (2017, see below). The study and comparison includes the petrography (Fig. 1), whole rock geochemistry, mineral chemistry (Fig. 2), Rb-Sr isotope analyses on plagioclase (Fig. 3), oxygen isotopes on quartz separates and an experiment on U-Pb dating of apatite (Fig. 4).

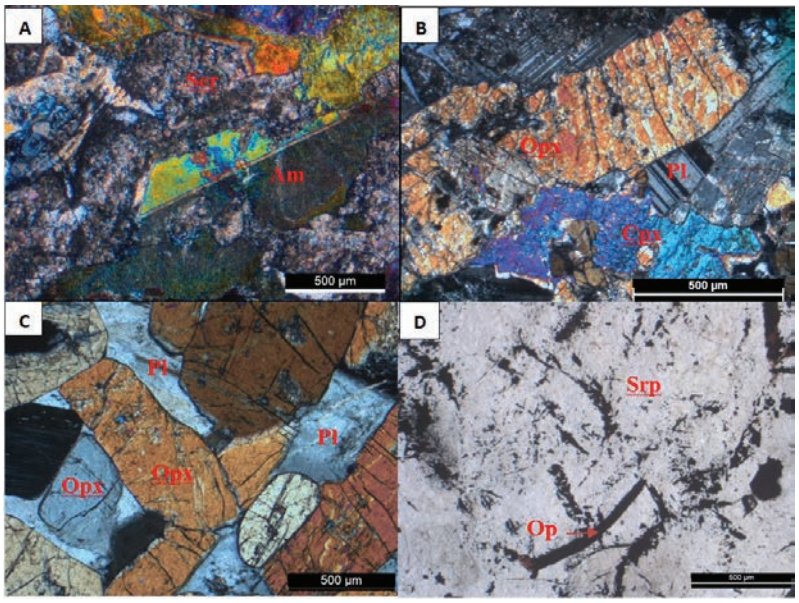

Figure 1: Representative micrographs for different boreholes, showing the dominant minerals and textures. Am-amphibole, Cpx-clinopyroxene, Opx-orthopyroxene, Ser-sericite, Pl-plagioclase, Srp-serpentine and Op-opaque minerals. A) MOM2 is a coarse-grained quartz-gabbro that is highly altered, and mainly consists of Ser and Am. B) MOM3 gabbronorite is partially altered, with Opx, Cpx and Pl as the main minerals. C) MOM8 feldspathic pyroxenite is a coarse grained, fresh sample with Opx and Pl. It shows a cumulus texture, where Opx is the cumulate mineral and Pl is the interstitial mineral. D) MOM7 serpentinite is highly altered, with Srp and Op pseudomorphing olivine.

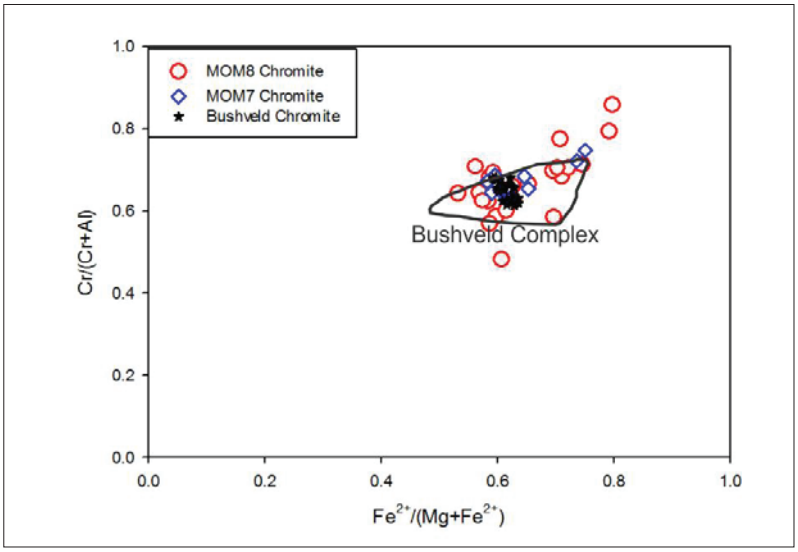

Figure 2: Plot of Fe# vs Cr# of chromite from the MFC (MOM7 and MOM8), compared to literature data for chromite from the BC (McCall, 2016; Rollinson et al., 2010; Yang and Gilbert, 2014). There is an overlap of the MFC data with the BC literature data and the chromite of the MFC plots inside the solid line which represents the chromite field for the BC.

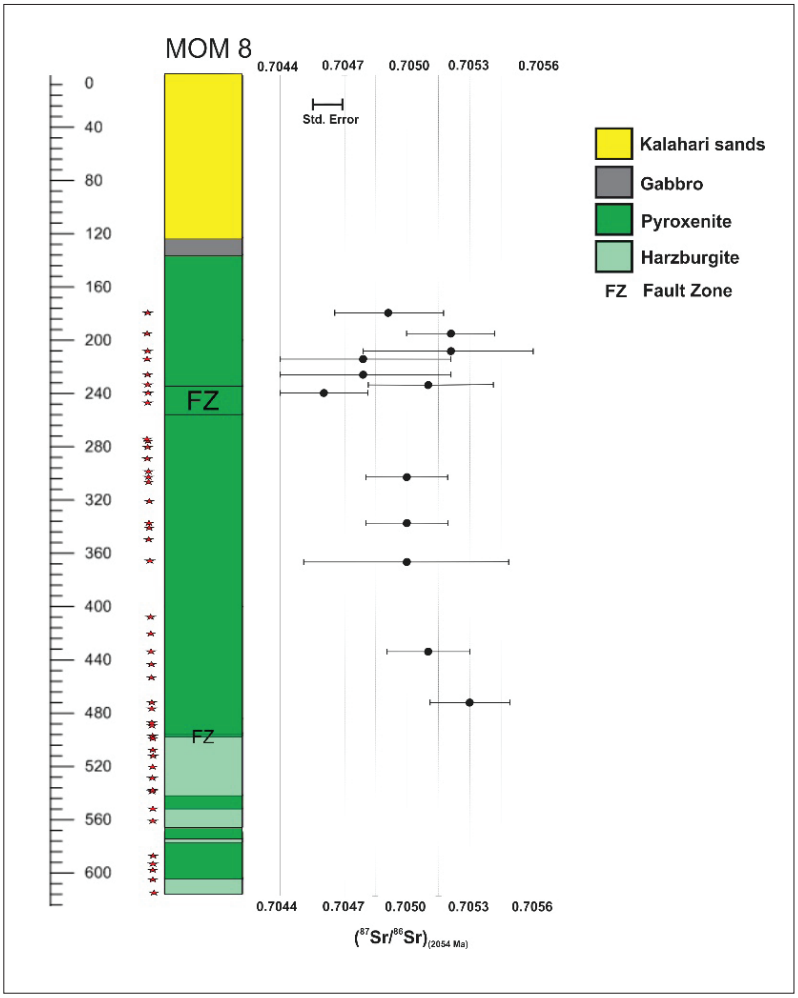

Figure 3: $^{87}Sr/^{86}Sr$ ratios at 2054 Ma of plagioclase in feldspathic pyroxenite plotted against a simplified stratigraphic column of MOM8. The data was obtained by LA-MC-ICPMS at the UJ isotope laboratory. The $^{87}Sr/^{86}Sr$ ratios range from 0.7044-0.7056, which is within range of the lower parts of the BC (Lower and Critical Zone).

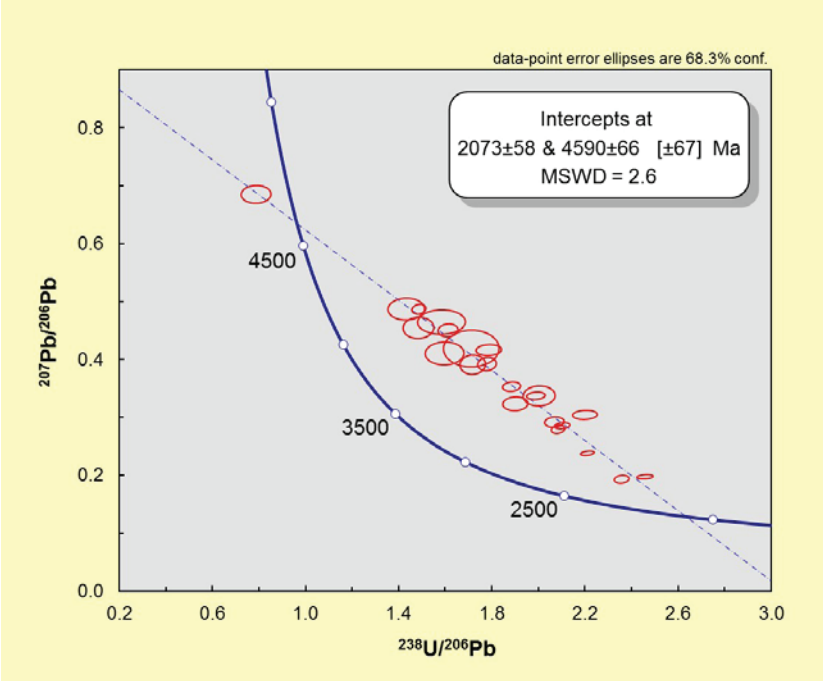

Figure 4: The Tera-Wasserburg diagram for U-Pb analyses of 22 apatite grains. The grains were analyzed by the LA-MC-ICPMS at the UJ isotope laboratory. The data appear highly discordant because of a high common Pb content, but the lower intercept is at 2073 ± 58 Ma.

The petrography shows that the MFC samples have been affected by alteration (Fig. 1), hence the petrographic information obtained is not conclusive when compared to the BC. However, the geochemistry shows that the two complexes are similar with regards to mineral chemistry, $^{87}Sr/^{86}Sr$ isotope ratios and oxygen isotope on quartz separates (not shown). The $\delta^{18}O$ results obtained on quartz separates of the quartz gabbro samples are 8.2 ‰ and 8.62 ‰ V-SMOW. These values are similar to that of Harris *et al.* (2005) for BC quartz at 8.7‰.

The results of the apatite dating experiment show the potential of the LA-ICP-MS method for this mineral, in spite of the large amount of common Pb present. It is within error of a baddeleyite U-Pb age of 2052±16 Ma for the Molopo Farms Complex (Ravhura, 2017; see below) and also with the most recent ages for the Bushverld Igneous Copmplex: 2057 ± 7.8 Ma from apatite (Wohlgemuth-Ueberwasser et al., 2017), and 2054.89 ± 0.37 Ma from zircon (Zeh et al., 2015).

Day, N.D (1984). Unpublished Report, Anglo American Prospecting Services (PTY) limited.
Harris, C. et al. (2005). Journal of Petrology 46, 579-601.
McCall, M.J. (2016). MSc Thesis, Stellenbosch University.
Prendergast, M.D. (2012). South African Journal of Geology 115, 77-89.
Ravhura, L.R. (2017) This volume
Rollinson, H.R. et al. (2010). *In* The Evolving Continents: Understanding the process of continental growth. Geological Society, London, special publications 338, 197-212.
Thomas, C.M., and Bowen, E.A. (1986). Independent geologist's report.
Wohlgemuth-Ueberwasser C.C. et al. (2017). American Mineralogist 102, 571-579.
Yang, X.M. and Gilbert, H.P. (2014). *In* Report of Activities 2014, Manitoba Geological Survey. p. 32-48.
Zeh, A. et al. (2015). Earth and Planetary Science Letters. 418, p. 103–114.

A MULTI-PRONGED APPROACH TO CONSTRAIN THE AGE OF THE MOLOPO FARMS LAYERED IGNEOUS COMPLEX, NORTHERN CAPE PROVINCE AND SOUTHEASTERN BOTSWANA

Livhuwani G. Ravhura

This ongoing study focuses on the major and trace element geochemistry and geochronology of the Molopo Farms Layered Igneous Complex (MFC), situated in the Northern Cape Province and south eastern Botswana, and complements the work of Hlungwani and Elburg (2017, see above). The MFC is thought to have intruded the sedimentary succession of the Paleoproterozoic Transvaal Supergroup. As the Complex is entirely covered by Cenozoic sediments of the Kalahari Formation, it can be studied only via intersection in exploration drill core and geophysical data.

Unlike other layered complexes e.g Bushveld Complex, Stillwater Complex, etc the MFC has no geochemical framework studies. At present, the available age is the poorly constrained Rb-Sr age of 2044±24Ma and for that reason and the fact that it is a layered igneous complex it has been correlated with Bushveld Complex. However, this age and correlation are as yet poorly constrained. This study provides additional data on the geochemical comparison of some of the igneous rocks, a baddeleyite age from the complex itelf and detrital zircon age data on the sedimentary country rocks.

The rocks of the MFC are medium to course grained gabbro, serpentinite, pyroxenite that intrude into sedimentary host rocks. The mafic igneous rocks of the MFC are dominantly sub-alkaline tholeiitic in composition and the magma is characterized as basaltic andesitic. The geochemical signature of the MFC is compared with other magmatic event (Bushveld Complex, Moshaneng dykes, Post Waterberg sills, Umkondo sills and Karro sills). The MFC is characterized by an enrichment in LREE relative to the HREE and shows negative Eu, Nb(Ta), P, Ti and positive K, Pb and U anomalies. This geochemical signature compares well with that of the B1-magma of the Bushveld Complex.

A U-Pb 2052±16 Ma age has been obtained from baddeleyite in a gabbro, yielding the emplacement age of the MFC. This age is within error with the Bushveld age (2054.4±1.3Ma, Zeh et al., 2015).The maximum age of sedimentary country rock into which MFC intrudes has been constrained using detrital zircon. The youngest concordant U-Pb ages obtained are between 2018±39 and 2276±19Ma. That could support correlation with sedimentary rocks of the Pretoria Group of the Transvaal Supergroup. Some of the quartzites, however, contain zircons with slightly younger apparent ages, and could be correlative to lower strata of the Waterberg Group.

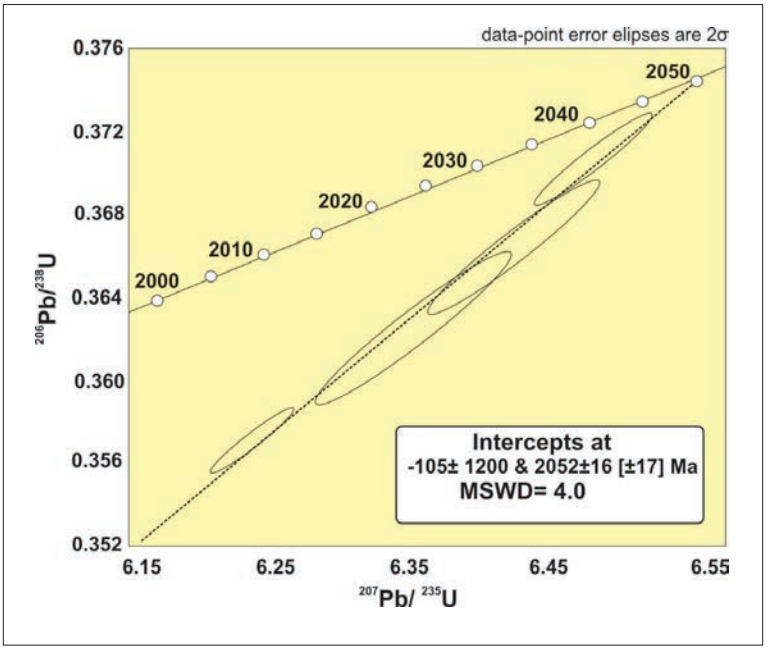

Figure 1. Concordia age diagram obtained for sample MOM2_139-142, showing an upper intercept and lower intercept ages at 2052±16- and -105±1200Ma respectively. MSWD stand for mean square of weighted deviates.

Hlungwani, P. and Elburg, M. (2017), this Volume (see above)
Zeh, A. et al. (2015). Earth and Planetary Science Letters. 418, p. 103–114.

PALEOMAGNETIC STUDY OF JURASSIC DYKES FROM WESTERN DRONNING MAUD LAND, ANTARCTICA

Johan O'Kennedy, Michael Knoper, Geoff Grantham, Michiel de Kock and Georgy Belyanin

Correspondence between the geology of southern African and western Dronning Maud Land (Antarctica) has been previously established (Barton et al., 1987; Arndt et al., 1991; Jacobs et al., 2003; Jones et al., 2003; Marschall et al., 2010). Nonetheless, the precise fit between Antarctica and Africa has seen little consensus. A wide range of different methods has been used to reconstruct configurations (e.g., Grantham et al., 2008; Hastie et al., 2013; Kristofferson et al., 2014), but there is a lack of paleomagnetic investigations based on Jurassic dykes. That is the focus of this study - to test various Gondwana reconstructions of Antarctica and Africa using paleomagnetic methods together with precise ArAr dating.

The Jurassic dykes of western Dronning Maud Land (WDML) have been sampled as orientated samples during the 2016/2017 austral summer field season. Paleomagnetic poles from these dykes from WDML will be compared to existing paleomagnetic poles from southern Africa. Analyses would be done by using both the SQUID (superconducting quantum interference devices) and the spinner magnetometers. Age determinations will be made by using the Ar-Ar dating method. This technique involves irradiating the samples at the Pelindaba Nuclear Research Centre, followed by measurements using the UJ noble gas laboratory. All the measuring instruments used (i.e., SQUID, spinner and noble gas spectrometer) are at the University of Johannesburg.

Preliminary Ar-Ar results indicate that the dykes from WDML have a range of ages from ~160 to 200 Ma, with the most common age of about 180 Ma.

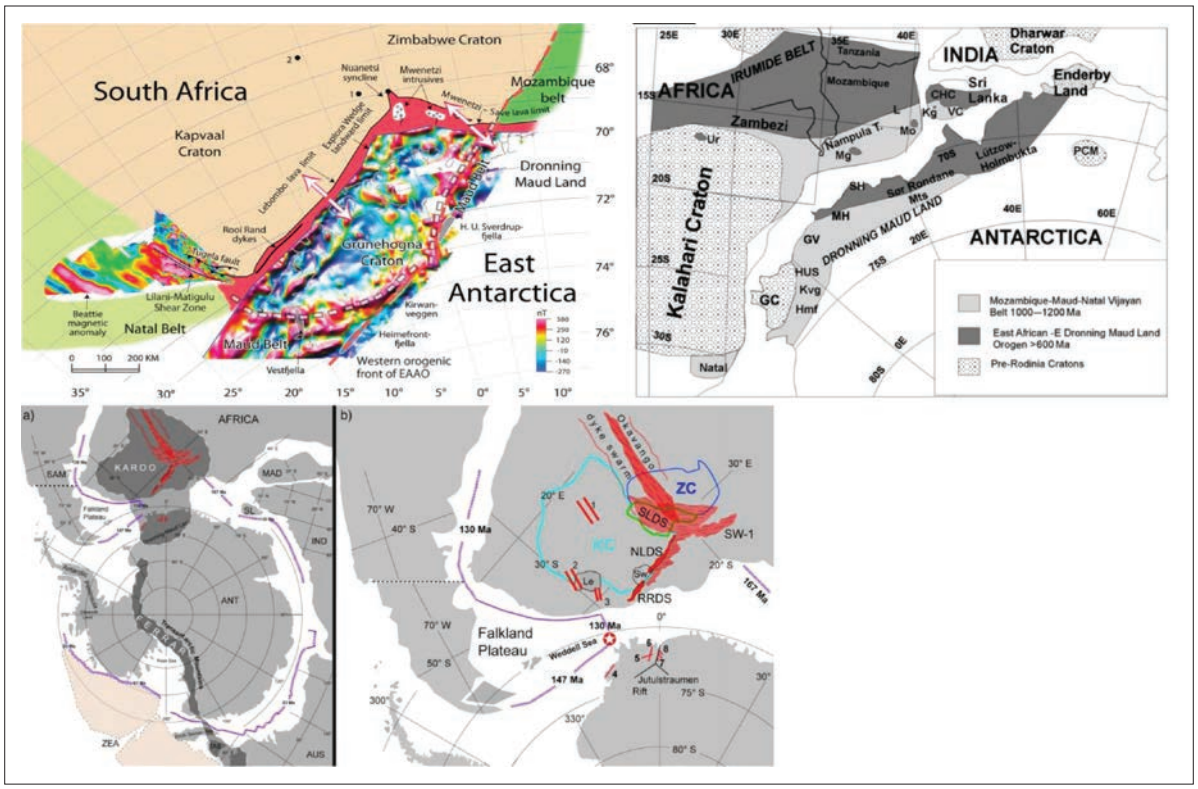

Figure 1: Examples of Gondwana configurations that will be tested for the purpose of this study. They include; Kristoffersen et al 2014 (A), Grantham et al 2008 (B) and Hastie et al 2013 (C).

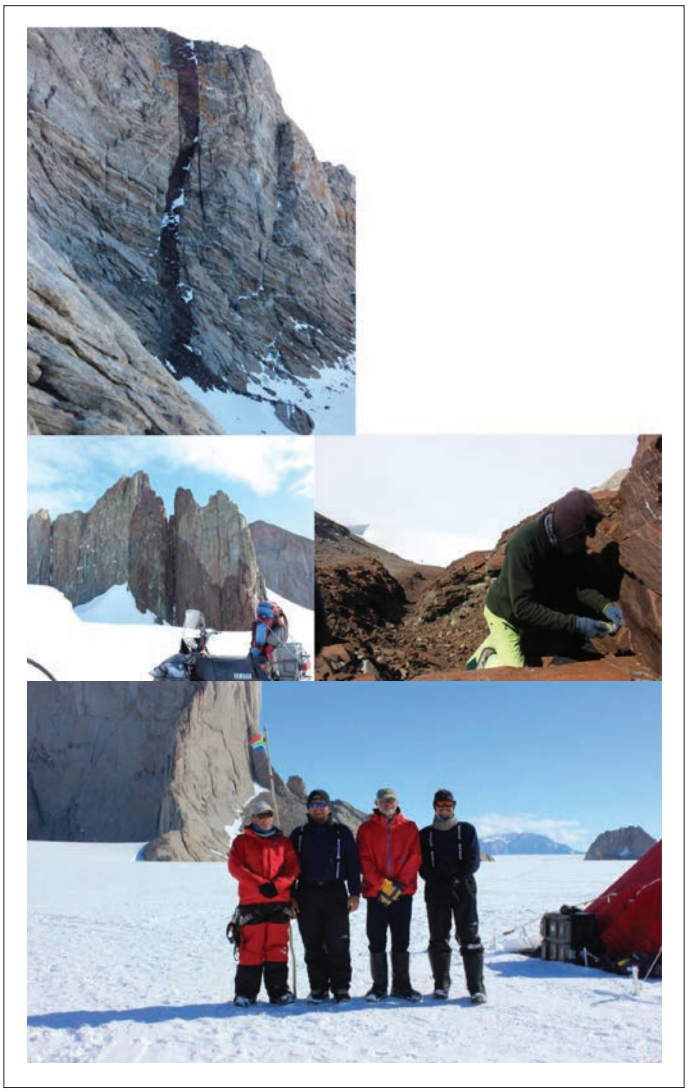

Figure 2: Clockwise from top left; Jurassic dyke intruding highly metamorphosed gneiss of the Maud Belt; measuring orientated block sample that will be used for this thesis; field team photo (from left to right - Herman van Niekerk, Riaan Bothma, Michael Knoper and me); mafic dyke with a snowmobile in the foreground.

Arndt, N.T., Todt, W., Chauvel, M., Tapfer, M., and Weber, K. (1991). U-Pb zircon age and Nd isotopic composition of granitoids, charnockites and supracrustal rocks from Heimefrontfjella, Antarctica. Geologisches Rundschau, vol. 80, pp. 759-777.

Barton, J.M., Jr., Klemd, R., Allsopp, H.L., Auret, S.H. and Coperthwaite, Y.L. (1987). The geology and geochronology of the Annandagstoppane granite, western Dronning Maud Land, Antarctica. Contributions in Mineral Petrology, vol. 97, pp. 488-496.

Grantham, G.H., Macey, P.H., Ingram, B.A., Roberts, M.P., Armstrong, R.A., Hokada, T., Shiraishi, K., Jackson, C., Bisnath, A., Manhica, V. (2008). Terrane correlations between Antarctica, Mozambique and Sri Lanka; comparisons of geochronology, lithology, structure and metamorphism and possible implications for the geology of southern Africa and Antarctica. Geological Society, London, Special Publication, vol. 308, pp. 91-119.

Hastie, W.W., Watkeys, M.K. and Aubourg, C. (2013) Magma flow in dyke swarms of the Karoo LIP: Implications for the mantle plume hypothesis, http://dx.doi.org/10.1016/j.gr.2013.08.010

Jacobs, J., Fanning, C.M., and Bauer, W. (2003). Timing of Grenville-age vs. Pan African medium- to high grade metamorphism in western Dronning Maud Land (East Antarctica) and Significance for correlations in Rodinia and Gondwana. Precambrian Research, vol. 125, pp. 1-20.

Jones, D.L., Bates, M.P., Li, Z.-X., Corner, B. and Hodgkinson, G. (2003). Paleomagnetic results from ca. 1130 Ma Borgmassivet intrusions in the Ahlmannryggen region of Dronning Maud Land, Antarctica, and tectonic implications. Tectonophysics, vol. 375, pp. 247-260.

Kristofferson, Y., Hofstede, C., Diez, A., Blenkner, R., Lambrecht, A., Mayer, C. and Eisen, O. (2014). Reassembling Gondwana: A new high quality constraint from vibroseis exploration of the sub-ice shelf geology of the East Antarctic continental margin. Journal of Geophysical Research: Solid Earth. DOI: 10.1002/2014JB011479.

Marschall, H.R., Hawkesworth, C.J., Storey, C.D., Dhume, B., Leat, P.T., Meyer, H.-P. and Tamm-Buckle, S. (2010). The Annandagstoppane Granite, East Antarctica: Evidence for Archaean Intracrustal Recycling in the Kaapvaal–Grunehogna Craton from Zircon O and Hf Isotopes. Journal of Petrology, vol. 51. pp. 2277-230

DISCOVERY OF AN ORANGEITE MAGMATIC EVENT IN THE CENTRAL KALAHARI: IMPLICATIONS FOR THE ORIGIN OF SOUTHERN AFRICAN KIMBERLITES

Marylou Vinès, Sebastian Tappe,*, Andreas Stracke[1], Allan Wilson[2], Andrew Rogers[3]

[1] Westfälische Wilhelms-Universität Műnster, Germany, [2] University of the Witwatersrand, South Africa
[3] Petra Diamonds South Africa (Pty) Ltd

Southern Africa hosts more than 1,600 kimberlite bodies, and over 75% of these fall within a 250 to 50 Ma age range. These Mesozoic-Cenozoic kimberlites have Group-1 and Group-2 compositional affinities, with occurrences of both groups providing significant primary diamond deposits. While Group-1 kimberlites represent a relatively homogenous type of CO_2- and H_2O-rich ultramafic magma in cratonic regions worldwide (Kjarsgaard et al., 2009), Group-2 kimberlites are compositionally more diverse potassic rocks that are confined to the Kaapvaal craton with emplacement ages between 200-110 Ma (Mitchell, 1995). Most models proposed for the origin of Group-1 kimberlites suggest sublithospheric depleted upper mantle sources (Tappe et al., 2017), whereas the compositions of Group-2 kimberlites require long-term enriched sources (Smith et al., 1985; Becker and Le Roex, 2006), with cratonic mantle lithosphere providing a suitable substrate to generate these H_2O-rich potassic magmas. The complexity of Group-2 kimberlites is consistent with the heterogeneous nature of the Kaapvaal craton root (Giuliani et al., 2015), and some authors emphasized strong petrogenetic links to olivine lamproites and ultramafic lamprophyres from cratons worldwide (Tappe et al., 2008). Group-2 kimberlites may therefore be interpreted as the magmatic expression of metasomatized mantle lithosphere beneath the Kaapvaal craton. Within such a model each craton produces its own compositional 'flavour' of ultramafic potassic magmatism due to the differences in composition, style, and timing of lithospheric mantle enrichment. The re-introduction of the term 'orangeite' for Group-2 kimberlite (Mitchell, 1995) reinforced the fact that these often diamond-bearing rocks differ significantly from archetypal kimberlites and, thus, they should be treated separately within models that seek to explain volatile-rich mantle-derived magmatism on thick continental shields.

The KX36 kimberlite pipe was discovered in 2008 during geophysical surveying of the central Kalahari in Botswana (Rogers et al., 2013). The pipe represents a ~5 ha large magmatic body that is covered by 80 m of Kalahari Group sedimentary overburden. The KX36 kimberlite pipe cuts through 400 m of Karoo Supergroup basaltic lava, and the kimberlite magma has locally entrained up to 10-20 vol% of basalt wall-rock, as well as some minor granitoid basement. On the basis of stratigraphy, the KX36 kimberlite pipe was emplaced between 180 and 50 Ma. The nearest known kimberlite occurrences are the Gope cluster some 60 km to the NW and the highly economic Orapa field some 250 km to the NNE of KX36, with kimberlite pipe emplacement ages between 115 and 80 Ma (Griffin et al., 2014). However, our first U/Pb perovskite age results for two magmatic kimberlite units within the KX36 pipe indicate magma emplacement at the NW margin of the Kaapvaal craton between 160 and 140 Ma. The robustness of these preliminary results is currently tested by additional analyses, also including an alternative analytical method.

Two main units, 'black' and 'green' kimberlite, can be distinguished within the KX36 pipe down to ~500 m depth. Both units represent coherent magmatic kimberlite, and the green variety appears to be a hydrothermally altered and more crustally contaminated variant of the fresh black kimberlite. The black kimberlite is highly macrocrystic with individual olivine crystals approaching 15 mm across (up to 30 vol%). Phlogopite macrocrysts up to 3 mm across are common (up to 5 vol%). Their rims typically enclose minute groundmass spinel crystals. The groundmass of the black kimberlite variety consists of variable proportions of phlogopite flakes (20-120 μm), carbonate and serpentine. Accessory groundmass phases comprise atoll-textured spinel and perovskite (<60 μm), and very rare Mg-rich ilmenite.

A sizable (20 cm across) micaceous autolith was recovered from KX36 kimberlite drill core. The fresh autolith is inequigranular and dominated by olivine, phlogopite and clinopyroxene, with minor spinel, Mn-rich ilmenite, calcite, serpentine, apatite and Ti-rich andradite garnet. Macrocrystic olivine has high forsterite content of Fo_{92}. Phlogopite has high TiO_2 content (1-4 wt%) and evolves by Al-depletion toward tetraferriphlogopite. Clinopyroxene is close to diopside end-member composition with minor amounts of Ti and Al. Spinel crystals occur in interstices and as inclusions in phlogopite and clinopyroxene. They have magnesian chromite composition with high Cr# of up to 93 and low

TiO_2 content (<6 wt%). Interstitial magmatic garnet has Ti-andradite composition with up to 1 wt% ZrO_2. These mineralogical features suggest that the parent magma was of orangeite affinity.

Although the fresh black kimberlite variety of the KX36 pipe macroscopically resembles archetypal kimberlite, several mineralogical and geochemical features suggest a petrogenetic affinity to Group-2 kimberlite. For example, the transitional nature of the KX36 kimberlite between archetypal kimberlite and orangeite is illustrated by the elevated K contents at constant and low Ti concentration levels. This trend culminates at the micaceous autolith (Fig.1). Primitive mantle normalized incompatible element patterns show a significant slope for the LILE (Cs, Rb, Ba), unfractionated low concentrations for the HFSE (Th, U, Nb, Ta), and highly fractionated LREE/HREE. These patterns strongly resemble the trace element distributions of orangeites (Fig.2). The trace element pattern of the micaceous autolith is highly fractionated and bears resemblance to primitive continental arc volcanic rocks. Such a geochemical signature is typically found in subduction zone settings.

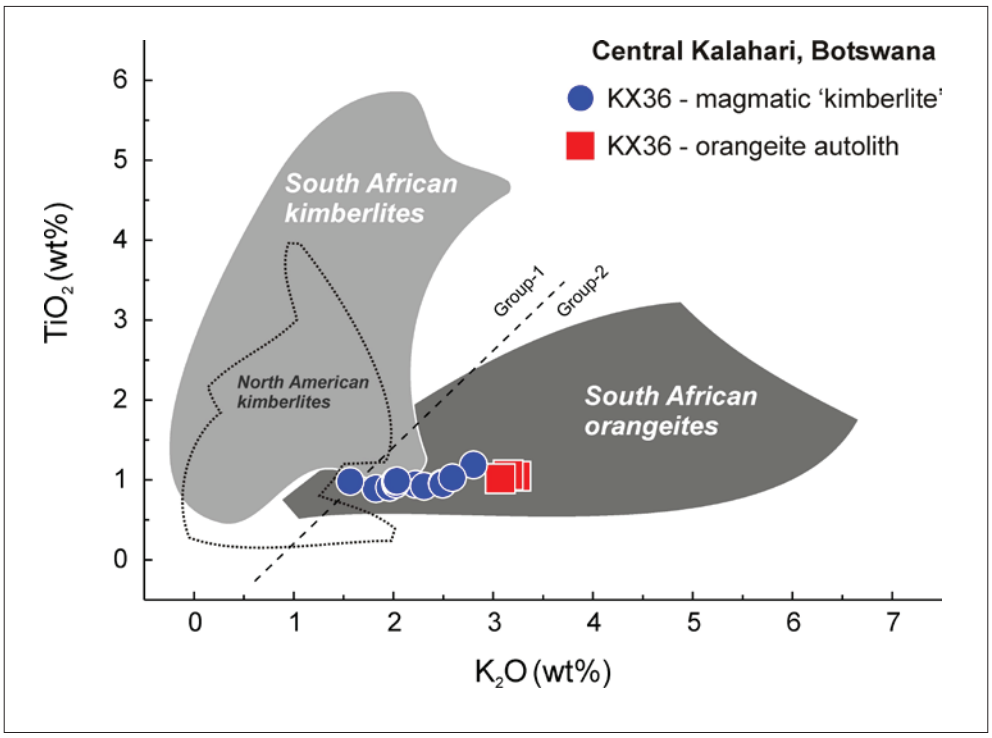

Figure 1: TiO_2 vs. K_2O for fresh uncontaminated (C.I. <1.25) magmatic KX36 kimberlite and an entrained micaceous autolith (fields for comparison from: Smith et al., 1985; Becker and Le Roex, 2006; Coe et al., 2008; Tappe et al., 2017).

Our study provides first evidence for the occurrence of kimberlite magmatism of Group-2 affinity in the central Kalahari basin. This discovery increases the geographic extent of ultramafic potassic magmatism in southern Africa by more than 300 km toward the NW Kaapvaal craton edge. As previously suggested for orangeite magmatism in other parts of the Kaapvaal craton (cf., Coe et al., 2008), the combination of a high-LILE and low-HFSE geochemical fingerprint at the NW craton margin is best explained by involvement of strongly K-metasomatized mantle lithosphere. The distinctive trace element signature can be linked to prior subduction-driven collision events during the Proterozoic evolution of the Kaapvaal craton and surrounding orogenic belts.

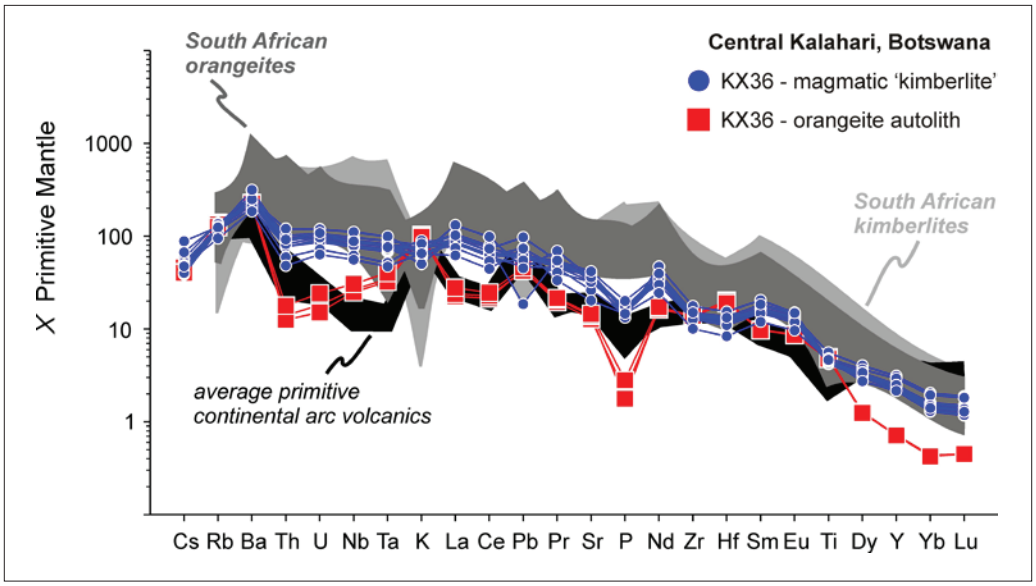

Figure 2: Normalized incompatible element patterns for fresh uncontaminated (C.I. <1.25) magmatic KX36 kimberlite and an entrained micaceous autolith (fields for comparison from: Becker and Le Roex, 2006; http://georoc.mpch-mainz.gwdg.de/georoc/).

Acknowledgments

This PhD study is conducted with support of the CIMERA DST-NRF Centre of Excellence at the University of Johannesburg.

Becker M, Le Roex AP (2006) Geochemistry of South African on- and off-craton, Group I and Group II kimberlites: Petrogenesis and source region evolution. J Petrol 47: 673-703

Coe N, Le Roex AP, Gurney JJ, Pearson DG, Nowell GM (2008) Petrogenesis of the Swartruggens and Star Group II kimberlite dyke swarms, South Africa: Constraints from whole rock geochemistry. Contrib Mineral Petrol 156: 627-652

Giuliani A, Phillips D, Woodhead JD, Kamenetsky VS, Fiorentini ML, Maas R, Soltys A, Armstrong RA (2015) Did diamond-bearing orangeites originate from MARID-veined peridotites in the lithospheric mantle? Nat Commun 6: 1-10

Griffin WL, Batumike JM, Greau Y, Pearson NJ, Shee SR, O'Reilly SY (2014) Emplacement ages and sources of kimberlites and related rocks in southern Africa: U-Pb ages and Sr-Nd isotopes of groundmass perovskite. Contrib Mineral Petrol 168: 1-13

Kjarsgaard BA, Pearson DG, Tappe S, Nowell GM, Dowall D (2009) Geochemistry of hypabyssal kimberlites from Lac de Gras, Canada: Comparisons to a global database and applications to the parent magma problem. Lithos 112: 236-248

Mitchell RH (1995) Kimberlites, orangeites, and related rocks. Plenum Press, New York

Rogers AJ, Hough TG, Davidson JM (2013) KX36 - rediscovering the diamond exploration potential of the central Kalahari in Botswana. The Journal of The Southern African Institute of Mining and Metallurgy 113: 539-545

Smith CB, Gurney JJ, Skinner EMW, Clement CR, Ebrahim N (1985) Geochemical character of Southern African kimberlites: A new approach based on isotopic constraints. Transactions of the Geological Society of South Africa 88: 267-280

Tappe S, Foley SF, Kjarsgaard BA, Romer RL, Heaman LM, Stracke A, Jenner GA (2008) Between carbonatite and lamproite: Diamondiferous Torngat ultramafic lamprophyres formed by carbonate-fluxed melting of cratonic MARID-type metasomes. Geochim Cosmochim Acta 72: 3258-3286

Tappe S, Romer RL, Stracke A, Steenfelt A, Smart KA, Muehlenbachs K, Torsvik TH (2017) Sources and mobility of carbonate melts beneath cratons, with implications for deep carbon cycling, metasomatism and rift initiation. Earth and Planetary Science Letters 466: 152-167

THERMODYNAMIC MODELLING CONSTRAINTS ON INCIPIENT MELTING IN THE EARTH'S MANTLE IN PRESENCE OF VOLATILES (CO_2-H_2O): A KEY TOOL FOR ECONOMICS DEPOSITS

Malcolm Massuyeau

Constraining mantle processes is essential to the understanding of the fundamental mechanisms ruling our world, such as plate tectonics, volcanism or the formation of economically relevant ore deposits. Of particular interest, partial melting in the Earth's mantle is one of these key processes in the global geodynamics.

The link between volatiles and mantle melting has so far been highlighted by experimental petrology, revealing that ppm concentration levels of carbon and other volatiles in the Earth's mantle can induce incipient melting (i.e. formation of small melt fractions being stable in a large pressure-temperature window) by: (1) decreasing the peridotite melting temperatures by some hundreds of degrees Celsius, and (2) expanding the range of melt compositions under influence of CO_2, and moderately H_2O (see Figure 1). Near-solidus melts are dominated by carbonate-rich compositions, which evolve towards basaltic compositions at higher temperatures (see Figure). However, this carbonate-silicate transition is generally non-ideal and can be complex, abrupt, depending on temperature, pressure and chemical composition (i.e., P-T-X conditions) of the system. Under specific conditions, the strong non-ideality of the system can show a miscibility gap between both types of liquids (i.e., immiscibility between a carbonate-rich liquid and a silicate-rich liquid).

Consequently, modelling incipient melting in the presence of volatiles can easily become a complex challenge, especially in the presence of CO_2. Up to now, thermodynamic modelling principally addressed mantle partial melting in both dry and H_2O-bearing peridotite systems (Ghiorso et al., 2002; Asimow and Langmuir, 2003; Katz et al., 2003; Hirschmann et al., 2009; Lee et al., 2009; Ueki and Iwamori, 2013, 2014; Jennings and Holland, 2015), notably motivated by the pioneering work of Mark Ghiorso and co-workers in the numerical modelling of liquid–solid phase equilibria applied to igneous systems with the well-known MELTS/pMELTS/Rhyolite-MELTS softwares (Ghiorso et al., 1983; Ghiorso and Sack, 1995; Ghiorso et al., 2002; Gualda et al., 2012). Current models, where the effect of CO_2 on incipient melting is considered, are empirically derived (Hirschmann, 2010; Dasgupta et al., 2013) and hardly applicable outside their compositional and pressure-temperature ranges of calibration (Massuyeau et al., 2015). In the only thermodynamic model dealing with CO_2 in mantle melting, the latter is considered as a soluble component in silicate-rich melts for CO_2-bearing systems within a recent update of MELTS (Ghiorso and Gualda, 2015).

Nevertheless, since many decades, the composition of CO_2-bearing melts, from carbonatite to basalt, coexisting with a peridotite assemblage is rather well constrained by experimental petrology in terms of P-T-X conditions. The experimental database produced is then used to calibrate our thermodynamic modelling in order at simulating the mantle melting and predicting the melt composition in the mantle as a function of P-T-X conditions.

In a first model, we used the activity of silica in the melt to constrain the melt composition in major elements from carbonate-rich (i.e., carbonatites) to silicate-rich melts (i.e., basalts). At a given pressure and temperature, the activity of the silica component in the melt, $a_{SiO_{2(l)}}$, is constrained (buffered) and calculated for a melt coexisting with mantle olivine and orthopyroxene (Massuyeau et al., 2015). Assuming the melt composition can be modelled as a mixture of different and experimentally constrained end-members, mixtures of these end-members in different proportions are then adjusted with the aim to obtain a silica content giving a value of $a_{SiO_{2(l)}}$, in equilibrium with olivine and orthopyroxene. This model has already been used, and its potential to capture the evolution of the melt composition in different geodynamic contexts has been shown (Massuyeau et al., 2015; Aulbach et al., 2017).

In future developments, this model will serve as a base for the self-consistent mantle melting model, with a major improvement which is to generalize the model via a complete description of the thermodynamic properties for the melt major components, i.e. SiO_2-TiO_2-Al_2O_3-CaO-MgO-FeO-Na_2O-K_2O-H_2O-CO_2. Already, some tests of feasibility have already been made. The biggest challenge we face here is calibrating a model predicting experimental observations, including the experimental uncertainties which are potentially high and highly variable depending on the component and thermodynamic parameters considered.

Finally, another major research axis in this thermodynamic modelling will concern the development of a thermodynamic model to predict the behaviour of the trace elements in melts described above, and their partitioning with the ambient peridotite mantle. One of the fundamental aspects of this model will

be the coupling of the trace element partitioning with (thermodynamic modelling relating) major element abundances in the melt to different P-T-volatiles conditions. One of the principal aims of such a coupled model is to track the physical and chemical conditions of the formation and mobility of diverse types of melt within Earth's upper mantle being responsible for mantle metasomatism including diamond formation and transport, geochemical enrichment and volatile cycling. In short, the new model will use the major and trace element compositions of mantle-derived magmatic rocks to determine the P-T conditions (i.e., locations) of their source regions.

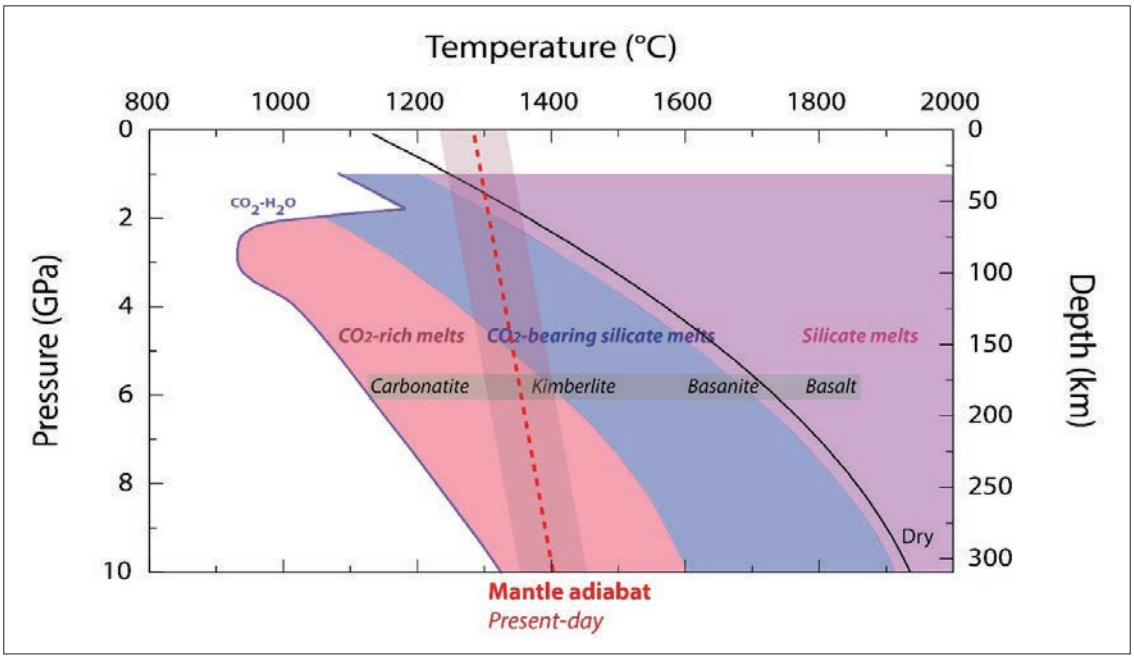

Figure 1: P-T window schematically representing a representative and simplified evolution of the melt composition in presence of water and CO_2 as a function of pressure-temperature conditions. Solidus temperatures of dry (black curve; Hirschmann, 2000) and H_2O-CO_2-bearing (purple curve; combination of different studies: Wallace and Green, 1988; Foley et al., 2009; Hirschmann et al., 2009) peridotite are also represented, together with the typical P-T conditions prevailing in the adiabatic mantle (i.e., asthenosphere; dashed red curve).

Asimow, P.D., Langmuir, C.H., 2003. The importance of water to oceanic mantle melting regimes. Nature, 421, 815-820.

Aulbach, S., Massuyeau, M., and Gaillard, F., 2017. Origins of cratonic mantle discontinuities: A view from petrology, geochemistry and thermodynamic models. Lithos, 268–271, 364–382.

Dasgupta, R., Mallik, A., Tsuno, K., Withers, A.C., Hirth, G., Hirschmann, M.M., 2013. Carbon-dioxide-rich silicate melt in the Earth's upper mantle. Nature, 493, 211-215.

Foley, S.F., Yaxley, G.M., Rosenthal, A., Buhre, S., Kiseeva, E.S., Rapp, R.P., Jacob, D.E., 2009. The composition of near-solidus melts of peridotite in the presence of CO2 and H2O between 40 and 60 kbar. Lithos, 112S, 274-283.

Ghiorso, M.S., Gualda, G.A.R., 2015. An H_2O–CO_2 mixed fluid saturation model compatible with rhyolite-MELTS. Contributions to Mineralogy and Petrology, 169, doi:10.1007/s00410-015-1141-8.

Ghiorso, M.S., Sack, R.O., 1995. Chemical mass transfer in magmatic processes IV. A revised and internally consistent thermodynamic model for the interpolation and extrapolation of liquid-solid equilibria in magmatic systems at elevated temperatures and pressures. Contributions to Mineralogy and Petrology, 119, 197-212.

Ghiorso, M.S., Carmichael, I.S.E., Rivers, M.L., Sack, R.O., 1983. The Gibbs Free Energy of mixing of natural silicate liquids; an expanded regular solution approximation for the calculation of magmatic intensive variables. Contributions to Mineralogy and Petrology, 84, 107-145.

Ghiorso, M.S., Hirschmann, M.M., Reiners, P.W., Kress, V.C., 2002. The pMELTS: A revision of MELTS for improved calculation of phase relations and major element partitioning related to partial melting of the mantle to 3 GPa. Geochemistry Geophysics Geosystems, 3, doi: 10.1029/2001GC000217.

Gualda, G.A.R., Ghiorso, M.S., Lemons, R.V., Carley, T.L., 2012. Rhyolite-MELTS: a Modified Calibration of MELTS Optimized for Silica-rich, Fluid-bearing Magmatic Systems. Journal of Petrology, 53, 875-890.

Hirschmann, M.M., 2000. Mantle solidus: Experimental constraints and the effects of peridotite composition. Geochemistry Geophysics Geosystems, 1, doi: 10.1029/2000GC000070.

Hirschmann, M.M., 2010. Partial melt in the oceanic low velocity zone. Physics of the Earth and Planetary Interiors, 179, 60-71.

Hirschmann, M.M., Tenner, T., Aubaud, C., Withers, A.C., 2009. Dehydration melting of nominally anhydrous mantle: The primacy of partitioning. Physics of the Earth and Planetary Interiors, 176, 54-68.

Jennings, E.S., Holland, T.J.B., 2015. A Simple Thermodynamic Model for Melting of Peridotite in the System NCFMASOCr. Journal of Petrology, 56, 869-892.

Katz, R.F., Spiegelman, M., Langmuir, C.H., 2003. A new parameterization of hydrous mantle melting. Geochemistry Geophysics Geosystems, 4, 1073, doi:10.1029/2002GC000433.

Lee, C.-T. A., Luffi, P., Plank, T., Dalton, H., Leeman, W.P., 2009. Constraints on the depths and temperatures of basaltic magma generation on Earth and other terrestrial planets using new thermobarometers for mafic magmas. Earth and Planetary Science Letters, 279, 20-33.

Massuyeau, M., Gardés, E., Morizet, Y., Gaillard, F., 2015. A model for the activity of silica along the carbonatite–kimberlite–mellilitite–basanite melt compositional joint. Chemical Geology, 418, 206-216.

Ueki, K., Iwamori, H., 2013. Thermodynamic model for partial melting of peridotite by system energy minimization. Geochemistry Geophysics Geosystems, 14, 342-366.

Ueki, K., Iwamori, H., 2014. Thermodynamic calculations of the polybaric melting phase relations of spinel lherzolite. Geochemistry Geophysics Geosystems, 15, 5015-5033.

Wallace, M.E., Green, D.H., 1988. An experimental determination of primary carbonatite magma composition. Nature, 335, 343-346.

Metamorphism and Tectonics, and their Chronology

SERPENTINIZATION OF PERIDOTITIC ROCKS AND ASSOCIATED MAGNETITE MINERALIZATION FROM THE LECHANA AREA, EASTERN BOTSWANA

Georgy Belyanin, Thuto Mokatse[1], Rajesh Hariharan[1]

[1] Department of Earth and Environmental Sciences, BIUST, Botswana

Serpentinization is a major metasomatic process primarily involving H_2O-rich fluids that alter olivine and pyroxene to serpentine group minerals in ultramafic rocks. Serpentinized peridotitic rocks occur as a prominent rock type, occupying low lying ridges and prominent hills, in the Lechana area, eastern Botswana. They are associated with amphibolites, and together occur as inclusions within Neoarchean biotite-bearing tonalitic gneiss. Two of the hills preserve prominent magnetite-bearing layers associated with peridotitic rocks, and can be traced for the entire outcrop length.

Detailed petrographic observation aided with reflected light/BSE imaging indicates the preservation of various stages of serpentinization in the peridotitic rocks (figure). Relics of olivine and orthopyroxene are variably preserved. Mesh, hourglass and bastitic textures characterize the serpentinization. Magnetite starts to occur as subhedral to anhedral grains associated with olivine and orthopyroxene. With the progress of serpentinization, the occurrence of magnetite varies from elongated adjoined grains to veins to layers. The magnetite-bearing layers are associated with heavily serpentinized rocks. Mineral chemical analyses indicate that the magnetites are chromium-rich with Cr_2O_3 contents varying from ~6 to 11 wt.%. The Mn content of the chromian-magnetites varies from ~0.15 to 0.4 wt.%. Although Kfs-metasomatic overprint occurs locally (seen in tonalitic gneiss and amphibolite), no such overprint is seen in the peridotitic rocks. At the present stage, the field mapping, petrographic and mineral chemical studies point towards an association of the magnetite mineralization with serpentinization of the peridotitic rocks. Ongoing studies aim to further evaluate this inference.

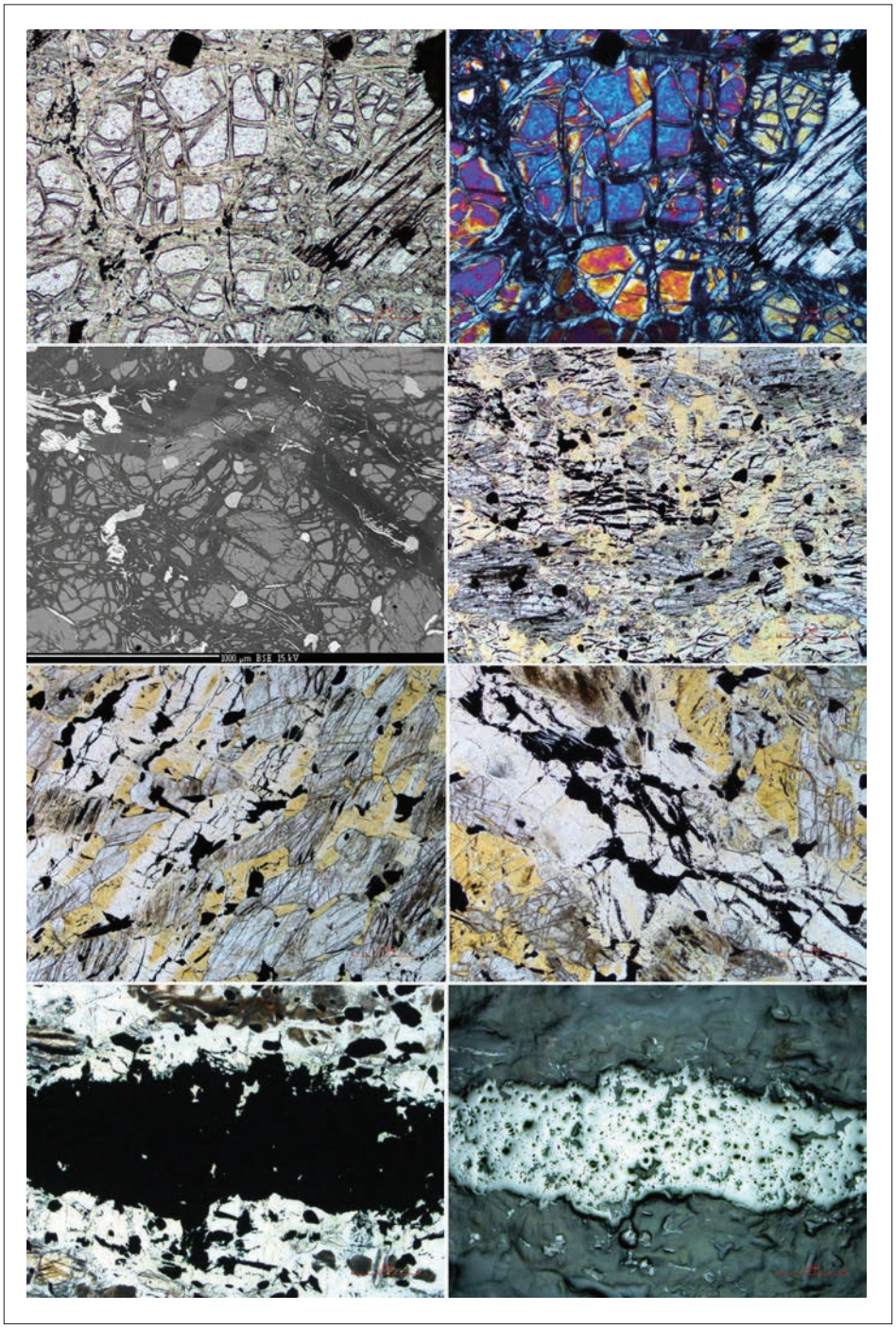

Figure 1. Representative plane-polarized, back-scattered electron and reflected light images from the peridotitic rocks indicating the progress of serpentinization and association with magnetite.

PETROGENESIS OF NEOARCHEAN PYROXENE-BEARING TTG CORE AND PYROXENE-ABSENT GRANITE RIM FROM THE AVOCA PLUTON (LIMPOPO COMPLEX)

Georgy Belyanin, Rajesh Hariharan[1] and Dirk Van Reenen

[1] Department of Earth and Environmental Sciences, BIUST, Botswana

The Neoarchean eon is characterized by a greater proportion of K-rich granitoids (biotite, two-mica granites, sanukitoids, etc.) relative to the Na-rich tonalite-trondhjemite-granodiorites (TTGs) than the Paleo- and Mesoarchean (Kemp and Hawkesworth, 2003), and the Neoarchean TTG's seem to have a different composition compared with their older counterparts (see reviews in Moyen and Martin, 2012). Considering the diversity of possible phases between the Na-rich and K-rich endmembers, studies on temporally and spatially associated Neoarchean granitoids in individual terranes can help to characterize the petrogenetic processes and likely tectonic setting that characterize this change in granitoid composition.

A variety of Neoarchean granitoid gneisses occur within the Central Zone of the Limpopo Complex in southern Africa. Both the voluminous and less voluminous of these granitoid gneisses are characterized by their widespread nature; rarely do they form individual plutons.

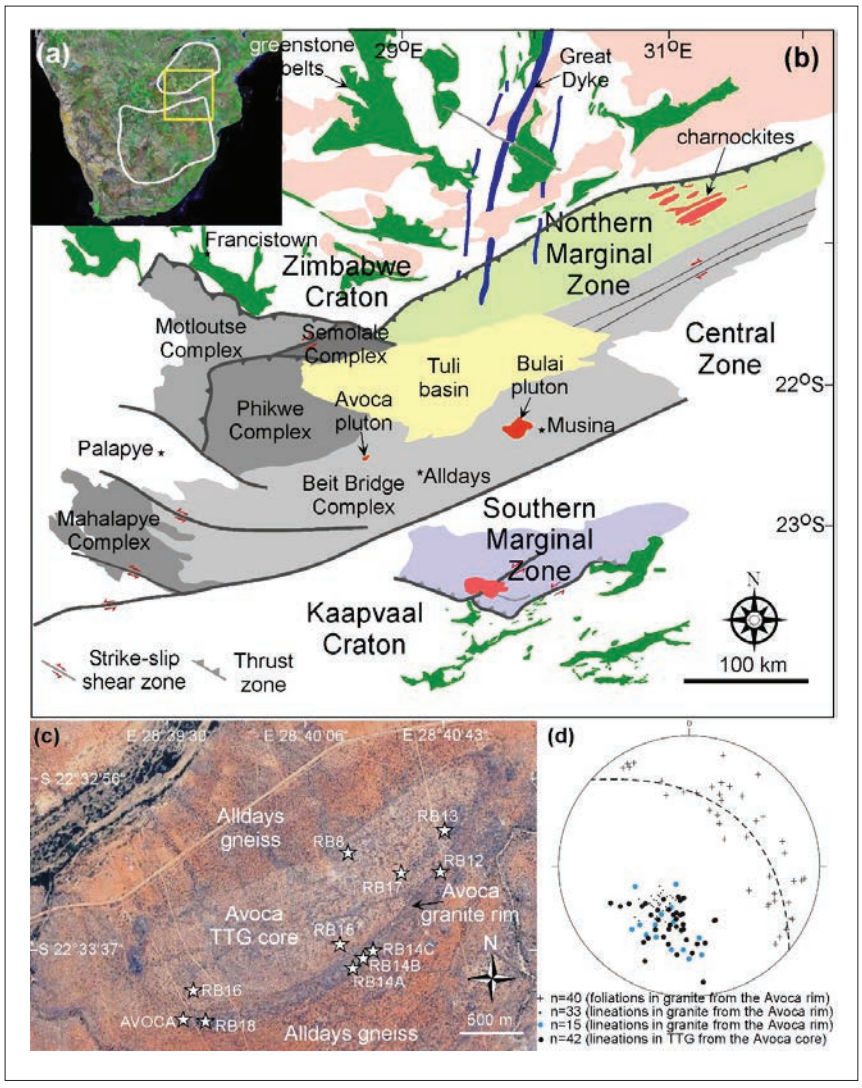

Figure 1. The approximate extent of the Archean Kaapvaal and Zimbabwe cratons. The box indicates the area covered in (b). (b) Generalized geologic map of the Limpopo complex showing the places of the Avoca and Bulai pluton in the Central Zone of the Complex. (c) Geologic map of the Avoca pluton and surroundings on a google satellite image, showing the sampling locations (indicated by stars). (d) Stereographic projection for the Avoca pluton. Crosses are poles to foliation, and dots are lineations (Boshoff, 2004).

The Neoarchean Avoca pluton from the northwestern margin of the Beit Bridge Complex segment of the Limpopo Complex consists of a dominant TTG core and a thin granite rim (Figure 1), with local occurrence of two-pyroxene-bearing metabasite intercalations and boudins. Field relations of granite enclaves in the TTG core rocks together with available ages indicate that the TTG intruded the granite. The TTG rocks are characterized by biotite, amphibole and orthopyroxene, with clinopyroxene occurring locally, while amphibole and biotite constitute the main mafic minerals in the granite. Both the core and rim rocks are characterized by difference in mineral chemistry, with the mafic minerals Mg-rich in the TTG, while they are Fe-rich in the granite and metabasite.

The TTG is magnesian to slightly ferroan and characterized by higher Al_2O_3, Mg#, Sr/Y and La/Yb than the ferroan granite. Primitive mantle-normalized trace element patterns of both TTG and granite show systematic negative Nb-Ta anomalies, with TTG characterized by positive Pb anomaly while granite has no such prominent Pb anomaly (Figure 2). Separate petrogenetic models can be suggested for the different phases of the Avoca core, with the trondhjemite-tonalites considered as high-pressure melts of metabasalt, while the granodiorite with lower SiO2 content, higher K2O and MgO contents, and higher incompatible element contents, than the trondhjemite-tonalites, is a product of hybridization of earlier TTG melts and peridodite in a subduction setting.

Granites from the Avoca rim reflect low-pressure melting of pre-existing crustal lithologies in a collisional setting. Comparison with available geochemical data of other temporally and spatially associated granitoid gneisses from the Beit Bridge Complex indicate alternating TTG-granite magmatism, arguing for the operation of Neoarchean accretionary tectonics along the northwestern margin of the Beit Bridge Complex. The change in granitoid composition preserved within the Beit Bridge Complex indicates the diversity of possible phases between Na-rich and K-rich end members, associated petrogenetic processes and a likely tectonic setting that characterize the transition from TTG to sanukitoid magmatism (see review in Laurent et al, 2014).

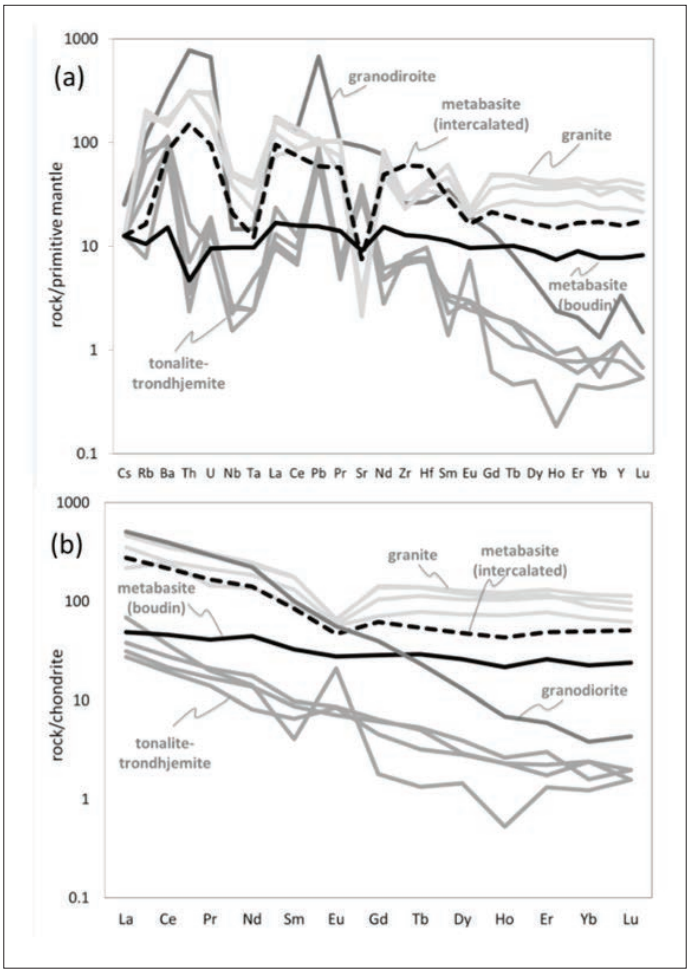

Figure 2. Avoca TTG, granite and metabasite compositions in terms of primitive mantle-normalized multi-element (a) and chondrite-normalized REE (b) plots.

Boshoff, R., 2004. Formation of major fold types during distinct geological events in the Central Zone of the Limpopo Belt, South Africa: new structural, metamorphic and geochronologic data. M.Sc. Thesis, Rand Afrikaans University.

Kemp, A.I.S., Hawkesworth, C.J., 2003. Granitic perspectives on the generation and secular evolution of the continental crust. In: Rudnick, R.L. (Ed.), The Crust, Treatise in Geochemistry 3, 349–410.

Laurent, O., Martin, H., Moyen, J.F., Doucelance, R., 2014. The diversity and evolution of late-Archean granitoids: Evidence for the onset of "modern-style" plate tectonics between 3.0 and 2.5 Ga. Lithos 205, 208–235.

Moyen, J.F., Martin, H., 2012. Forty years of TTG research. Lithos 148, 312–336.

THE JOHANNESBURG DOME DILEMMA

Robyn Ormond, Jérémie Lehmann, Georgy Belyanin

The Johannesburg Dome, located in the centre of the Kaapvaal Craton, is a slightly elliptical inlier (50 km in E-W direction by 30 km in N-S direction) of Archean rocks surrounded by younger, outward-dipping supracrustal rocks of the Witwatersrand, Ventersdorp and Transvaal supergroups (Fig. 1A), thus corresponding to the shape of a structural dome. Despite several studies carried out regarding the petrography, geochemistry and magmatic evolution of the Johannesburg Dome rocks [1][2][3], the question still remains: why is the Johannesburg Dome a dome? The mechanisms of formation, structural evolution and relative timing of formation of the domal geometry of the Johannesburg Dome remain poorly constrained. Through ongoing investigation of the relationships between the core and the supracrustal cover of the Johannesburg Dome, some insight could be gained regarding the timing and mechanism of its formation as a structural dome.

The Zwartkops Hills located along the NW margin of the Johannesburg Dome, described as being a north-verging nappe, represent an outlier of West Rand Group rocks, Witwatersrand Supergroup (Figure 1A), overlying the rocks of the Archean basement [4]. Our ongoing structural investigation documents S to SW-dipping greenschist-facies cleavages locally carrying down-dip mineral lineations, asymmetric open to closed upright folds, as well as conjugate contractional kink folds at Zwartkops, all compatible with a top-to-the-north movement (Figure 1B).

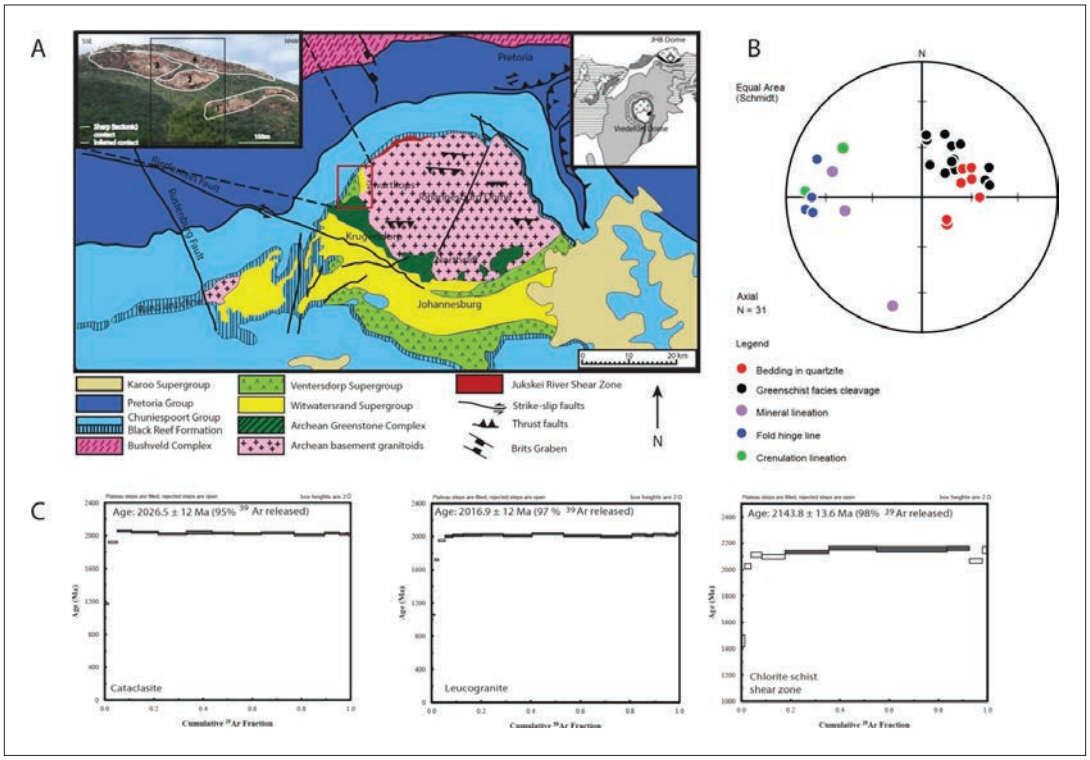

Figure 1: (A) Map showing the geology of the Johannesburg Dome region, adapted from [6], with a cartoon (upper right hand corner) showing the position of the Johannesburg Dome in relation to the VIS, adapted from [7]. An annotated photograph (upper left hand corner) shows an E-facing cliff in the southern part of the Zwartkops Hills in which four quartzite lenses are well exposed. (B) Equal area lower-hemisphere stereonet showing structural data pertaining to the southern Zwartkops Hills, including bedding and cleavage orientations plotted as poles to the plane, as well as lineation (mineral, crenulation, and fold hinge line) orientations. (C) $^{40}Ar/^{39}Ar$ stepwise heating age spectra (2σ) showing plateau ages obtained from white mica separated via suspension settling and hand picking from cataclasite, leucogranite and chlorite schist (from a shear zone in the gneissic metadiorite of the basement) samples.

New $^{40}Ar/^{39}Ar$ stepwise heating plateau ages (Figure 1C) were obtained on white micas separated from Zwartkops Hills samples by both hand-picking and suspension settling. They reveal two age populations. An older age of 2143.8 ± 13.6 Ma (2σ) was obtained from a shear zone recording greenschist facies metamorphism (white micas sized 0.4-3 mm) developed within gneissic metadiorite of the Archean basement and is interpreted as approximating the age of shearing. A younger age population of ca. 2016-2026 Ma (2σ) was obtained from a leucogranite and schistose cataclasite, white micas sized ± 2 mm and < 100 µm respectively.

The 2016-2026 Ma age population is very similar to the 2023 ± 4 Ma U-Pb zircon age obtained from a pseudotachylitic breccia, recorded for the Vredefort Impact Structure (VIS) [5]. It is thought that the VIS could have played a role in the deformation of the Zwartkops Hills and consequently the Johannesburg Dome, yet is it uncertain to what extent.

[1] Willemse J. (1933). Transactions of the Geological Society of South Africa 36: 1-27
[2] Kynaston H. (1907). Transactions of the Geological Society of South Africa 10: 51-61
[3] Anhaeusser C.R. (1973). Special Publication of the Geological Society of South Africa 3: 361-385
[4] Roering C. (1984). Transactions of the Geological Society of South Africa 87: 87-99
[5] Kamo S.L. et al. (1996). Earth and Planetary Science Letters 144: 369-387
[6] Alexandre P. et al.(2006). South African Journal of Geology 109: 393-410
[7] Koglin N. et al. (2010). Precambrian Research 183: 817-824

Coal and hydrocarbons

IN-SITU CARBON ISOTOPE ANALYSIS OF ARCHAEAN CARBONACEOUS GRAINS OF THE WITWATERSRAND BASIN, SOUTH AFRICA

Axel Hofmann, Giuliana Costa, Emilie Thomassot[1]

[1] CRPG-CNRS, Université de Lorraine, 54500 Vandoeuvre-lès-Nancy, France

The Archaean Witwatersrand Basin in South Africa (Figure 1) is the classic example of a palaeoplacer gold deposit hosted in quartz pebble conglomerates, also known as reefs. It hosts the richest and the single most important gold province in the world (Frimmel et al., 2005). The reefs host a large array of detrital heavy minerals - mainly pyrite, but also zircon, rutile, uraninite and many others, but also gold - indicating prolonged times of sedimentary reworking and mineral concentrations. Following deposition, hydrothermal and metamorphic fluids modified the primary mineralogy of the reefs, giving rise to remobilization of some of the primary ore constituents, gold in particular.

An additional aspect of the gold ore involves the presence of carbon in the reefs, as bitumen seams and sand-sized nodules (Figure 2). Bitumen was largely derived from oil that was generated at different times in the evolution of the Witwatersrand Basin. Migration of oil along fractures within or adjacent to detrital uraninite grains and radiogenic oil immobilization may have given rise to bituminous nodules (England et al., 2002). Gold is commonly closely associated with the carbonaceous matter, with gold grades of carbon seams frequently in the order of several hundred ppm. In order to better understand the origin of bitumen seams and nodules, we have undertaken an in-situ carbon isotope analysis of carbon nodules of several mineralized reefs using the Cameca ims 1270 ion probe. Instrumental mass fractionation was determined using an in-house graphite standard Sri Lanka ($\delta^{13}C$ = -3.6 ‰) analysed prior to each sample run.

Carbon isotope data from four samples of three reefs (Fig. 3) vary between -41 to -22 ‰, which is a similar range of values as reported previously from bulk analyses (Hoefs and Schidlowski, 1967; Spangenberg and Frimmel, 2001). There is generally a relatively small within-reef variability of $\delta^{13}C$ values, whereas the inter-reef variability is large. Assuming that the nodules were derived from migrating oils, large inter-reef variability may point to the migration of isotopically distinct hydrocarbons in the reefs investigated, with migration likely taking place at different times during the burial history of the basin.

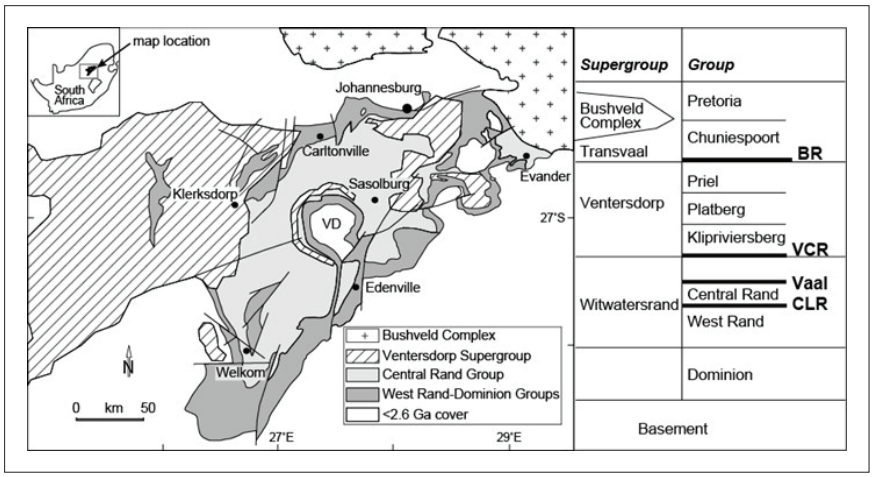

Figure 1. Witwatersrand basin location and simplified stratigraphic column of the Witwatersrand Basin and Transvaal Supergroup. CLR: Carbon Leader Reef; Vaal: Vaal Reef; VCR: Ventersdorp Contact Reef; BR: Black Reef; VD:

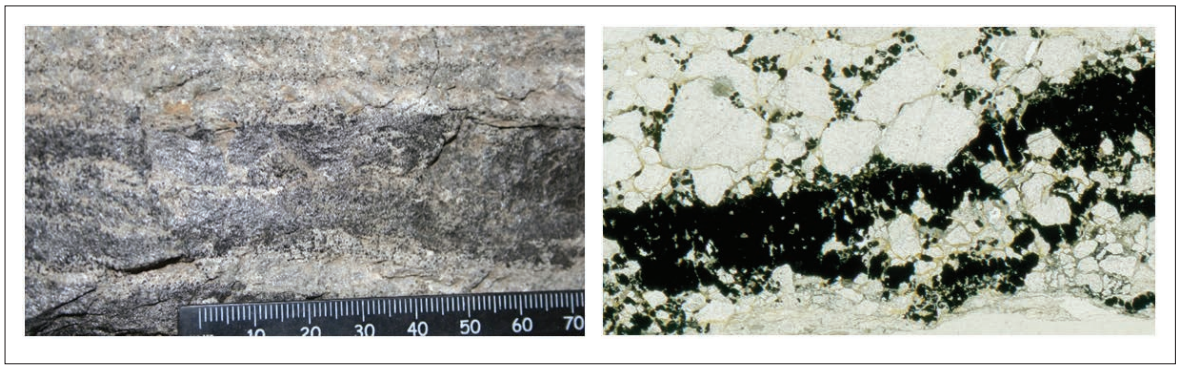

Figure 2. Carbon seam in sandstone (left). Thin section scan of carbon seam made of sand-sized carbonaceous nodules at the base of the Vaal Reef (right; width of field of view is c. 1 cm).

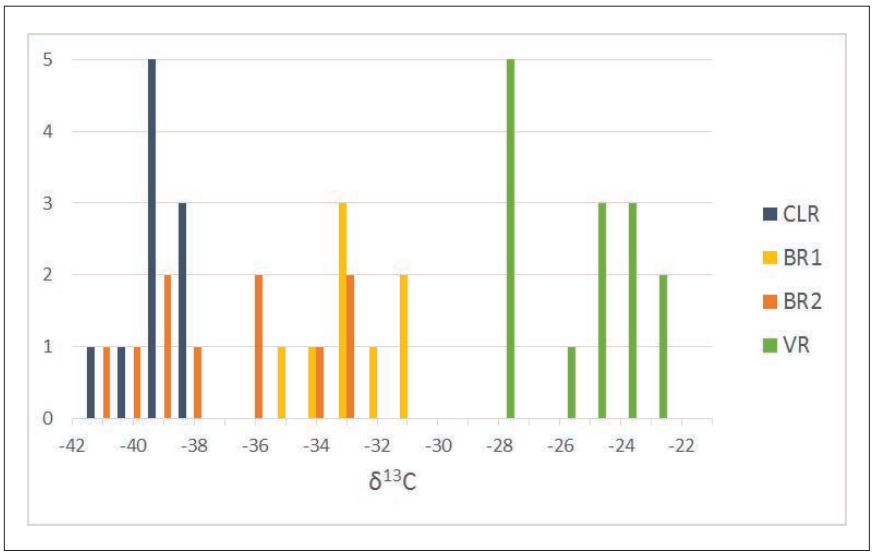

Figure 3. Histogram of δ13C values of individual sand-sized carbonaceous nodules in one sample of Carbon Leader Reef (CLR), one sample of Vaal Reef (VR) and two samples of Black Reef (BR).

England, G.L., Rasmussen, B., Krapez, B. & Groves, D.I. (2002). Archaean oil migration in the Witwatersrand Basin of South Africa. Journal of the Geological Society 159, 189–201.

Frimmel, H. E., Groves, D. I., Kirk, J., Ruiz, J., Chesley, J. & Minter, W. E. L. (2005). The formation and preservation of the Witwatersrand Goldfields, the world's largest gold province. Economic Geology 100th Anniversary Volume, 769-797.

Hoefs, J., & Schidlowski, M. (1967). Carbon isotope composition of carbonaceous matter from the Precambrian of the Witwatersrand system. Science, 155, 1096-1097.

Spangenberg, J. E., & Frimmel, H. E. (2001). Basin-internal derivation of hydrocarbons in the Witwatersrand Basin, South Africa: evidence from bulk and molecular δ 13 C data. Chemical Geology, 173, 339-355.

ON THE FORMATION OF INERTINITE MACERALS THROUGH COMBUSTION OF PLANT MATTER – PRELIMINARY OBSERVATIONS

O. Marvin Moroeng[1,2], R. James Roberts[2] and Nikki J. Wagner[1]

1 Geology Department, UJ; 2 Department of Geology, University of Pretoria

The formation of inertinite macerals in coal through combustion and/or oxidation continues to be a topic of much discussion, and the conclusions remain largely controversial. Gondwana coals, including coals in South Africa, are dominated by various inertinite macerals, including semifusinite, inertodetrinite and fusinite[1-8]. Falcon[9] attributes the dominance of these macerals to oxidation and incomplete decomposition brought about by a waning ice age. In contrast, Glasspool[5-6] argues that the macerals were formed by prehistoric combustion of plant matter. The preservation of anatomical structure in both fusinite and semifusinite would suggest minimal microbial degradation in contrast to other inertinite macerals such as macrinite.

A Medium rank C bituminous coal sample was obtained from the Witbank Coalfield, South Africa. The sample was subsequently crushed (-2 mm) and subjected to float-sink separation to produce vitrinite and inertinite-rich products. The three samples (parent, low density vitrinite-rich and high density inertinite-rich) were prepared for petrographic analysis. The low density product was found to have a vitrinite content of 83.1 vol. % (mmf) dominated by collotelinite and collodetrinite. In contrast, the high density product (65.7 vol. % inertinite) is dominated semifusinite (of varying reflectance) and inertodetrinite. Solid-state electron spin resonance (ESR) and carbon-13 cross-polarization magic-angle-spinning nuclear magnetic resonance (^{13}C CP-MAS NMR) were undertaken on the samples.

Based on the results of the ESR analysis, the inertinite-rich product has the significantly higher free radical content in contrast to the parent and especially the vitrinite-rich samples. Differences in the spin density of the float-sink products of the sample suggests differences in the coalification pathways. Thermally driven "pre-diagenesis metamorphism" has previously been suggested to account for differences in spin density between iso-rank maceral groups[10]. Based on the NMR structural parameters, lignin-derived benzene rings in the vitrinite-rich product have merged to form polycyclic clusters. In contrast, the average cluster size in the inertinite-rich float product corresponds to isolated benzene rings. The presence of monocyclic rings in the former is interpreted to be consistent with "the possession of rigidity before incorporation in peat" as suggested by Scott[11]. Physically, rigidity may manifest through the preservation of cell walls, whereas, on a molecular level, rigidity may be expressed by the prevention of ring mergers (?). Ring merger in the vitrinite-rich sample corresponds to the destruction of anatomical structure.

Following combustion, the affected plant matter may subsequently be brought into a peat-forming environment, wherein it is superimposed against vitrinite-forming plant matter (Figure 1).

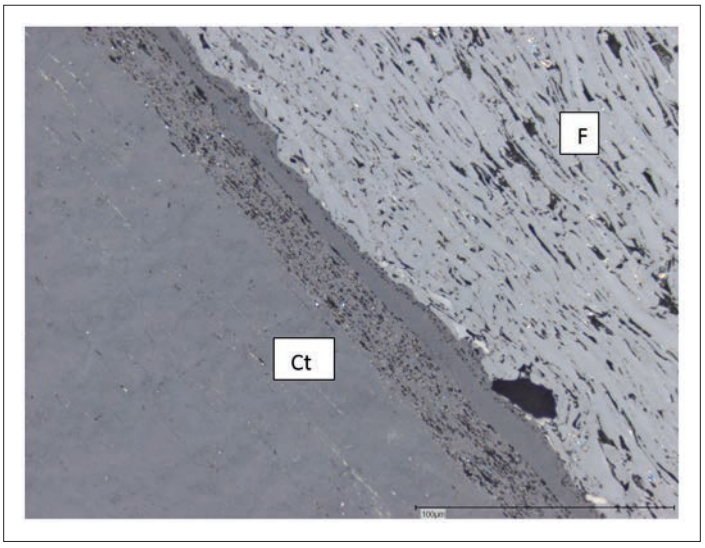

Figure 1: Photomicrograph showing the vitrinite maceral collotelinite (Ct, structure absent) and fusinite (F; with cell walls preserved, albeit compressed).

1. Falcon, R. and Ham, A.J. (1988). The characteristics of Southern African coals. The Journal of the South African Institute of Mining and Metallurgy, 88 (5), 145-161.
2. Hagelskamp, H.H.B. and Snyman, C.P. (1988). On the origin of low-reflecting inertinites in coals from the Highveld Coalfield, South Africa. Fuel, 67, 307-313.
3. Snyman, C.P. (1989). The role of coal petrography in understanding the properties of South African coal. In: Pickhardt, W. (Ed.). Erich Stach Memorial Issue. International Journal of Coal Geology, 14, 83-101.
4. Cadle, A.B., Cairncross, B., Christie, A.D.M. and Roberts, D.L. (1993). The Karoo Basin of South Africa: type basin for coal-bearing deposits of southern Africa. International Journal of Coal Geology, 23, 117-157.
5. Glasspool, I. (2003a). Palaeoecology of selected South African export coals from the Vryheid Formation, with emphasis on the role of heterosporous lycopods and wildfire derived inertinite. Fuel, 82, 959–970.
6. Glasspool, I.J. (2003b). Hypautochthonous–allochthonous coal deposition in the Permian, South African, Witbank Basin No. 2 seam; a combined approach using sedimentology, coal petrology and palaeontology. International Journal of Coal Geology, 53, 81-135.
7. Van Niekerk, D., Mitchell, G.D. and Mathews, J.P. (2010). Petrographic and reflectance analysis of solvent-swelled and solvent-extracted South African vitrinite-rich and inertinite-rich coals. International Journal of Coal Geology, 81, 45-52.
8. Van Niekerk, D., Pugmire, R.J., Solum, M.S., Painter, P.C. and Mathews, J.P. (2008). Structural characterization of vitrinite-rich and inertinite-rich Permian-aged South African bituminous coals. International Journal of Coal Geology, 76, 290-300.
9. Falcon, R.M.S. (1986). A brief review of the origin, formation, and distribution of coal in southern Africa. In: Anhaeusser, C.R. and Maske, S. (Eds.). Mineral Deposits of Southern Africa, Vols. I and II. Geological Society of South Africa. Johannesburg. 1879-1898.
10. Retcofsky, H.L., Stark, J.M. and Friedel, R.A. (1968). Electron Spin Resonance in American Coals. Analytical Chemistry, 40 (11), 1699-1704.
11. Scott, A.C. (1989). Observations on the nature and origin of fusain. International Journal of Coal Geology, 12, 443-475.

TIMING OF THE THERMAL OVERMATURATION OF THE ECCA GROUP'S PETROLEUM SOURCE ROCKS, MAIN KAROO BASIN, SOUTH AFRICA

Elijah O. Adeniyi, Frantz Ossa Ossa, Jan D. Kramers, Michiel O. De Kock, Georgy Belyanin and Nicolas J. Beukes.

The renowned estimates of the Main Karoo Basin shale gas reserves (368 billion cubic meter (bcm) to 13734bcm) have been recently deflated to a much lower margin of around 368bcm. Recent findings reveal that low hydrocarbon generation potential exists in the surroundings of dolerite intrusions across the basin. The source rocks are believed to have undergone thermal exhaustion as a result of the Jurassic-aged Karoo Large Igneous Province (KLIP) dolerite sills/dykes intrusions and other thermal events such as the Cape Fold Belt (CFB) within the basin. Yet, the mechanism and timing of these source rock exhaustion events remain controversial.

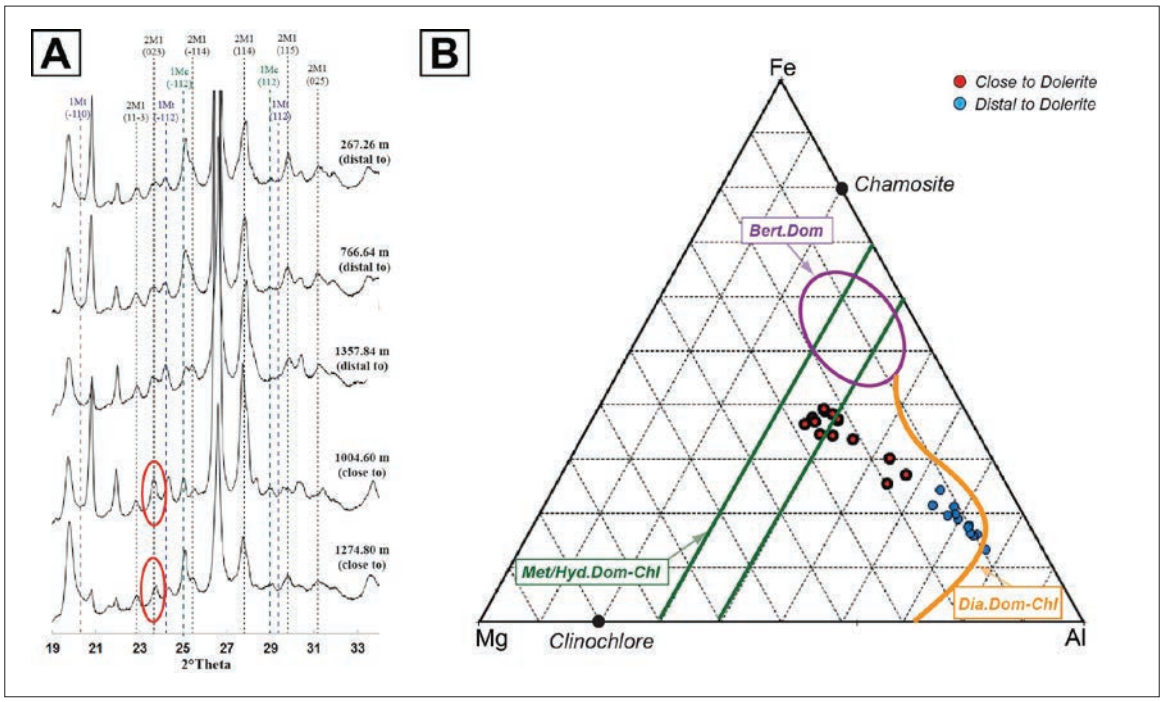

Figure 1: Clay mineralogy of the Ecca's petroleum source rock. (A) Representative XRD patterns of disoriented clay-rich powders showing illite polytype populations between 19 and 34 [°2Theta] in samples distal to and close to the dolerite intrusions. (B) Chlorite chemistry represented in a Mg-Al-Fe ternary plots (after Velde, 1985) for samples close and distal to the dolerite intrusions.

Based on drill core samples from the central Main Karoo Basin, we have used clay mineralogy of the 2:1:1 and 2:1 phyllosilicate groups including chlorite and illite respectively, as well as $^{40}Ar/^{39}Ar$ radiometric dating of illite, to constrain the nature and cause of mineral transformation processes that affected petroleum source rocks of the Ecca Group situated close and distal to the mafic sills/dykes, as well as their related timing. The X-ray diffractograms and mineral chemistry revealed that chlorite and illite phases of samples close to the dolerite intrusions are characterised by higher crystal growth rate/crystallinity with a chemical composition indicative for a formation in metamorphic environment (Figure 1). In contrast, chlorite and illite distal to any dolerite intrusion show lower crystal growth rate/crystallinity with chemical composition suggesting a formation in diagenetic environment (Figure 1).

$^{40}Ar/^{39}Ar$ radiometric dating indicates that illite in samples distal to the dolerite intrusions formed between 292 and 245 Ma with some ages clustering around 281 Ma (Figure 2). The oldest ages are consistent with a detrital fraction probably recycled from the erosion of the ash bed at the top of the underlying Dwyka Group. However, ages around 281 Ma can be linked with estimated depositional age of the Ecca Group at ~ 280 Ma, while the youngest ages may reflect late diagenesis to regional metamorphism (Figure 2). Therefore, our results may reflect multi-stage illitization from early to late diagenesis or regional metamorphism. Illite fractions from samples close to dolerite shows formation age between 204.6 and 170.1 Ma, consistent with the time of the Jurrassic-aged Karoo Large Igneous Province (KLIP) dolerite sills and dykes intrusions at ~ 180 Ma (Figure 2). This illustrates that these illites experienced a partial or total age resetting through recrystallization due to the late thermal anomaly/ contact metamorphism induced by the intrusion of dolerites. The correlation between the timing of the youngest mineral transformation processes and the KLIP represents strong evidence suggesting that petroleum source rocks of the Ecca Group experienced a thermal overprinting event ~ 180 Ma ago. This late thermal anomaly is consistent with previous organic geochemical data illustrating thermal over-maturation and exhaustion of the Ecca's shales considerably destroying their shale gas potential in the vicinity of dolerite intrusions.

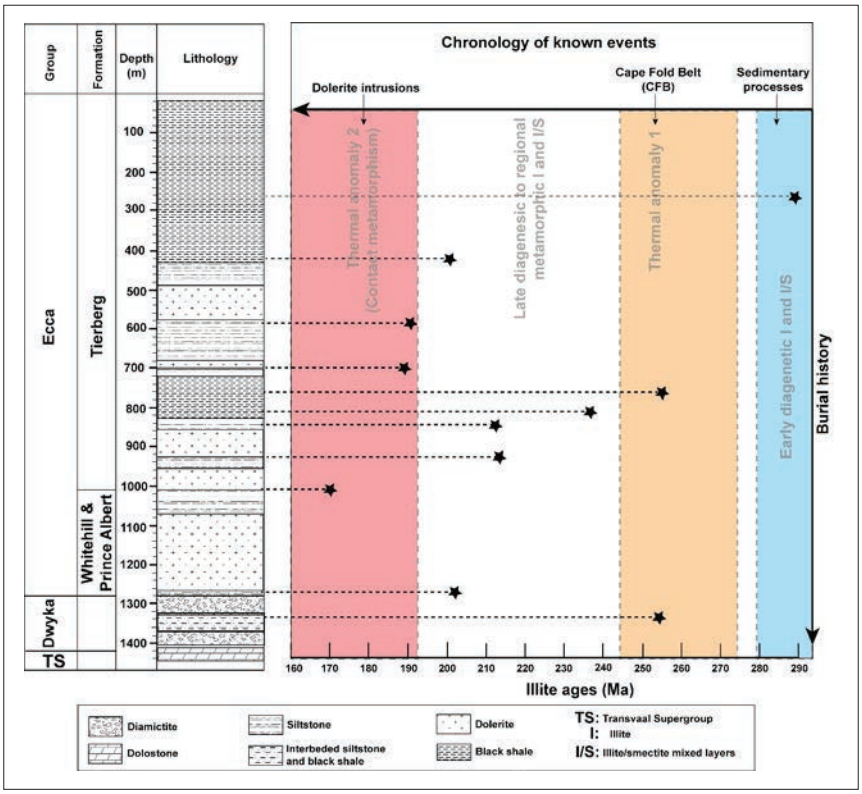

Figure 2: Illite Ar – Ar Ages plotted against sample depths in BH 47 (black stars). The length of dashed lines represents the distance of samples to the dolerite intrusions (longer = distal to the dolerite; shorter = closer to the dolerites) while blue, orange and red fields represent age-constrained events related to the Main Karoo Basin's history. Samples close to the dolerite intrusions plot in the red field indicating illite age-reset/contact metamorphism during the Jurassic-aged LIP.

Past Glacial Episodes and Geomorphology

PALEOMAGNETISM AND GEOCHEMISTRY OF THE MESOARCHEAN KLIPWAL DIAMICTITE, MOZAAN GROUP, PONGOLA SUPERGROUP, SOUTH AFRICA.

Tshepang Lechekoane

The Mozaan Group of the Pongola Supergroup together with the correlative Witwatersrand Supergroup host the oldest, best-preserved cover successions deposited on a stable craton between 2.96 – 2.84 Ga ago. Little is known about the tectonic processes which operated on the young Earth in the Archean. Paleomagnetism remains the most robust method with which early cratonic movements can be constrained. There is a poor paleomagnetic record for the Kaapvaal Craton during the Archean. This study aims to contribute to the pole density and constrain the apparent polar wander path (APWP) for the Kaapvaal Craton during this period, as well as to interrogate the sediment source of the Klipwal Member diamictite. The provenance of Klipwal diamictite was previously poorly understood. This study is set to contribute new insight on the origin of the sediments making up this unit. The geochemical data suggests a strong mafic to ultramafic source with minor felsic input. The CIA is consistent with moderate weathering which probably took place at the source. The elevated levels of iron are attributed to the precipitation of ferric-oxyhydroxides from the anoxic seawater with a high concentration of dissolved iron. Petrographic and field studies suggest that sediments were sourced from an off craton greenstone terrane adjacent to the Witwatersrand – Mozaan basin indicating that the extent of glaciation was more extensive than previously thought. A glacial influence is envisioned but more reliable data is required. During thermal demagnetisation, a low temperature (250 - 350˚C), steep northerly negatively inclined component HIG was observed. Because of the negative bootstrap fold test, this component has been interpreted to be an overprint. A total of six sites were sampled but only five produced meaningful results. Sites KWU, KWV, KWW, KWX and KWZ show no preferred grouping which impedes the calculation of a reliable pole. Individual VGPs were calculated for these sites to reveal three groups when plotted together with Meso – Neoarchean poles. Sites KWX, KWZ and other previously proposed poles for the Klipwal diamictite record an overprint around 2.8 - 2.7 Ga This overprint is associated with post-Pongola granites which intruded the Pongola Supergroup during this interval. Another group is observed around 1.05 Ga as recorded by sites KWU and KWV. This event is interpreted as an overprint associated with the Namaqua-Natal orogeny which affected the eastern margin of the Kaapvaal Craton during this time. All the sites were ultimately combined to calculate an average pole situated at longitude = -40.3˚ and latitude 69.1˚ with α^{95} = 12 presented in this study. This new pole together with those previously proposed demonstrates that a reliable APWP for the Kaapvaal Craton during the Archean remains elusive.

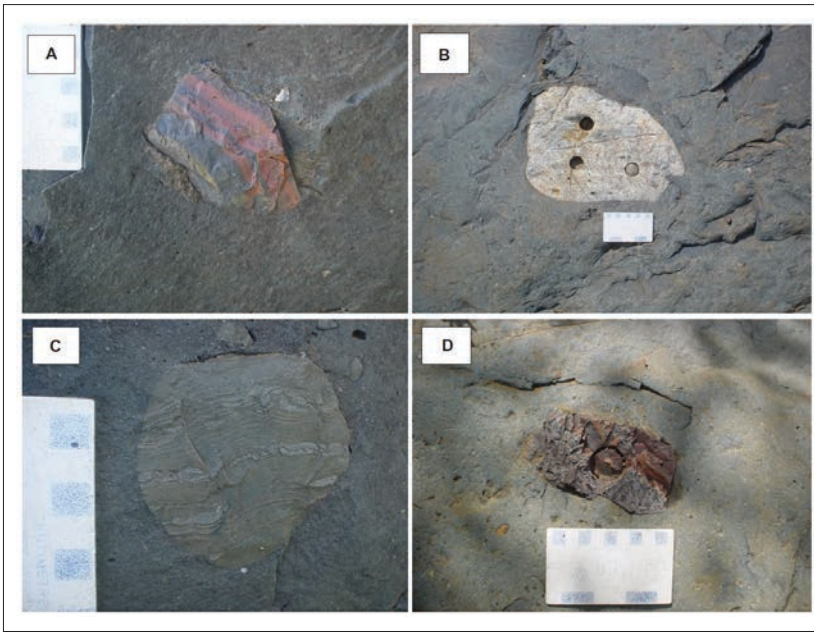

Figure 1. Photographs of some of the clast types occurring in the Klipwal diamictite in Swaziland. A - angular iron-formation clast, B - well-rounded quartzite clast. C- well-rounded banded chert clast and D - subangular chert clast.

GLACIAL AND INTERGLACIAL SEDIMENTARY RECORD IN PALEO-FJORDS: EVIDENCE FOR PERMO-CARBONIFEROUS ICE-MARGIN FLUCTUATIONS AND GLACIO-ISOSTATIC REBOUND (DWYKA GROUP, SOUTH-EASTERN SOUTH AFRICA)

Pierre Dietrich and Axel Hofmann

The Gondwana-wide Permo-Carboniferous glaciogenic deposits are assumed to record the growth and decay of ice masses separated by intermittent interstadials. In Namibia and south-western South Africa, up to four deglacial sequences have been identified in the Dwyka Group, forming the basal succession of the classic Karoo Supergroup. The Dwyka Group in KwaZulu-Natal, south-east South Africa, directly lies on a highly uneven preglacial topography characterized by 100-200 m-deep and 1-3 km-wide U-shaped valleys (Figure 1A) carved in the bedrock by glacial abrasion (Glacial Erosion Surface, GES, 1). Glaciogenic deposits are up to 200 m thick (Figure 1B) in the axis of these valleys while they pinch out on paleo-highs. Although mainly made up of massive diamictite, the Dwyka Group in this region also comprises interstratified turbiditic, coastal and fluvioglacial sandstone and conglomerate layers that point out for ice margin advance-retreat cycles and relative sea level fluctuations, at least partly forced by glacio-isostatic adjustment process. Glacial valleys represent paleo-fjords as observed elsewhere in Southern Gondwana.

Three superimposed units made up of both glacial and non-glacial deposits compose the Dwyka Group (Fig. B). The up to 70 m-thick lower unit consists of massive to faintly-laminated diamictite bearing abundant boulder-sized lonestones (Figure 1C). This lower unit wedges out and onlaps on valley flanks while its top is characterized by glacial striae and grooves (GES 2) remobilized into wave ripples (Figures 1D & E). Above, a 50-m thick coarsening-upward sequence forms the second unit which consists in massive lonestone-bearing diamictite interstratified with normally-graded sandstone beds devoid of lonestones. These facies grade upward into a 10 to 20 m-thick planar, trough and sigmoidal cross-bedded conglomeratic sandstones disturbed by subglacial deformation (GES 3). The third unit, consisting of massive diamictite bearing concretions and rare lonestones, is topped by discontinuous patches of highly glacially-deformed (extensional step fractures, subglacial glaciotectonic deformation, GES 4) conglomeratic sandstones characterized by cross bedding and undulating laminations (Figure 1F). Black shales of the Ecca Group, usually interpreted as postglacial deposits, directly rest on this ultimate glacial surface.

Diamictite intervals likely result from deposition in a glaciomarine environment by important rain-out beneath or immediately in front of a floating ice shelf and/or a tidewater glacier. The reworking of GES 2, which itself onlaps on glacial valley flanks, by wave action in a shallow coastal environment indicate: (1) local ice free condition, and (2) that valley interfluves were emerged at that time and valleys themselves thus constituted fjords. In the second unit, normally-graded sandstone beds and cross-bedded sandstone horizons, interpreted as subaqueous sediment density flow and fluvioglacial deposits, also indicate minor ice margin retreat. The upward transition from sediment density flow deposits interstratified within glaciomarine diamictite to fluvioglacial conglomeratic sandstones is interpreted as the emergence of a subaqueous ice-contact fan into an ice-contact delta characterized by a distinctive fluvioglacial delta plain. Finally, glacially-deformed conglomeratic sandstones of the third unit, capping glaciomarine deposits, are also interpreted as being emplaced in a proximal fluvioglacial to glacio-deltaic environment.

The vertical superimposition of glaciomarine and proglacial facies within the Dwyka Group constitutes a strong indicator of ice margin fluctuations throughout the study area. In such a context, the glacial maximum is likely marked by the basal erosion surface that carved U-shaped valleys out. The glacial surface recorded on top of the first unit is suspected to represent a temporary stillstand marked into an ice margin retreat; ice grounding and reworking of the glacial surface into a shallow environment likely resulting from RSL fall forced by the glacio-isostatic rebound (Boulton, 1990). Similarly, as the second and third units form shallowing-upward successions, they are also interpreted as having been deposited in a context of RSL fall forced by the glacio-isostatic rebound during ice margin retreat phases (Dietrich et al., 2017). Capping glacial surfaces (GESs 3 and 4), on the other hand, could relate to subsequent glacial advances (Powell and Cooper, 2002). In such a setting, marine and glaciomarine deposits directly resting on top of these glacial surfaces are interpreted as being deposited in front of rapidly retreating (collapse?) ice margins in glacio-isostatic depressions, as also indicated by the relative scarcity of lonestones. The virtual absence of lonestone-free,

fine-grained deposits throughout the Dwyka Group in this area strongly suggests that the ice margin did not retreat far away from the studied area and then sedimentation rates remained unusually high. In such a proximal depositional setting, we propose that the whole Dwyka succession was deposited rapidly, in agreement with the work of Haldorsen et al. (2001). Recorded relative sea level fluctuations were then most likely provided by crustal movements forced by glacio-isostatic processes (deflexion and rebound) and by glacio-eustatic sea level change, without any contribution from the subsidence (Dietrich et al., 2017). Preglacial topography played a preponderant role in defining paleogeography (fjords) and influencing glacial dynamic and stratigraphic architecture, for instance in focusing ice flows and sedimentary fluxes.

Boulton, G.S. 1990, Sedimentary and sea level changes during glacial cycles and their control on glaciomarine facies architecture, in Dowdeswell, J.A., Scourse, J.D. eds., *Glacimarine Environments: Processes and Sediments*, Geological Society of London, Special Publication, 53, p. 15-52.

Haldorsen, S., Von Brunn, V., Maud, R. and Truter, D.E. 2001, A Weichselian deglaciation model applied to the Early Permian glaciation in the Northeastern Karoo Basin, South Africa. Journal of Quaternary Science, 16, p. 583-593.

Powell, R.D. and Cooper, J.M. 2002, A glacial sequence stratigraphic model for temperate, glaciated continental shelves, in Dowdeswell, J.A., O Cofaigh, C. eds., *Glacier-influenced Sedimentation on High-Latitude Continental Margins,* Geological Society of London, Special Publication, 203, p. 215-244.

Dietrich, P., Ghienne, J.-F., Schuster, M., Lajeunesse, P., Nutz, A., Deschamps, R., Roquin, C. and Duringer, P. 2017, From outwash to coastal systems in the Portneuf-Forestville deltaic complex (Québec North Shore): Anatomy of a forced regressive deglacial sequence, Sedimentology, 64, p. 1044-1078.

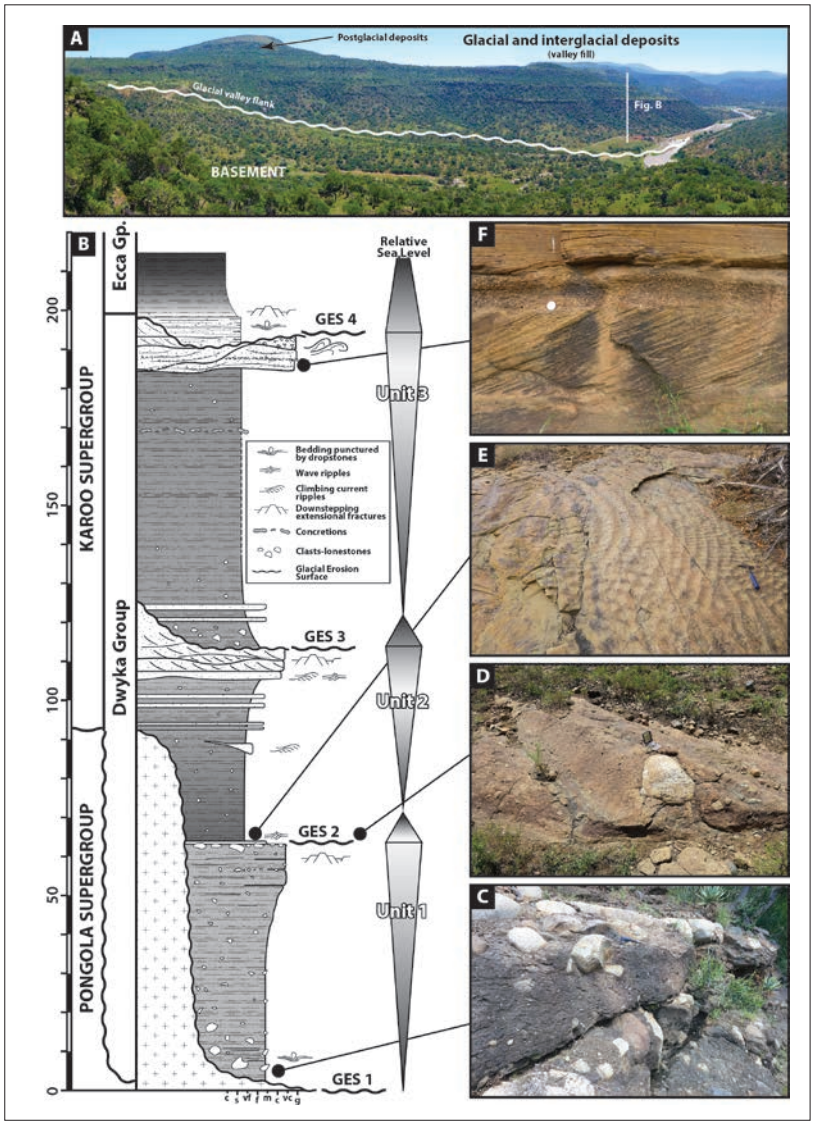

Figure 1 (A) Panoramic picture of a valley carved into the bedrock (Pongola Supergroup) and filled up by the glaciogenic Dwyka Group. (B) Synthetic sedimentary log of the Dwyka Group, and interpretation for relative sea level changes. (C) Boulder-bearing, massive to faintly-laminated diamictite. (D) Glacial striae and grooves on top of the first sedimentary unit. (E) Polygonal wave ripples, in place reworking the second glacial erosion surface (GES). (F) Planar cross bedding and conglomeratic layers characterising the top of the third sedimentary unit, interpreted as fluvioglacial deposits.

COSMOGENIC 10Be AND 26Al STUDIES ON THE SURFACE OF THE RISING STAR SITE, CRADLE OF HUMANKIND: MYSTERY OF THE TRUE DENUDATION RATES

Tebogo V. Makhubela, Jan D. Kramers, Dirk Scherler[1], Hella Wittmann[1], Paul H.G.M. Dirks[2], Stephan R. Winkler[3]

[1] Deutsches Geoforschunszentrum Potsdam, [2] James Cook University, Townsville, Australia, [3] iThemba Labs Johannesburg

Assessing the history and rate of landscape change of the Cradle of Humankind (CoH), UNESCO World Heritage Site, South Africa, is important for better understanding of paleo-ecosystems and hominin evolution in southern Africa, as well as fossil deposition and preservation in caves. In the last three decades, the use of cosmogenic nuclides has become a preferred method to quantitatively study and understand earth surface processes, landscape changes and their rates (Granger et al., 2013). Beryllium-10 (^{10}Be) produced in quartz is the most widely used cosmogenic radionuclide (half-life = 1.39 Myr) for studies of denudation rate. In situ produced Aluminium-26 (^{26}Al) in quartz is used less frequently for denudation studies but commonly paired with ^{10}Be for studies of cosmogenic nuclide burial dating.

In the CoH, cosmogenic nuclides have previously been used for studies of landscape changes (Dirks et al., 2010; 2016), as well as for burial dating of the fossil-bearing cave deposits (Partridge et al., 2003; Gibbon et al., 2014; Granger et al., 2015). We present new *in situ* cosmogenic 10Be and ^{26}Al concentrations ([^{10}Be] and [^{26}Al], respectively) in quartz and chert from soils, chert float and chert horizons in outcropping dolomite, on the peneplain surface above the Rising Star cave system (Figure 1). The Rising Star landscape is characterized by shallowly dipping planar surfaces (slope angles of < 5°) with a few monadnocks-like ridges that give the area a rolling or undulating surface of low relief. Entrance to the Rising Star cave system occurs on a NE facing scarp of one of these ridges (~ 12 m above the altitude of the Bloubank River channel). A 1.3 m-thick capping chert unit overlies a 15–20 m thick, horizon of the Monte Christo Formation, which hosts most chambers within the system. The Monte Christo Formation is a stromatolitic dolomite, rich in chert, with thin oolitic beds near its base, and interbedded with generally thin (< 50 cm) shale horizons. In addition to the capping chert unit, the dolomite bedrock also contains abundant thin (< 10 cm) chert horizons.

Soil samples yield the highest [^{10}Be] and [^{26}Al] in the range 2.28 – 3.91 ($\times10^6$) atoms per gram (a/g) and 13.13 – 19.58 ($\times10^6$) a/g, respectively. Bedrock samples yield the lowest cosmogenic nuclides concentrations which range between 0.457 – 0.904 ($\times10^6$) a/g for [^{10}Be], and 3.79 – 6.66 ($\times10^6$) a/g for [^{26}Al]. The [^{10}Be] and [^{26}Al] for the clast samples range between those of the soil and bedrock samples: 1.02 – 2.43 ($\times10^6$) a/g and 7.79 – 14.04 ($\times10^6$) a/g.

The [^{10}Be] were used to calculate average apparent denudation rates, and the soil and clast samples yield average erosion rates similar within 1σ: 3.58 ± 1.91 m/Ma and 4.29 ± 0.69 m/Ma, respectively. The average apparent denudation rate for the bedrock chert is up to three times faster (11.28 ± 1.09 m/Ma) than for soils and clasts in this study and previous studies (Figure 2). All soil samples have ^{26}Al/^{10}Be ratios significantly lower than the 6.75 surface steady state ratio.

Based on the average 10Be denudation rates previously found (3.6 m/Ma, Dirks et al., 2010; 3.44 m/Ma, Dirks et al., 2016), the landscape across the CoH is considered old and eroding slowly. High erosion rates similar to our results (5.13 - 15.02 m/Ma, Dirks et al., 2010; 2016; Figure 2) for chert bedrock are ascribed to fast river incision or a recent partial collapse event. In contrast, we think our high outcrop erosion rates reflect true denudation and the low apparent values from soil samples indicate long retention of quartz on surface, while dolomite is largely removed in solution. The quartz then experiences periods of burial and reworking in caves, river terraces and/or deep soils, resulting in low ^{26}Al/^{10}Be ratios.

Dirks et al., 2010. Science, 328, 205-208.
Dirks and Berger, 2013. J. Afr. Earth Sci. 78, 109-131.
Dirks et al., 2016. J. Hum. Evol., 96, 19-34.
Gibbon et al., 2014. Quat Geochron., 24, 10-15.
Granger et al., 2013. Geol. Soc. Am. Bull. 125, 1379-1402.
Granger et al., 2015. Nature, 522, 85-88.
Partridge et al., 2003. Science, 300, 607-612.

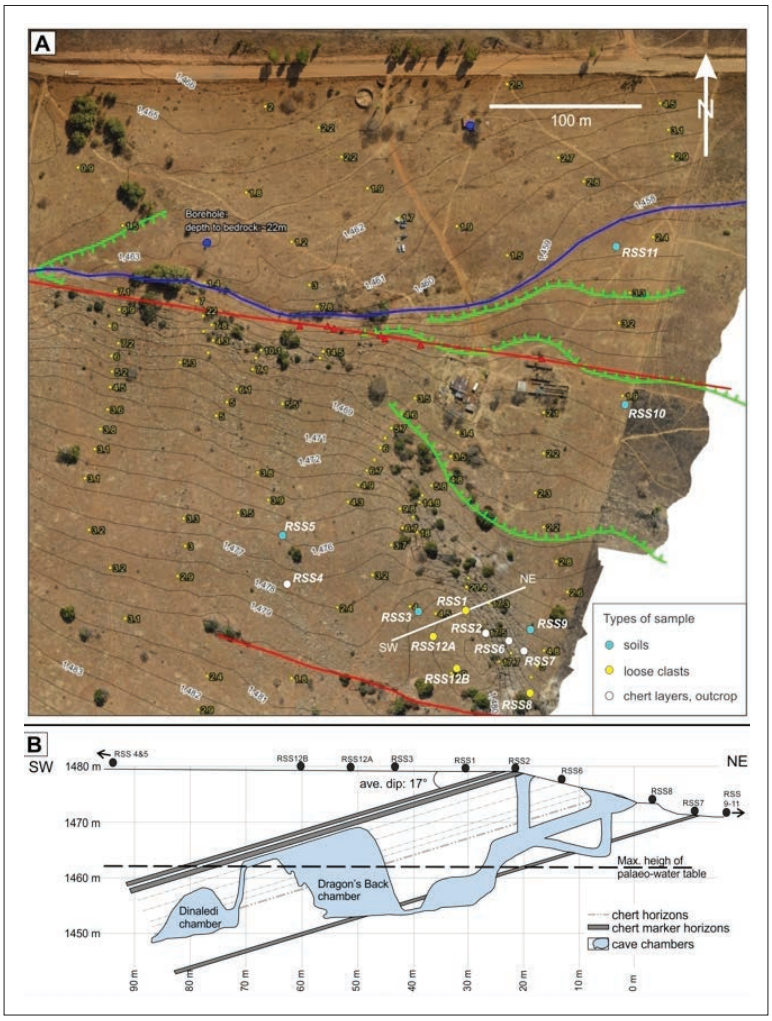

Figure 1: Samples collected and their location on the surface of the Rising Star cave system. (a) UAV map of the Rising Star property, with topography (1 m intervals) and spot measurements for slope (based on spacing of topo lines), showing the geomorphological interpretation of the evolving landscape, terrace formation and channel migration. Note that the streambed is bounded by two faults, in a rift-like geometry with alluvial deposits along the rift. (Alluvial terrace scarps: green; fault: red; river bed: blue) Three types of samples were collected: soils, loose cobble-sized clasts and fragments of chert from the horizons in the dolomite bedrock. (b) Profile of the Rising Star showing the location of the samples on the surface above the cave system.

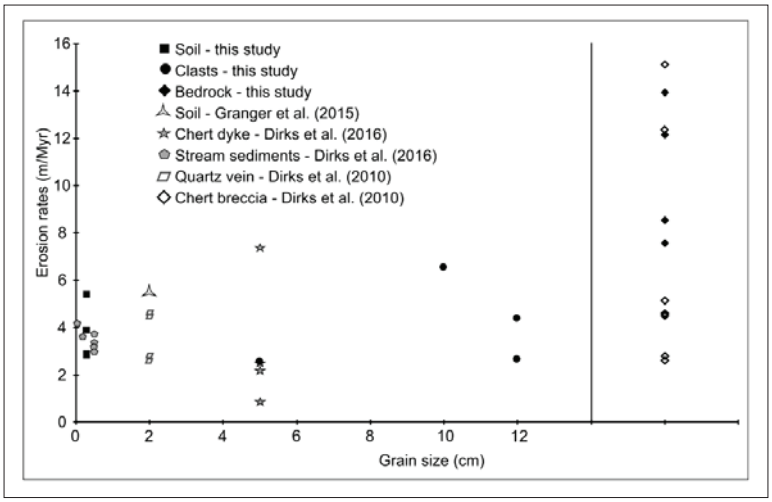

Figure 2: Apparent erosion rates plotted against grain size for soil and clast samples (left) and bedrock samples (right). Data from this study compared to published data. Apparent erosion rates for samples collected in situ from chert horizons within the dolomite bedrock (average 11.28 m/Ma) are 2-3 times faster than erosion rates for the soils and clasts.

POSTGRADUATE STUDENTS IN PPM (2016)

STUDENT	P/F time	THESIS TOPIC	SUPERVISORS
Abraham, Rowen	F	CO_2 adsorption in Karoo shales	N. Wagner
Adeniyi, Elijah (MSc)	F	Gas potential in Karoo (Karen project)	N. Beukes
Badenhorst , Charlotte (PhD)	F	Charphite – char as a replacement for natural graphite	N. Wagner
Blignaut, Lauren (PhD)	P	Ore genesis in Manganese Fields	K.S. Viljoen, H. Tsikos
Boshoff, Pedro (MSc)	P	Speleogenesis in Cradle of Humankind	J. Kramers, H. van Niekerk
Bowden, Laura (PhD)	F	Detrital zircon age determination of Karoo age sediments	N.J. Beukes, C Vorster
Bukanga, Amuli (MSc)	P	Small scale mining, olivine	F. Senzani
Chabalala, Vongani (PhD)	P	Coal petrology applied to gas exploration	N. Wagner
Da Costa, Giuliana (PhD)	F	Evaluation of syn-sedimentary gold deposition in the Witwatersrand Basin	A. Hofmann
De Kock, Conrad (MSc)	F	Mineralization at Sishen iron mine	A.J.B. Smith, N.J. Beukes
Dzvinamurungu, Thomas (PhD)	F	Metallogenesis of Nkomati nickel mine	K.S. Viljoen
Fabien, Francis (MSc)	P	Coal oxidation in underground mines	N. Wagner
Fitschen, Juergen (MSc)	P	Stress-strain analysis, Barberton M.L.	A. Hofmann
Fitzpatrick, Stuart (MSc)	F	Palaeomagnetism, continent reconstruction	M.O. de Kock, H. van Niekerk, C. Vorster
Gevera, Patrick (MSc)	F	Medical Geology	H. Mouri
Hlongwani, Caroline (MSc)	F	Study of iron mineralization	A.J.B. Smith
Hlungwani, Peace	F	The petrography and geochemistry of the layered Molopo Farms Complex.	M. Elburg
Jodder, Jaganmoy (PhD)	F	Unraveling the chronostratigraphy of the Iron Ore Group (IOG) of the Singhbhum craton, India	A. Hofmann
Kekana, Papi (MSc)	F	Temporal and spatial variation coal quality	N. Wagner
Koki, Christa (MSc)	F	Medical Geology	H. Mouri
Lum, Jullieta (MSc)	F	Beryl minerals of Southern Africa	K.S. Viljoen, B. Cairncross
Luskin, Casey (PhD)	F	Paleomagnetism of the Nsuze Group, Pongola Supergroup, Kaapvaal Craton	M. de Kock, H. Wabo
Magwaza, Boniswa (MSc)	F	Zircons in metamorphism	M. Elburg
Makhubela, Tebogo V. (PhD)	P	Geochronology of cave deposits, landscape evolution	J. Kramers, D. Scherler, G. Belyanin
Makukule, Xitshembiso	F	Petrography and image analysis to validate coal washability	N. Wagner
Masangane, Noma (MSc)	F	Iron mineralization, Wolhaarkop Dome	A.J.B. Smith, N.J. Beukes
Mashamba, M. Lucas (MSc)	P	Acid mine drainage, Brugspruit, MP	J. Kramers, H. Coetzee (CGS)
Matiane, Arnold (MSc)	F	Rare Earth Elements in coal ashes	N. Wagner
McGeer, Bianca	F	Cause of earthquakes in South Africa, specifically larger magnitude ones in the Wits gold mining region	H. van Niekerk, J. Lehmann, M. Manzi (Wits)
Mgoqi, Aviwe (MSc)	F	Acid rock drainage, MP and Limpopo	J. Kramers, D. Love (Golder assoc.)
Mkhatshwa, Sindile (PhD)	F	Geometallurgical studies	K.S. Viljoen
Monareng, Fisah (MSc)	F	Paleomagnetism, Kalahari Manganese Field	M.O. de Kock, N. Beukes, L. Blignaut
Morake, Mabuela (MSc)	F	Karoo-related dykes in Antarctica	M. Knoper, M. Elburg, J. Kramers

Mpanza, Zama (MSc)	F	Cratonic mantle beneath Premier kimberlite	K.S. Viljoen, S. Tappe
Mphaphuli, Maseda (MSc)	F	Soutpansberg Coalfield	N. Wagner
Naude, Grethe (MSc)	P	Process temperature in a semi-coke plant	N. Wagner
Ndhlovu, Brian (MSc)	F	Geometallurgy of sulphides in the Plat Reef	K.S. Viljoen
Nendouvhada, Ndivhuho (MSc)	F	Comparison coal composition in Botswana	N. Wagner
Ngobeli, Rebeun (MSc)	F	Detrital zircon age determination of the Makganyene Formation	N.J. Beukes, C Vorster
Nkomo, Thobeka (MSc)	F	Pb-Zn-Cu ores of Aggeneys-Gamsberg	K.S. Viljoen
Nthloro, Boitumela (MSc)	F	Iron mineralization Kolomela Mine	A.J.B. Smith, N. Beukes
Nxumalo, Valerie (PhD)	P	Springbok Flats Coalfield, uranium and sediment provenance	J. Kramers, B. Cairncross, C. Vorster
O'Kennedy, Johan	F	Jurassic dykes from western Dronning Maud Land, Antarctica	M. Knoper
Opperman, Alicia (MSc)	P	Structural geology, Kalahari Mn field	N.J. Beukes, L.C. Blignaut
Radzivhoni, Charles (MSc)	P	Geometallurgy Mogalakwena Mine	K.S. Viljoen
Rammilla, Ephriam (MSc)	F	Izermyn iron formation, Sinqeni Fm.	N.J. Beukes, A.J.B. Smith
Ravhura, Livhuwani (MSc)	F	Geochronology of Molopo Farms Complex	N.J. Beukes, C. Vorster, M.O. de Kock
Rose, Derek (PhD)	P	Geometallurgy of PGE ore at two Rivers	K.S. Viljoen. H. Mouri
Singo, N. Kenneth (PhD)	P	Remediation of abandoned mines	J. Kramers
Terblanche, Sullivan (MSc)	F	Geomorphology of Buffalo River Catchment	H. van Niekerk, C. Vorster
Tsunke, Mpho (MSc)	P	Sethlabotse project, Highveld coalfield	B. Cairncross
Vines, Marylou (PhD)	F	Studies on kimberlites and their xenoliths	S. Tappe
Zardad, Sabiyya (MSc)	F	Sedimentology and age determination for the Rooihoogte Formation	A.J.B. Smith, C Vorster, N.J. Beukes

POSTDOCTORAL ASSOCIATES IN PPM (2016)

Ballouard, Christophe
Igneous petrology and geochemistry

Dietrich, Pierre
Sedimentology, particularly of glacial deposits, and past glacial episodes

Dongre, Ashish
Geochemical studies of kimberlites

Eickmann, Benjamin
Mineralogy, geochemistry and isotope studies related to the environment of early life

Humbert, Fabien
Structural and paleomagnetic studies on the Paleoproterozoic Hekpoort and Ongeluk volcanic formations, and implications for the evolution of the Transvaal Basin

Massuyeau, Malcolm

Mantle melting processes and thermodynamics, with emphasis on the effect of H2O and CO2

Ossa Ossa, Frantz Gerard
Mineralogical and geochemical studies of low grade metamorphism and diagenesis, with focus on clay mineralogy

MSc STUDENTS THAT GRADUATED IN 2016

Ramakoloi, Ntshebo Christinah (MSc, 12th April 2016)
Compositional variation of the Pt-Pd bismuthotellurides in the Platreef Akanani Prospect, Lonmin PLC. (s: KS Viljoen)

Moitsi, Matome Ernest (MSc, 28th September 2016)
A geometallurgical study of the mineralized footwall of the Brakspruit Facies of the Merensky Reef at the Lonmin Karee Pt mine, Bushveld Complex. South Africa. (s: KS Viljoen, co: M. Knoper)

Motloba, Gloria Boikanyo (MSc, 28th September 2016)
A geometallurgical Assessment of the P2 and P1 units of the Platreef at Lonmin's Akanani Project, Northern Limb, Bushveld Complex (s: K.S. Viljoen, co: AJB Smith)

Vafeas, Nicholas Andrew (MSc, 28th September 2016, with Distinction)
Petrography and Geochemistry of the Hotazel Formation on Mukulu 265, Kalahari Manganese Field, Northern Cape Province (s: N. Beukes, co: AJB Smith, L. Blignaut).

PUBLISHED PAPERS, 2016 (peer-reviewed international journals and book chapters)

Agangi, A., Hofmann, A., Eickmann, B., Marin-Carbonne, J. and Reddy, S. M. (2016) An atmospheric source of S in Mesoarchaean structurally-controlled gold mineralisation of the Barberton Greenstone Belt. Precambrian Research, 285, 10-20.
Alebouyeh Semami, F., De Kock, M.O., Söderlund, U., Gumsley, A.P., Da Silva, R., Beukes, N.J. and Armstrong, R. (2016) New U–Pb geochronologic and palaeomagnetic constraints on the late Palaeoproterozoic Hartley magmatic event: evidence for a potential large igneous province in the Kaapvaal Craton during Kalahari assembly, South Africa. Gff, 138(1):164-182. DOI:10.1080/11035897.2015.1124917
Andersen, T., Kristoffersen, M. and Elburg, M. (2016) How far can we trust provenance and crustal evolution information from detrital zircons? A South African case study. Gondwana Research, 34, 129-148. doi: 10.1016/j.gr.2016.03.003. SCI 2015: 8.74.
Andersen, T., Elburg, M.A. and Cawthorn-Blazeby, A. (2016) U-Pb and Lu-Hf zircon data in young sediments reflect sedimentary recycling in eastern South Africa. Journal of the Geological Society of London, 173, 337-351. SCI 2105: 2.5
Aulbach, S., Gerdes, A. and Viljoen, K.S. (2016) Formation of diamondiferous kyanite-eclogite in a subduction zone mélange. Geochimica et Cosmochimica Acta, 179, 156-176.
Beukes, N.J., Swindell, E.P.W. and Wabo, H. (2016) Manganese deposits of Africa. Episodes, 39, 285-317.
Cairncross, B. (2016) Ajoite: Connoisseur's Choice, Rocks & Minerals, 91, 426-432.
Cairncross, B. (2016) Shigaite: Connoisseur's Choice. Rocks & Minerals, 91, 150-153.
Cairncross, B., Fraser, A. and McGregor, S. (2016) The Thabazimbi mine cave, Limpopo Province, South Africa. Rocks & Minerals, 91, 322-331.
Chalapathi Rao, N.V., Dongre, A., Wu, F. and Lehmann, B. (2016) A late cretaceous (ca. 90 Ma) kimberlite event in southern India: Implication for sub-continental lithospheric mantle evolution and diamond exploration. Gondwana Research, 35, 378-389.
Chitsiga T.L, Daramola, M.O., Wagner N.J., Ngoy, J.M. 2016. Effect of the presence of water-soluble amines on the Carbon Dioxide (CO2) adsorption capacity of amine-grafted poly-succinimide (PSI) adsorbent during CO2 Capture. Energy Procedia 86, p 90 - 105.
Clemens, J.D. and Elburg, M.A. (2016) Possible spatial variability in the Selwyn Block of Central Victoria: evidence from Late Devonian felsic igneous rocks. Australian Journal of Earth Sciences, 63, 187-192, doi: 10.1080/08120099.2016.1158736. SCI 2015: 2.29.
Cornell, D., Zack, T., Andersen, T., Corfu, F., Frei, D. and van Schijndel, V. (2016) Th-U-Pb zircon geochronology of the Palaeoproterozoic Hartley Formation porphyry by six methods, with age uncertainty approaching 1 Ma. South African Journal of Geology, 119, 473-494.

Czaja, A.D., Beukes, N.J. and Osterhout, J.T. (2016) Sulfur-oxidizing bacteria prior to the Great Oxidation Event from the 2.52 Ga Gamohaan Formation of South Africa. Geology, 44, 983-986.

Da Costa, G., Hofmann, A.. and Agangi, A. (2016). Provenance of detrital pyrite in Archean sedimentary rocks: Examples from the Witwatersrand Basin. In: Mazumder, R. (Ed.), Sediment provenance: influences on compositional change from source to sink. Elsevier, pp. 509-531 (http://dx.doi.org/10.1016/B978-0-12-803386-9.00018-6).

Delvigne, C., Opfergelt, S., Cardinal, D., Hofmann, A. and André, L. (2016) Desilication in Archean weathering processes traced by silicon isotopes and Ge/Si ratios. Chemical Geology, 420, 139-147.

Dongre, A.N., Viljoen KS, Chalapathi Rao NV, Gucsik A (2016) Origin of Ti-rich garnets in the groundmass of Wajrakarur field kimberlites, southern India: Insights from EPMA and Raman spectroscopy. Mineralogy and Petrology, 110, 295-307.

Dorland, H.C., Campbell, Q.P., Le Roux, M., McMillan, K., Dorland, M.I., Erasmus, P. and Wagner, N. (2016) Simulation of washability and liberation information from photographs. In: Proceedings of the XVIII International Coal Preparation Congress. (Editor: Litvinenko, V.) 28 June – 1 July 2016, Saint-Petersburg, Russia, Springer, pp. 249-254.

Elburg, M., Andersen, T., Jacobs, J., Läufer, A., Ruppel, A., Krohne, N. and Damaske, D. (2016) One hundred and fifty million years of intrusive activity in the Sør Rondane Mountains (East Antarctica): implications for Gondwana assembly. Journal of Geology, 124, 1-26. SCI 2015: 2.58.

Elliott, M.C., Dirks, P.H.G.M., Berger, L.R., Roberts, E.MKramers, J.D., John Hawks, J., Patrick S Randolph-Quinney, P.S., Musiba, C.M., Churchill, S.E., De Ruiter, D.J., Schmid, P., Backwell, L.R., Belyanin, G.A., Boshoff, P., Hunter, K.L., Feuerriegel, E.M., Gurtov, A., Harrison, J.G., Hunter, R., Kruger, A., Morris, H. and Peixotto, B., (2016) Geological and taphonomic context of excavations within the Rising Star cave system. American Journal of Physical Anthropology, 159, 138-138.

Fritz, J., Tagle, R., Ashworth, L., Schmitt, R. T., Hofmann, A., Luais, B., Harris, P., Hoehnel, D., Özdemir, S., Mohr-Westheide, T. and Koeberl, C. (2016) Nondestructive spectroscopic and petrochemical investigations of Paleoarchean spherule layers from the ICDP drill core BARB5, Barberton Mountain Land, South Africa. Meteoritics and Planetary Science, 51, 2441–2458.

Frost-Killian, S., Master, S., Viljoen, R.P. and Wilson, M.G.C. (2016) The great mineral fields of Africa: Introduction. Episodes, 39, 85-103.

Hoffmann, J.E., Kröner, A., Hegner, E., Viehmann, S., Xie, H., Iaccheri, L.M., Schneider, K.P., Hofmann, A., Wong, J., Geng, H. and Yang, J. (2016) Source composition, fractional crystallization and magma mixing processes in the 3.48–3.43 Ga Tsawela tonalite suite (Ancient Gneiss Complex, Swaziland) – Implications for Palaeoarchaean geodynamics. Precambrian Research, 276, 43-66.

Keeditse, M., Rajesh, H.M., Belyanin, G.A., Fukuyama, M., Tsunogae, T. (2016) Primary magmatic amphibole in Archaean meta-pyroxenite from the central zone of the Limpopo Complex, South Africa. South African Journal of Geology, 119, 607-622.

Kramers, J.D., 2016. Isochron, In: Gilbert, A.S., Goldberg, P., Holliday, V.T., Mandel, R.D., Sternberg, R.S., Encyclopedia of Geoarchaeology, Springer Verlag, ISNN 978-94-007-4827-9, pp 448-449.

Kristoffersen, M., Andersen, T., Elburg, M.A. and Watkeys, M. (2016) Detrital zircon in a supercontinental setting: Locally derived and far-transported components in the Ordovician Natal Group, South Africa. Journal of the Geological Society of London, 173, 203-215. SCI 2105: 2.5.

Kurzweil, F., Wille, M., Ganteret, N., Beukes, N.J. and Schoenberg, R. (2016) Manganese oxide shuttling in pre-GOE oceans – evidence from molybdenum and iron isotopes. Earth and Planetary Science Letters, 452, 69-78.

Lehmann, J., Saalmann, K., Naydenov, K.V., Milani, L., Belyanin, G.A., Zwingmann, H., Charlesworth G. and Kinnaird, J.A. (2016) Structural and geochronological constraints on the Pan-African tectonic evolution of the northern Damara Belt, Namibia. Tectonics, 35, 103-135.

Lum, J., Viljoen, K.S. and Cairncross, B. (2016) Mineralogical and geochemical characteristics of emeralds from the Leydsdorp area, South Africa. South African Journal of Geology, 119, 359-378.

Lum, J., Viljoen, K.S., Cairncross, B. and Frei, D. (2016) Mineralogical and geochemical characteristics of beryl (aquamarine) from the Erongo volcanic complex, Namibia. Journal of African Earth Sciences 124, 104-125.

Luo, G., Ono, S., Beukes, N.J., Wang, D.T., Xie, S. and Summons, R.E. (2016) Rapid oxygenation of Earth's atmosphere 2.33 billion years ago. Science Advances 13 May 2016: Vol. 2, no. 5, e1600134 DOI: 10.1126/sciadv.1600134.

Mare, L.P., De Kock, M.O., Cairncross, B. and Mouri, H. (2016) Magnetic evaluation of the palaeothermal variation across the Karoo Basin, South Africa. South African Journal of Geology, 119, 435-452. DOI:10.2113/gssajg.119.2.435.

Mavhengere, P., Vittee, T., Wagner, NJ., Kauchali, S. 2016. An Algorithm for Determining Kinetic Parameters of the Dissociation of Complex Solid Fuels. SAIMM, vol 116, 55-63.

Munyangane, P., Mouri, H. and Kramers, J., 2016. Assessment of some potential harmful trace elements (PHTEs) in the borehole water of Greater Giyani, Limpopo Province, South Africa: possible implications for human health. Environ Geochem Health. Publ. online October 10, 2016, DOI 10.1007/s10653-016-9887-0

Naydenov, K.V., Lehmann, J., Saalmann K., Milani, L,. Poterai, J., Kinnaird, J. A., Charlesworth, G., Kramers, J.D., 2016. The geology of the Matala Dome: an important piece of the Pan-African puzzle in Central Zambia. International Journal of Earth Sciences, 105: 695-712. doi: 10.1007/s00531-015-1222-y

Ossa Ossa, F. O., Hofmann, A., Vidal, O., Kramers, J. D., Belyanin, G. and Cavalazzi, B. (2016) Unusual manganese enrichment in the Mesoarchean Mozaan Group, Pongola Supergroup, South Africa. Precambrian Research, 281, 414–433.

Schröder, S., Beukes, N.J. and Armstrong, R.A. (2016) Detrital zircon constraints on the tectonostratigraphy of the Paleoproterozoic Pretoria Group, South Africa. Precambrian Research, 278, 362-393

Siahi, M., Hofmann, A., Hegner, E. and Master, S. (2016) Sedimentology and facies analysis of Mesoarchaean carbonate rocks of the Pongola Supergroup, South Africa. Precambrian Research, 278, 244–264.

Smart, K.A., Tappe, S., Stern, R.A., Webb, S.J. and Ashwal. L.D. (2016) A record of early Archaean plate tectonics and mantle redox preserved in Witwatersrand Diamonds. Nature Geoscience, 9, 255-259.

Smith, A.J.B. and Beukes, N.J. (2016) Palaeoproterozoic banded iron formation hosted high-grade hematite iron ore deposits of the Transvaal Supergroup, South Africa. Episodes, 39, 269-284.

Smith, A.J.B., Henry, G. and Frost-Killian, S. (2016) A review of the Birimian Supergroup and Tarkwaian Group-hosted gold deposits of Ghana. Episodes, 39, 177-197.

Tappe, S., Smart, K.A., Stracke, A., Romer, R.L, Prelevic, D. and van den Bogaard, P. (2016) Melt evolution beneath a rifted craton edge: 40Ar/39Ar geochronology and Sr-Nd-Hf-Pb isotope systematics of primitive alkaline basalts and lamprophyres from the SW Baltic Shield. Geochimica et Cosmochimica Acta, 173, 1-36.

Van Leeuwen, T., Allen, C., Elburg, M., Masonne, H.-J., Palin, M. and Hennig, J. (2016) The Palu Metamorphic Complex, NW Sulawesi, Indonesia: Origin and evolution of a young metamorphic terrane with links to Gondwana and Sundaland. Journal of Asian Earth Science, 115, 133-152. SCI 2015: 2.65.

Viljoen, F., Ramakoloi, N., Rose, D. and Reinke, C. (2015) Mineral chemistry of (Pt,Pd)-bismuthotelluride minerals in the Platreef at Zwartfontein, Akanani Project, Northern Bushveld Complex, South Africa. The Canadian Mineralogist 53,1109-1127. (Paper published by Canadian Mineralogist in November of 2016, but accepted for publication early 2016 and published under the 2015 series).

Vorster, C., Kramers, J.D., Beukes, N.J. and Van Niekerk, H.S. (2016) Detrital zircon U-Pb age determination and provenance of the Paleozoic Natal Group and Msikaba Formation, Kwazulu-Natal, South Africa. Geological Magazine, 15, 460-486.

Wabo, H., De Kock, M.O., Klausen, M.B., Söderlund, U. and Beukes, N.J. (2016) Paleomagnetism and chronology of B-1 marginal sills of the Bushveld Complex from the eastern Kaapvaal Craton, South Africa. Gff, 138(1):133-151. DOI:10.1080/11035897.2015.1099566.

Wabo, H., Olsson, J.R., De Kock, M.O., Humbert, F., Söderlund, U. and Klausen, M.B. (2016) New U–Pb age and paleomagnetic constraints from the Uitkomst Complex, South Africa: clues to the timing of intrusion. Gff, 138(1):152-163. DOI:10.1080/11035897.2015.1098726

PRESENTATIONS AT INTERNATIONAL CONFERENCES, with abstracts, 2016

Adeniyi, E., Beukes, N., Ossa Ossa, F. and de Kock, M.O. (2016) The impact of dolerite intrusions on the organic-rich mudstones of the Ecca Group in a borehole from the central Karoo Basin. Abstracts. 35th International Geological Congress, 27 August-4 September, Cape Town, South Africa. Paper Number 206.

Agangi, A., Reddy, S.M., Hofmann, A., Eickmann, B. and Marin-Carbonne, J. (2016) The source of sulfur in the Mesoarchaean gold deposits of the Barberton Greenstone Belt, southern Africa. . Abstracts. 35th International Geological Congress, 27 August-4 September, Cape Town, South Africa. Paper Number 4028.

Albut, G., Schoenberg, R., Kleinhanns, I.C., Beukes, N.J., Benger, M.,Wille, M., Babechuk M.G.,and Smith, A.J.B. (2016) Cr stable isotopic signatures of 2.32 to 2.9 Ga old marine chemical sediments. Abstracts. 35th International Geological Congress, 27 August-4 September, Cape Town, South Africa. Paper Number 5056.
Andersen, T., Elburg, M and Erambert, M. (2016) The miaskitic-to-agpaitic transition in the Pilanesberg alkaline complex, South Africa. Abstracts. 35th International Geological Congress, 27 August-4 September, Cape Town, South Africa. Paper Number 3745.
Andersen, T., Elburg, M and Kristofferson, M. (2016) Source to sink – or sink to sink? Sedimentary recycling and its effects on detrital zircon-based provenance analysis. Abstracts. 35th International Geological Congress, 27 August-4 September, Cape Town, South Africa. Paper Number 4327.
Aulbach S., Woodland A, Vasilyev P, Viljoen F (2016) Fe-based redox state of mantle eclogites: Inherited from oceanic protoliths, modified during subduction or overprinted during metasomatism? American Geophysical Union Fall Meeting, San Francisco, 12 – 16 December 2016.
Beukes, N.J. (2016) Oxygen-based redox systems in dynamic Archean oceans. Abstracts. 35th International Geological Congress, 27 August-4 September, Cape Town, South Africa. Paper Number 5476.
Beukes, N.J., De Kock, M.O. and Götz, A.E. (2016) KARIN explores the Karoo Basin and its fossil energy resources: New findings and perspectives from deep drill cores. Abstracts. 35th International Geological Congress, 27 August-4 September, Cape Town, South Africa. Paper Number
Beukes, N.J., Swindell, E.P.W. and Wabo, H. (2016) BIF-hosted manganese deposits of Africa. Abstracts. 35th International Geological Congress, 27 August-4 September, Cape Town, South Africa. Paper Number 5438.
Beukes, N.J., Swindell, E.P.W. and Wabo, H. (2016) Manganese deposits of Africa – Black shale associated deposits. Abstracts. 35th International Geological Congress, 27 August-4 September, Cape Town, South Africa. Paper Number 3111.
Blignaut, L.C., Viljoen, K.S. and Tsikos, H. (2016) A petrographic and geochemical analysis of the Kalahari manganese deposit, northern Cape, South Africa. Abstracts. 35th International Geological Congress, 29 August-2 September 2016, Cape Town, South Africa. Paper Number 3432.
Bowden, L., Beukes, N.J., Van Niekerk, H.S. and Vorster, C. (2016) Detrital zircon age population study from rocks of the Karoo Supergroup, Eastern Cape Province of South Africa. . Abstracts. 35th International Geological Congress, 27 August-4 September, Cape Town, South Africa. Paper Number 1871.
Brower, A. M., Corfu, F., Bybee, G. M., Lehmann, J., Owen-Smith, T. M. Understanding magmatic timescales and magma dynamics in Proterozoic anorthosites: a geochronological investigation of the Kunene Complex (Angola), AGU General Assembly 2016, San Francisco, USA, December 2016
Burness, S., Smart, K.A., Stevens, G, and Tappe, S. (2016) The role of sulphur during partial melting of the eclogitic cratonic mantle. Abstracts. 35th International Geological Congress, 27 August-4 September, Cape Town, South Africa. Paper Number 3929.
Cairncross, B. (2016). The Okiep copper mines – the most historic mining district in South Africa. . Abstracts. 35th International Geological Congress, 27 August-4 September, Cape Town, South Africa. Paper Number 541.
Cairncross, B. (2016) Gemstones of Southern Africa: a tour of the subcontinent. . Abstracts. 35th International Geological Congress, 27 August-4 September, Cape Town, South Africa. Paper Number 542. INVITED KEYNOTE SPEAKER.
Cairncross, B. (2016). The Johannesburg Geological Museum: An Underappreciated National Geoheritage Asset. . Abstracts. 35th International Geological Congress, 27 August-4 September, Cape Town, South Africa.
Chagondah G.S. and Hofmann A. (2016). Preliminary results on the petrogenesis and metallogenesis of Archaean rare-metal granitic pegmatites along the southern margin of the Zimbabwe craton. . Abstracts. 35th International Geological Congress, 27 August-4 September, Cape Town, South Africa. Paper Number 5482.
Collin, W.R., Gomez-Rivas, E., Martín-Martín, J.D. and Elburg, M. (2016) Unravelling the origin of diagenetic fluids in carbonate reservoirs with REE geochemistry. Petroleum Exploration (PETEX) Conference. London, UK. November 2016.
Da Costa G. V., Hofmann A. and Agangi A. (2016) Detrital pyrite: a revised classification scheme and application to placer gold deposits. Abstracts. 35th International Geological Congress, 27 August-4 September, Cape Town, South Africa. Paper Number 3260.
De Kock, M. O., Ravhura, L, Vorster, C., Beukes, N.J., Gumsley, A.P. (2016) Constraining the Timing of the Molopo Farms Complex Emplacement and Provenance of Its Country Rock. 7th International Dyke Conference, Beijing, China.

Dongre, A. and Viljoen, K.S. (2016) Classification of diamond source rocks in the Wajrakarur kimberlite field of southern India: A mineral genetic approach. Abstracts. 35th International Geological Congress, 27 August-4 September, Cape Town, South Africa. Paper Number 3412.
Dorland H.C., Campbell P.Q., Le Roux M., McMillan K., Dorland M.I., Erasmus P. and Wagner, N. (2016) Simulation of washability and liberation information from photographs. ICPC, Russia, June.
Dorland, H.C., Wagner, N.J. and Makukule, X. (2016) The product yield problem and the history and future of washability analyses. 33rd Annual International Pittsburgh Coal Conference, Cape Town, 9 – 12 August.
Dorland, H.C., Campbell, Q.P., Le Roux, M., Van Vuuren, P.A., Venter, W.C., Makukule, X.M., Wagner, N.J., Erasmus, P. and Dorland, M.I. (2016). Coal Geometallurgy: A place geologists may add value to the coal industry? . Abstracts. 35th International Geological Congress, 27 August-4 September, Cape Town, South Africa. Paper Number 1413.
Dorland,H.C., Wagner, N.J., Makukule, X.M., Campbell, Q.P., Le Roux, M., Van Vuuren, P.A., Venter, W.C., Erasmus, P., Dorland, M.I. (2016). The product yield problem and the history and future of washability analysis. Proceedings of the Pittsburgh Coal Conference, Cape Town, South Africa, 8-12 August.
Elburg, M., Cawthorn, R.G.C. and Andersen, T. (2016) The Mesoproterozoic Pilanesberg Complex - age and whole rock geochemistry. . Abstracts. 35th International Geological Congress, 27 August-4 September, Cape Town, South Africa. Paper Number 3627.
Elburg, M.A., Jacobs, J., Läufer, A., Andersen,T., le Roux, P., Harris, C., Ruppel, A., Krohne, N., and Damaske, D. (2016) Pan-African syenites and A-type granites in the Sør Rondane Mountains, Antarctica. . Abstracts. 35th International Geological Congress, 27 August-4 September, Cape Town, South Africa. Paper Number 3629.
Glynn, S., Master, S., Wiedenbeck, M., Armstrong, R.A., Frei, D., Davis, D. and Kramers, J.D. (2016) Geochronology of the Palaeoproterozoic Magondi Belt (Zimbabwe) and the Choma-Kalomo Block (Zambia), with regional implications. Abstracts. 35th International Geological Congress, 27 August-4 September, Cape Town, South Africa. Paper Number 5320.
Götz, A.E., Beukes, N.J. and De Kock, M.O. (2016) A multidisciplinary approach to decipher the complexity and potential of an unconventional gas resource: The Permian Whitehill Formation (Karoo Basin, South Africa). Abstracts. 35th International Geological Congress, 27 August-4 September, Cape Town, South Africa. Paper Number 3373.
Greco F., Cavalazzi B. and Hofmann A., (2016). Carbonates from the ~3.4 Ga old Buck Reef Chert of South Africa: testing potential microbial activity in an Archean hydrothermal system. Abstracts. 35th International Geological Congress, 27 August-4 September, Cape Town, South Africa. Paper Number 5016.
Gumsley, A., Bleeker, W., Chamberlain, K., Söderlund, U., De Kock, M.O., Larsson, E. and Bekker, A. (2016) U-Pb age for the Ongeluk Basalts: implications for GOE and global glaciations. Abstracts. 35th International Geological Congress, 27 August-4 September, Cape Town, South Africa. Paper Number 5417.
Gumsley, A., Chamberlain, K, Bleeker, W., Söderlund, U., De Kock, M.O., Kampmann, T, Larsson, E., Bekker, A. (2016) The timing of the Paleoprotereozoic Great Oxidation Event using dykes, sills and volcanics of the Ongeluk Large Igneous Province, Kaapvaal Craton. IDC7 Beijing, China.
Hatton, C., De Kock, M.O., and Altermann, W. (2016) On using the Kaapvaal Craton to naturalise the International Chronostratigraphic Chart for the Precambrian. Abstracts. 35th International Geological Congress, 27 August-4 September, Cape Town, South Africa. Paper Number 4593.
Hoehnel, D., Reimold, W. U., Mohr-Westheide, T., Hofmann, A., & Altenberger, U. (2016). Petrography of Archean Spherule Layers from the CT3 Drill Core, Barberton Greenstone Belt, South Africa. LPI Contributions, 1921.
Hoehnel, D., Tagle, R., Hofmann, A., Reimold, W. U., Mohr-Westheide, T., Fritz, J. and Altenberger, U. (2016). Micro-XRF Analysis of Archean Spherule Layers and Host Rocks from the CT3 Drill Core, Barberton Greenstone Belt, South Africa. LPI Contributions, 1921.
Hlongwani, N.C., Smith, A.J.B., Beukes, N.J. and Blignaut, L. (2016) The stratigraphic, petrographic and geochemical subdivision of the upper manganese ore bed of the Hotazel Formation at Kudumane Mining Resources, Northern Cape Province. Abstracts. 35th International Geological Congress, 27 August-4 September, Cape Town, South Africa. Paper Number 3481.
Hofmann A. (2016) Early Earth surface processes 3.5 to 3.0 Ga ago. Abstract, XIIth Rencontres du Vietnam, Search for life: from early Earth to exoplanets, Quy Nhon, Vietnam.
Hofmann A., Jodder J. and Xie, H. (2016) On the remarkable similarity of the Archaean geological evolution of the Singhbhum and Kaapvaal cratons. Abstracts. 35th International Geological Congress, 27 August-4 September, Cape Town, South Africa. Paper Number 5390.

Hofmann, A, Pitcairn, I. and Wilson A (2016) Gold mobility during Palaeo- and Mesoarchaean surface processes. Abstracts Volume, 26th Colloquium of African Geology, Ibadan, Nigeria, p. 80.
Jodder, J. and Hofmann, A. (2016) Carbonaceous cherts of the Daitari Greenstone Belt, Singhbhum Craton, India: A well preserved record of early life. . Abstracts. 35th International Geological Congress, 27 August-4 September, Cape Town, South Africa. Paper Number 5247.
Jodder, J. and Hofmann, A. (2016) Probing into the Palaeoarchaean record of the Singhbhum Craton (India) in search for vestiges of life older than 3.5 Ga. Abstract, XIIth Rencontres du Vietnam, Search for life: from early Earth to exoplanets, Quy Nhon, Vietnam.
Kekana, P. and Wagner, N.J. (2016) The application of Coal Quality Database over Time and Space across the Mpumalanga Coalfield. 33rd Annual International Pittsburgh Coal Conference, Cape Town, 9 – 12 August.
Kekana P. and Wagner, N.J. (2016) The Mpumalanga Coalfields: Quality, quantity variations and environmental issues through time and space. Abstracts. 35th International Geological Congress, 27 August-4 September, Cape Town, South Africa. Paper Number 3129.
Kramers, J.D., Beukes, N., Gumsley, A., Guy, B., Naegler, Th., Pettke, Th.3, Smith, A.B. and Voegelin, A. (2016) Evidence from molybdenum isotopes for a transient and localized nature of free aquatic oxygen around 3 Ga. . Abstracts. 35th International Geological Congress, 27 August-4 September, Cape Town, South Africa. Paper Number 4330.
Kristoffersen, M., Andersen, T., Elburg, M., (2016). Is There Any Provenance Information Contained In Highly Discordant Detrital Zircon From The Mesoarchaean Pongola Supergroup Sandstones? IMSG Conference, Langebaan, Western Cape, January 2016.
Kröner, A., Nagel, T., Hoffmann, J.E., Xie, H., Wong, J., Geng, H., Hegner, E., Liu, X., Hofmann, A., Liu, D. and Yang, J. (2016) High-grade metamorphism and crustal melting at ca. 3.2 Ga in the eastern Kaapvaal craton, southern Africa. Abstracts. 35th International Geological Congress, 27 August-4 September, Cape Town, South Africa. Paper Number 695.
Luais B., Fritz J., Hofmann A., Mohr-Westheide T., Reimold W.U., C. Koeberl C. (2016) Germanium elemental and isotopic tracing of ca 3.2Ga impact spherule layers from the Barberton Greenstone Belt (South Africa) Meteoritics & Planetary Science 49, Supp A239, #5417.
Lum, J.E., Viljoen, K.S., Cairncross, B. and Frei, D. (2016) Geochemical characteristics of beryl from the Erongo Volcanic Complex, Namibia. Abstracts. 35th International Geological Congress, 27 August-4 September, Cape Town, South Africa. Paper Number 3610.
Lum J.E., Viljoen, F., Cairncross, B, and Frei, D. (2016) Geochemical characterization of aquamarines and emeralds from Namibia and South Africa. Abstracts. Geological Society of America Annual Meeting, 25-28 September 2016, Denver, Colorado, USA (Paper 136-7).
Makhubela, T.V. and Kramers, J.D. (2016) (U-Th)/He dating of CaCO3 speleothems: a new perspective for dating fossil-bearing cave deposits. Abstracts. 35th International Geological Congress, 27 August-4 September, Cape Town, South Africa. Paper Number 763.
Maphaphuli M., Wagner, N.J. 2016. Mineral matter in coals from the Soutpansberg Coalfield, South Africa. 33rd Annual International Pittsburgh Coal Conference, Cape Town, 9 – 12 August.
Marageni, M. and P.E. Janney (2016) An investigation of rare earth element enrichment processes in diatremes and related carbonatites in western South Africa. . Abstracts. 35th International Geological Congress, 27 August-4 September, Cape Town, South Africa. Paper Number 1585.
Maré, L.P., De Kock, M.O., Cairncross, B. and Mouri, H. (2016) The use of thermomagnetic curves for paleotemperature evaluation in sedimentary basins. . Abstracts. 35th International Geological Congress, 27 August-4 September, Cape Town, South Africa. Paper Number 1131.
Matiane A. and Wagner, N.J. (2016) Determination of rare earth elements (REE's) in coals and their associated ash products from selected localities in South Africa. 33rd Annual International Pittsburgh Coal Conference, Cape Town, 9 – 12 August.
Matiane A. and Wagner N.J.(2016) Determination of rare earth elements (REE's) in coals and their associated ash products from selected localities in South Africa. Abstracts. 35th International Geological Congress, 27 August-4 September, Cape Town, South Africa. Paper Number 3187.
Moitsi, M., Viljoen, F. and Knoper, M. (2016) A geometallurgical study of the mineralized footwall underlying the Brakspruit facies of Merensky Reef at the Lonmin Karee Pt mine, Bushveld Complex, South Africa. Abstracts. 35th International Geological Congress, 27 August-4 September, Cape Town, South Africa. Paper Number 1635.
Molekwa M.A., Hofmann, A. and Eickmann, B. (2016). The origin of granular chert in the BARB3 drill core from the 3.4 Ga Buck Reef Chert, Onverwacht Group, Barberton Greenstone Belt, South Africa. . Abstracts. 35th International Geological Congress, 27 August-4 September, Cape Town, South Africa. Paper Number 4390.
Monareng, F.B., De Kock, M.O., Beukes, N. and Blignaut, L. (2016) Geochemistry of a paleoweathering profile on the "bostonites" mafic intrusives of Avontuur Deposit, Northern Cape. Abstracts. 35th International Geological Congress, 27 August-4 September, Cape Town, South Africa. Paper Number 3801.

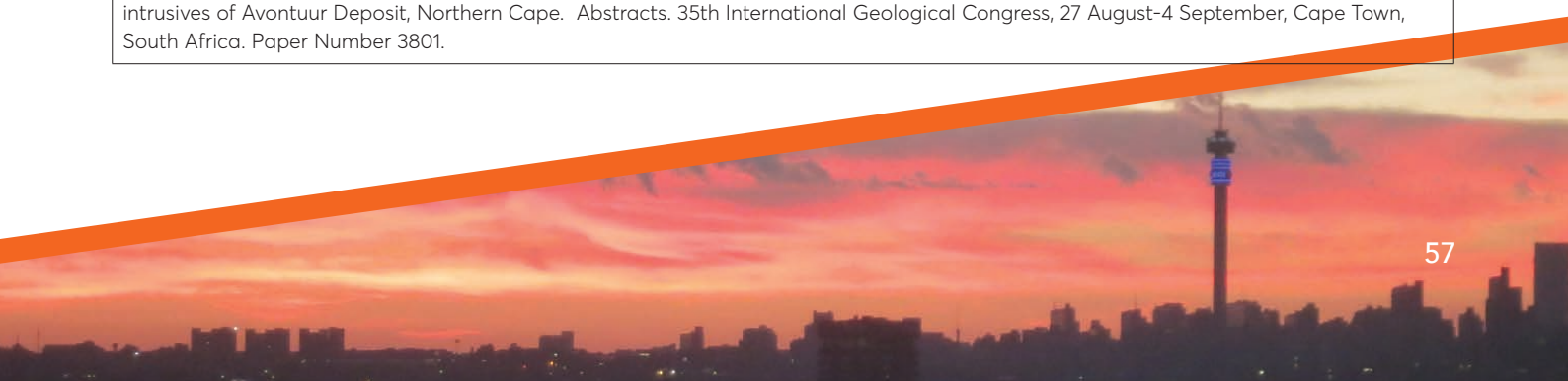

Morake, M.A., Knoper, M.W., Grantham, G.H., Kramers, J. and Elburg, M.A. (2016) Early-Middle Jurassic Mafic Dykes from the H.U. Sverdrupfjella, Antarctica. Abstracts. 35th International Geological Congress, 27 August-4 September, Cape Town, South Africa. Paper Number 5383.
Motloba, G.B., Viljoen, K.S. and Smith A.J.B. (2016) A Geometallurgical Assessment of the P2 and P1 units of the Platreef at Lonmin's Akanani Project, Northern Limb, Bushveld Complex. Abstracts. 35th International Geological Congress, 27 August-4 September, Cape Town, South Africa. Paper Number 3305.
Mphaphuli M., Wagner N.J. and Sparrow J. (2016) Variation in coal petrographic composition on either side of the Tshipise fault, Soutpansberg coalfield, South Africa. Abstracts. 35th International Geological Congress, 27 August-4 September, Cape Town, South Africa. Paper Number 4391.
Mthabela Z. and Wagner N.J. (2016) Prediction of Spontaneous Combustion in coal by use of Thermogravimetry. 33rd Annual International Pittsburgh Coal Conference, Cape Town, 9 – 12 August.
Nendouvhada, N., Wagner, N.J. and Golding, A. (2016) Application of coal petrography in understanding the variation of coal composition in the coalfields of Botswana. 33rd Annual International Pittsburgh Coal Conference, Cape Town, 9 – 12 August.
Nendouvhada N., Wagner N.J. and Golding, A. (2016) Comparison of petrographic composition in samples from six different coalfields of Botswana. Abstracts. 35th International Geological Congress, 27 August-4 September, Cape Town, South Africa. Paper Number 4346.
Nxumalo, V., Wagner N.J., Kramers J., Vorster, C. and Cairncross B. (2016) Trace elements Associated with the Upper Coal Zones of the Springbok Flats Basin, South Africa.33rd Annual International Pittsburgh Coal Conference, Cape Town, 9 – 12 August.
Nxumalo, V., Wagner, N., Cairncross, B., Kramers, J., Vorster, C., Przybylowicz, W. and Setladi, C. (2016) Coal geology and quality of the Springbok Flats Basin, South Africa. Abstracts. 35th International Geological Congress, 27 August-4 September, Cape Town, South Africa. Paper Number 1137.
Özdemir, S., Koeberl, C., Schulz, T., Reimold, W.U., Mohr-Westheide, T. and Hofmann, A. (2016) Archean spherule classification of CT3 drill core, Barberton Greenstone Belt (South Africa) based on petrography and mineral chemistry. In EGU General Assembly Conference Abstracts EGU2016-15691.
Ozdemir, S., Schulz, T., Koeberl, C., Reimold, W. U., Mohr-Westheide, T. and Hofmann, A. (2016) Paleoarchean Spherule Beds in the CT3 Drill Core from the Barberton Greenstone Belt, South Africa: Geochemistry and Os Isotopic Signatures. LPI Contributions, 1921
Ravhura, L., De Kock, M., Vorster, C., Beukes, N.J. and Gumsley, A.P. (2016) A multipronged approach to constraining the timing of the Molopo Farms Complex, southern Africa. Abstracts. 35th International Geological Congress, 27 August-4 September, Cape Town, South Africa. Paper Number 4872.
Robey, K., de Lange, S.S., Bredenkamp, E. and Beukes, N.J. (2016) Investigating the hydrogeological conditions of the deep formation in the southern Karoo Basin – Case study of the KARIN-CIMERA KFZ-1 hole. Abstracts. 35th International Geological Congress, 27 August-4 September, Cape Town, South Africa. Paper Number 4762
Schaefer T.L., Tomasek J., Hofmann A., Dunkl I., von Eynatten H., Xie H., Vollbrecht A., van den Kerkhof A., Techmer, K. (2016) A mineralogical-geochemical study of Mesoarchaean quartz-pebble conglomerates from the Pongola Supergroup and implications for U/Au placer deposits. Abstracts. 35th International Geological Congress, 27 August-4 September, Cape Town, South Africa. Paper Number 5388.
Schröder, S., Beukes, N. J., Warke, M. R. and Armstrong, R. A. (2016) Age constraints on Paleoproterozoic glacials and oxygenation from South Africa. Abstracts. 35th International Geological Congress, 27 August-4 September, Cape Town, South Africa. Paper Number 2448.
Siahi, M., Hofmann, A., Hegner, E., Master, S. and Müller, C.W. (2016) Textural and geochemical characteristics, and process of formation, of ooids in the Mesoarchaean Pongola Supergroup, South Africa. Abstracts. 35th International Geological Congress, 27 August-4 September, Cape Town, South Africa. Paper Number 4843.
Smith, A.J.B. and Beukes, N.J. (2016) Paleoproterozoic banded iron formation-hosted high-grade hematite iron ore deposits of the Transvaal Supergroup, South Africa. Abstracts. 35th International Geological Congress, 27 August-4 September, Cape Town, South Africa. Paper Number 1916.
Smith, A.J.B., Henry, G. and Frost-Killian, S. (2016) A review of the Birimian Supergroup- and Tarkwaian Group-hosted gold deposits of Ghana. Abstracts. 35th International Geological Congress, 27 August-4 September, Cape Town, South Africa. Paper Number 3354.

Vorster, C., Beukes, N.J, Kramers, J.Van Niekerk, H.S. (2016) Atlantic- to Andean type basin inversion along the southern margin of Gondwana: U-Pb detrital zircon evidence form the Cape- and lower Karoo Supergroups and correlatives in Argentina and the Falkland Islands. Abstracts. 35th International Geological Congress, 27 August-4 September, Cape Town, South Africa. Paper Number 1534.

Wabo, H., Belyanin, G., De Kock, M.O., Humbert, F., Söderlund, U, Mare, L.P. and Kramers, J. (2016) Preliminary geochronology, geochemical and paleomagnetic results from NE-trending dykes in the Lydenburg area, South Africa. IDC7 Beijing, China.

Wilson A.H., Hofmann A. and Siahi M. (2016) The Mid-Archaean Pongola Supergroup: volcanism, sedimentation and early life development on Earth's oldest stable continental margin. Abstracts. 35th International Geological Congress, 27 August-4 September, Cape Town, South Africa. Paper Number 866.

Zardad, S., Smith, A.J.B., Vorster, C. and Beukes, N.J. (2016) The Sedimentology of the Rooihoogte Formation of the Transvaal Supergroup in the Carletonville area. Abstracts. 35th International Geological Congress, 27 August-4 September, Cape Town, South Africa. Paper Number 3533.

SUPPORT STAFF IN PPM AND GEOLOGY

Lisborn Mangwane and Baldwin Tshivhiahuvhi: Technical assistants, thin section laboratory.

Daniel Selepe: Technical assistant, field vehicle maintenance.

Thuso Ramaliba: Laboratory Assistant, thin section laboratory.

Herbert Gugwane: Technical assistant, rock preparation laboratory.

Diana Khoza: Finance and transport.

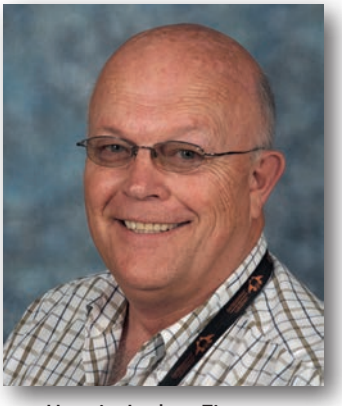

Hennie Jonker: Finance and field schools.

Herbert Leteane: Technical assistant.

Elaine Minnaar: Departmental Secretary.

PPM ANNUAL RESEARCH COLLOQUIUM

Date: Thursday, 26 October 2017

Venue: University of Johannesburg Kingsway Campus, Chinua Achebe Auditorium, 6th floor of the Library building (adjacent to the main Kingsway entrance)

Programme of talks to be announced closer to the date

Time: 12.00 to 16.00, followed by drinks and snacks

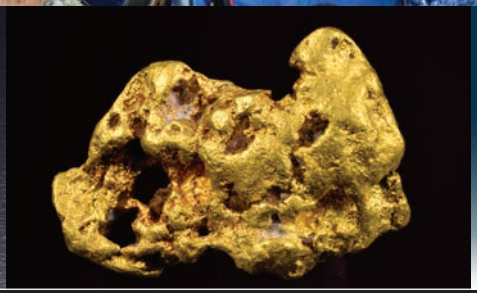

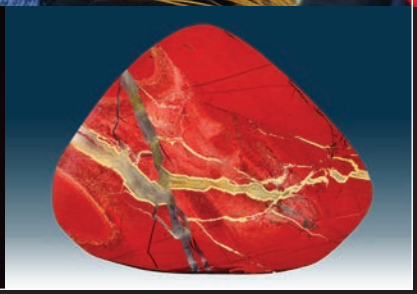

SPECTRUM

SPECTRUM, the Central Analytical Facility of the Faculty of Science at UJ, was established in 1999 to serve as a one-stop state-of-the-art unit, managed and staffed to ensure an accessible analytical service not only for UJ staff and students but also for outside cooperation and clients.

SPECTRUM offers comprehensive solutions for a broad range of applications, utilizing modern high-technology equipment. This includes PANalytical X'Pert Pro X ray diffraction (XRD) and Magix Pro X ray fluorescence (XRF) instruments, a Tescan Vega3 scanning electron microscope (SEM) with EDX detector for semiquantitative chemical analysis, a JEOL 733 microprobe, a Spectro ARCOS ICP optical emission spectrometer (OES), a Perkin Elmer NexION 350 ICP quadrupole mass spectrometer (ICP-QMS) for solution analysis, a Varian Unity Inova NMR system, and Zeiss Axioplan 2 compound and Zeiss Discovery stereo microscopes.

Argon extraction and mass spectrometer

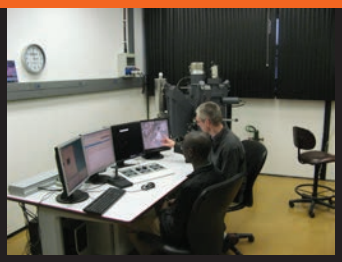

Electron microprobe

Laser ablation ICP-MS

Laser ablation multicollector ICP-MS

SPECIALIZED GEOSCIENCE APPLICATIONS AT SPECTRUM

Other than the more general instrumentation at SPECTRUM mentioned above, the facility also houses five units (two of them unique in Africa) geared specifically to Geoscience applications, among them the needs of PPM:

- A FEI Quanta 600F field emission Mineral Liberation Analyzer (MLA). This instrument is the one mainly used in geometallurgical research.
- A CAMECA SX100 electron microprobe with 4 wavelength dispersive spectrometers (WDS) and an energy dispersive spectrometer (EDS), used extensively for in situ micrometer-scale quantitative chemical analysis of minerals in a broad spectrum of projects.
- A ThermoFischer X-Series II ICP quadrupole mass spectrometer coupled to a New Wave UP-213 Nd YAG laser ablation system, as well as a Nu Instruments Nu Plasma II multicollector ICP mass spectrometer, coupled to a Resolution 199 nm excimer laser ablation system, are dedicated to in situ isotope and chemical analysis of minerals on a microscopic scale. The quadrupole system is particularly suited to rapid series of uranium-lead zircon age determinations, for instance in sediments, and trace element geochemical profiling. The multicollector system enables high-precision uranium-lead dating of zircon and other uranium-bearing minerals, as well as high precision isotope ratio analyses on strontium, neodymium, hafnium and many other elements, from both laser ablation and samples in solution.
- A MAP-215 noble gas mass spectrometer coupled to an ultra-high vacuum gas extraction system using a continuous 1064 nm Nd-YAG laser as a heat source. This is the only functional unit of its kind in Africa and is chiefly used for both $^{40}Ar/^{39}Ar$ and (in conjunction with the solution ICP-QMS system) U-Th-He geochronology.
- A paleomagnetic laboratory, likewise unique in Africa. This

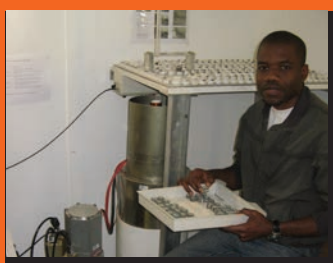

SQUID magnetometer with sample magazine

Solution ICP-MS

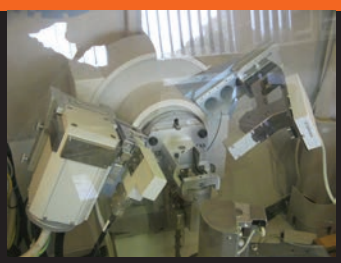

X ray diffraction

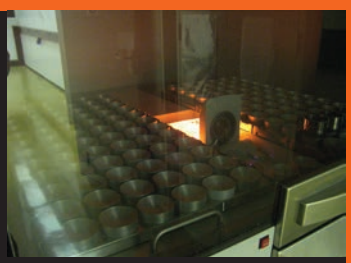

X ray fluorescence

For further information and cost of services please contact: Dr Willie Oldewage, Tel: 011 559 2274; Fax: 011 559 3361; e-mail: willieho@uj.ac.za